719940

ORNL-4584
UC-41 — Health and Safety

Contract No. W-7405-eng-26

HEALTH PHYSICS DIVISION ANNUAL PROGRESS REPORT

For Period Ending July 31, 1970

K. Z. Morgan, Director

W. S. Snyder, Assistant Director
E. G. Struxness, Assistant Director

REPOSITORY MMES/X-10/Vault
COLLECTION Central Files
BOX No. ORNL-4584
FOLDER

OCTOBER 1970

OAK RIDGE NATIONAL LABORATORY
Oak Ridge, Tennessee
operated by
UNION CARBIDE CORPORATION
for the
U. S. ATOMIC ENERGY COMMISSION

1147930

A-00389

Human Studies Project

Contents

SUMMARY ix

PART I. RADIOACTIVE WASTE DISPOSAL

1. FATE OF TRACE ELEMENTS AND RADIONUCLIDES IN TERRESTRIAL ENVIRONMENT 1
   - Evaluation of Zonal Centrifugation Techniques 1
   - Applications of Zonal Centrifugation 4
   - Distribution of ^{137}Cs in Soil of a *Liriodendron* Forest 8
   - Water Quality Studies in Walker Branch Watershed 9
2. DISPOSAL BY HYDRAULIC FRACTURING 11
   - Investigations at Oak Ridge 11
   - Investigations in New York State 11
3. DISPOSAL IN NATURAL SALT FORMATIONS 16
   - Design Criteria and Facility Description 16
   - Detailed Information Developed in Support of Facility Design 18
4. ENGINEERING, ECONOMIC, AND SAFETY EVALUATIONS 37
   - Siting and Operation of Nuclear Facilities 37
   - Routine Atmospheric Releases of Radioactive Materials 37
   - Pathway Analysis 38
   - Regional Planning 39
5. EARTHQUAKES AND REACTOR SAFETY 41
   - ORNL Seismograph Station ORT 41
6. DOSE ESTIMATION STUDIES RELATED TO PEACEFUL USES OF NUCLEAR EXPLOSIVES 42
   - Utilization of Natural Gas from Nuclearly Stimulated Wells 42
   - Development of Radiation Safety Guides for Transient Exposures 49
   - Dose Estimation Studies Related to Construction of an Interoceanic Canal with Nuclear Explosives 53

1147931

7. RELATED COOPERATIVE PROJECTS 57

Cooperation of Other Agencies in ORNL Studies 57

Visiting Investigators from Abroad 57

Nuclear Safety Review 57

Participation in Educational Programs and Cooperation with Other Agencies 57

Laboratory Projects 57

PART II. RADIATION PHYSICS

8. THEORETICAL RADIATION PHYSICS 58

Radiation Quantities and Their Significance in Health Physics 58

Dosimetry of High-Energy Nucleons and Pions 59

Determination of LET Spectra from Energy-Proportional Pulse-Height Measurements 60

Critical Dipole Moments for Electron Binding to a Nonstationary Dipolar System 61

Approximate Hartree-Fock Energies for Autoionizing States in Neon and Argon 63

Variational Bound Method for Elastic Scattering Phase Shifts 64

Oscillator Strength 65

Potential Energy Curves for Diatomic Molecules 66

The Mean Free Path of Relativistic Electrons for Plasmon Excitation 66

Z_1^3 Effect in the Stopping Power of Charged Particles 67

Double-Plasmon Excitation in a Free-Electron Gas 68

Anomalous Damping of Volume Plasmons in Polycrystalline Metals 68

Photon–Surface-Plasmon Coupling at a Dielectric Solid 70

Revised Formulation of the Macroscopic Maxwell Theory 71

Revised Formulation of the Kinetic Plasma Theory 72

9. INTERACTION OF RADIATION WITH LIQUIDS AND SOLIDS 74

Collective Effects in the Optical Properties of Cesium 74

Optical Properties of MgO and MgF_2 in the Soft-X-Ray Region 76

Study of the Optical Properties of Solids by Ellipsometry 78

Radiative Decay of Collective Oscillations in Metals 79

Radiation Damping of Surface Plasmons from Aluminum-Coated Concave Diffraction Gratings 82

Efficiency of Dielectric-Coated Concave Diffraction Gratings 83

Observations of Surface Roughness 83

Exoelectron Emission During Oxygen and Water Chemisorption on Fresh Magnesium Surfaces 85

1147932

10. PHYSICS OF TISSUE DAMAGE 87
Electron-Slowing-Down Studies 87
Optical Properties of Some Organic Liquids 88

11. ELECTRON AND ION COLLISION PHYSICS 92
Electron Impact Excitation and Ionization of the Rare Gases 92
Threshold Electron Impact Excitation of Some Simple Molecules 94
Interaction of Electrons with Substituted Benzenes, Substituted Pyridines, and Pyrizine 95
Attachment Rate of Thermal Electrons to SF_6 96
Thermal-Electron Attachment Rates and Negative-Ion Lifetimes of Other Molecules 97
Quadrupole Ion-Mass Analysis of Swarm Experiments 98
Collisions of Slow Cesium Atoms with Electronegative Gases 98
Low-Energy Negative-Ion–Molecule Reactions 100

12. ATOMIC AND MOLECULAR RADIATION PHYSICS 105
Thermal-Electron Scattering by Polar Molecules 105
Electron Attachment and "Carrier Gas" Energy Distribution Functions 108
Cross-Section Functions for Thermal-Peaking Electron Attachment Resonances 108
Electron Attachment to Sulfur Hexafluoride 114
Electron Attachment to Organic Molecules 116
Capture of Slow Electrons by Organic Molecules in the Field of an Excited Electronic State 118
Lifetimes of Long-Lived Polyatomic Negative Ions Formed by Electron Capture in the Field of the Ground Electronic State 118
Energy Dependence of the Lifetime of Long-Lived Transient Negative Ions 119
Electron Attachment to Halogenated Hydrocarbons 121
Threshold-Electron Excitation Spectra of Organic Molecules: Location of Triplet and Compound Molecular Negative-Ion States 121
Emission and Decay of Fluorescent Organic Liquids Under Electron Impact 121
Photophysical Studies of Liquids 122
On Molecular Parameters of Physical, Chemical, and Biological Interest 123
Stopping Powers of Slow Electrons in Hydrocarbons 123
Resonance Radiation Imprisonment Phenomena 123
Comparison of Direct and Photosensitized Ionization Efficiencies 124

13. GRADUATE EDUCATION AND VOCATIONAL TRAINING 125

1147933

PART III. RADIATION DOSIMETRY RESEARCH

GENERAL OBJECTIVES AND ACTIVITIES 128

14. DOSIMETRY FOR HUMAN EXPOSURES AND RADIOBIOLOGY 129

Japanese Dosimetry Program 129

Leakage Studies for "Fat Man" and "Little Boy" 134

Dose Distributions in Cylinders Exposed During Operation HENRE 135

Depth-Dose Distributions in Small Animals 137

Californium-252 138

15. SPECTROMETRY RESEARCH AND DEVELOPMENT 152

An Extrapolation Chamber for the Measurement of Dose Distributions at Bone-Tissue Interfaces 152

Dose Distributions at Bone-Tissue Interfaces 153

Purification of Sulfur by Zone Refining 155

Experimental Measurements of LET 155

Unusual X-Ray Sources 157

Description of Neutron Leakage from the Operation HENRE Neutron Generator 159

Organic Scintillator Experiment 159

DOSAR Portable Scaler Modification 161

Nuclear Data Analyzer Tape Conversion 161

TSEE and Spark-Counter Preamplifiers 162

Measurement of the Neutron Spectrum from the HPRR Between 50 keV and 450 keV 164

16. APPLIED DOSIMETRY RESEARCH 165

TSEE Research 165

Nuclear Track Registration in Polymers 180

17. HPRR AND ACCELERATOR OPERATIONS 187

Neutron Generator Target Research $D(d,n)^3He$ and $T(d,n)^4He$ Reactions 187

HPRR Operations 189

Intercomparison Studies 191

Van de Graaff Operations 197

18. INTERACTION OF CHARGED PARTICLES WITH MATTER 198

PART IV. INTERNAL DOSIMETRY

19. INTERNAL DOSE ESTIMATION 200

Estimates of Dose to Red Bone Marrow from Monoenergetic Sources of Photons in Lungs and Other Organs 200

1147934

Estimation of Dose to Gonads from Gamma Emitters Present in the Body 203

Estimation of Dose and Dose Commitment to Bladder Wall from a Radionuclide Present in Urine 206

Application of Berman's Ten-Compartment Model for Human Iodine Metabolism to Estimation of Microcurie-Days Residence of ^{123}I, ^{124}I, ^{125}I, ^{126}I, and ^{131}I 208

Application of the Mammillary Compartment Model to Estimation of Microcurie-Days Residence of ^{232}Th, ^{228}Ra-^{228}Ac, ^{228}Th, and ^{224}Ra in Man 214

Scattered Energy Spectrum for a Monoenergetic Gamma Emitter Uniformly Distributed in an Infinite Cloud 216

20. STABLE ELEMENT METABOLISM 223

Elemental Intake and Excretion in Long-Term Balance Studies 223

Gross Composition of Bone and Cartilage 223

THESES, PAPERS, PUBLICATIONS, AND LECTURES

THESES 227

PAPERS 228

PUBLICATIONS 233

LECTURES 242

1147935

Summary

PART I. RADIOACTIVE WASTE DISPOSAL

1. Fate of Trace Elements and Radionuclides in Terrestrial Environment

Banding of several reference clay minerals was evaluated in a continuous density-gradient solution using zonal centrifugation. Variables examined were particle sizes, cationic saturations, and centrifugal forces. Zonal centrifugation was also used to segregate mineral fractions of several environmental samples, and then these were investigated for phosphate or radionuclide distribution. For phosphate distribution, samples were obtained from the bottom and suspended sediments of the ORIC pond and a soil whose runoff drains into the pond. The principal finding is that most of the phosphate is present in the iron and aluminum phosphate forms.

For radionuclide distribution samples, bottom sediments from White Oak Lake Bed and Creek were examined. Cesium-137 was found primarily in the clay mineral band; ^{90}Sr was found in most bands, including the bands containing calcium carbonate, which tentatively confirms earlier conclusion. Distribution of ^{137}Cs in a soil from previously tagged trees (*Liriodendron* forest) suggests that the mineral illite plays a dominant role in fixing this radionuclide.

Water quality studies of Walker Branch Watershed were continued. Water temperatures were measured continuously at several locations in the two streams which drain the watershed. Differences in water temperatures were observed with time and location, and the differences were not predictably uniform. The differences are discussed, with reference to the source of groundwater and to air temperatures.

2. Disposal by Hydraulic Fracturing

Operational waste injection ILW-6 was made in June 1969. Some 80,000 gal of waste, containing nearly 100,000 Ci of activity, were disposed of without incident.

The work in New York State is well under way. The injection well and the four surrounding observation wells have been completed, and two test injections have been made. Both injections were into the same slot at a depth of 1450 ft. The first was made with water only in October 1969, and apparently made a dominantly horizontal but complex fracture. The second, containing 2.7 Ci of ^{95}Zr-^{95}Nb, was made on June 26, 1970, and is already known to be horizontal. A dye, Rhodamine B, was mixed with the radioactive tracer to make a visible marker.

3. Disposal in Natural Salt Formations

The principal effort in the current program is a study leading to the development of a conceptual design (and the required safety analyses) of a combined solidified high-level power reactor fuel-reprocessing waste repository and low-activity alpha-contaminated waste repository. This one facility should be capable of handling all waste of these two types until about the end of this century.

For the high-level wastes a total (gross) salt mine area of about 850 acres, all newly mined for the purpose, will be required. The present design for the low-level facility calls for the use of an existing inactive mine which has around 40 million cubic feet of space already mined. The tentatively selected location is near Lyons, Kansas.

A geologic and hydrologic study based on available information indicates that the central Kansas area meets the criteria established for the location of the first demonstration repository (e.g., salt beds at least 200 ft thick and lying at depths of no more than 2000 ft). Also the Arbuckle formation appears to be suitable for disposal of excess salt as brine. However, contacts with local salt producers have indicated the possibility for sale of the salt either as brine or as rock salt. Therefore, sale of the excess salt is considered to be the desirable disposal method, with the Arbuckle formation as a backup.

1147936

A number of preliminary studies of temperatures (due to radioactive decay heat) at mine level and in the rock formations around the mine have been carried out. Based on all considerations (such as mine stability, aquifer temperature rises, etc.), it appears that 200°C peak salt temperature is neither too conservative nor too liberal for at least the initial stages of a high-level disposal facility operation.

A study of salt tectonics in relation to the disposal of solidified high-level waste was made. Considering the specific case of the formation at Lyons, Kansas, it was concluded that the possibility of extensive salt deformation affecting the safety of the disposal area for a period of a few hundred thousand years can be excluded. Also the heating caused by the decay heat generated in the high-level waste would be of such short duration (from a geologic point of view) that no significant consequences would be expected.

4. Engineering, Economic, and Safety Evaluation

Investigation has continued of factors involved in the siting and operation of nuclear facilities. Radioactive production and decay processes can now be included directly in computer calculation of downwind air concentrations that result from routine release of gaseous effluents. After deposition, the movement of radionuclides in food chains can be simulated by the preliminary computer program PATHWAY. An example is used to illustrate application of this program. Information has been assembled on nuclear power plant locations and the surface waters contiguous to each site for use in discussions on regional planning.

5. Earthquakes and Reactor Safety

Routine operation of the ORNL seismograph station has continued during the year, including the regular reporting of data to the U.S. Coast and Geodetic Survey and the periodical issuance of a station bulletin. In addition, a seismic history of the southeast region of the United States was compiled and a study of the seismicity of this area made.

6. Dose Estimation Studies Related to Peaceful Uses of Nuclear Explosives

The concentration of tritium and ^{85}Kr in gas samples from the Gasbuggy well, the first nuclearly stimulated natural gas well, declined exponentially as contaminated gas was removed during flaring operations and diluted with uncontaminated formation gas. The ratio of these radioactive impurities in the gas to the concentration of carbon dioxide and hydrogen also diminished for reasons that are not clear at present. Recent census data were used for an estimate of the home occupancy factor, the fraction of the time that an average home is occupied, to aid calculations of home exposure to radioisotopes in contaminated gas used for heating and other purposes.

Data on gas consumption in two West Coast metropolitan areas, Los Angeles and San Francisco, have been combined with meteorological information to provide estimates of the hypothetical doses resulting from the use of contaminated natural gas in these areas. Calculated concentrations of radioisotopes in the atmosphere were higher in Los Angeles than in San Francisco, but the hypothetical doses resulting from the maximum exposures were almost the same in both areas (2.2 and 2.5 millirems/year respectively) because of greater domestic use of gas in the cooler region.

In addition to potential radiation exposures from home and industrial combustion of contaminated natural gas, the hypothetical exposure of users of gas by-products has been considered, including carbon black, fertilizer ammonia, tritiated alcohol, and hydrogenated fats and oils. In all cases the hypothetical exposure to consumers of these products was shown to be negligible at the levels of radioactivity anticipated in large-scale use of nuclear explosives for stimulation of natural gas production.

Considerable effort has been directed toward the development of radiation safety guides for transient exposures because of the need to evaluate the possible hazard of radioactive releases from peaceful uses of nuclear explosives at or near the earth's surface. Cumulative exposure guides (CUE's), based either on ICRP maximum permissible annual doses or on maximum permissible organ burdens, have been calculated for short-term inhalation exposures in terms of concentration (microcuries per cubic centimeter) and time (hours). These transient exposure guides, calculated by means of computer programs, are useful for "first-cut" assessment of the possible impact of short-term releases of radioactive materials to the environment.

Other exposure modes which are, in general, more difficult to evaluate than inhalation, have also been considered in calculating CUE's. A computer program available for calculating the exposure resulting from immersion in radioactive clouds for short periods. A simplified model has also been developed to describe one exposure pathway, the fallout-milk-man food chain, that can aid evaluation of ingestion hazards resulting from either transient or long-term fission product deposition on vegetation.

1147937

Potential doses to indigenous populations along Route 17 in eastern Panama and Route 25 in northwestern Colombia were estimated for a combination of hypothetical exposures to radiation. The studies attempted to determine when it might be appropriate for populations to reenter areas adjacent to the two routes.

7. Related Cooperative Projects

Representatives of other agencies continued to participate in the Radioactive Waste Disposal Section's studies. One alien guest was in residence during the year. One member served as assistant news editor for the United States for *Health Physics* and as an assistant editor of *Nuclear Safety*. One member of the Section served on the Southern Governors' Conference Task Force for Nuclear Power Policy. Members of the Section participated part time in the Nuclear Safety Information Center, the Civil Defense Research Project, and the agroindustrial complex study.

PART II. RADIATION PHYSICS

8. Theoretical Radiation Physics

A critical appraisal has been made of quantities and units in radiation protection work, and a different approach has been suggested for establishing permissible limits of radiation exposure.

A Monte Carlo method has been developed for determining LET spectra from energy-proportional pulse-height measurements, and work has begun to use this method to develop a more convenient and more reliable means of determining LET distributions.

Work is in progress in collaboration with the experimental Health Physics Group at CERN on the dosimetry of high-energy pions. Calculations are being tailored to simulate actual experimental conditions such as beam density profile, energy distributions, and target size, shape, and composition, and initial results have been in good agreement with experiment.

A new theoretical investigation has been made of electron binding to a finite dynamic dipolar system where the Hamiltonian operator in the Schrodinger equation contains, in addition to the electron kinetic energy, the rotational energy of the dipole. Approximate Hartree-Fock energies have been calculated for autoionizing states in neon and argon atoms. A new variational method has been formulated and applied to the determination of elastic scattering phase shifts. A generalization of the oscillator strength of a molecular system which includes nuclei as well as electrons has been enunciated. A rapid method of obtaining the potential energy of a diatomic molecule has been devised. An expression for the mean free path of a swift charged particle for plasmon excitation, valid for relativistic energies of the particle, has been given. A theoretical treatment of the difference in stopping power of a charged particle and its antiparticle has been made using a semiclassical approach. Working in the RPA, a formula for the mean free path for double-plasmon excitation by a fast charged particle has been derived. Festenberg's experimental results showing anomalously large damping of volume plasmons in polycrystalline aluminum have been explained in terms of elastic scatter of the plasmon on the grain structure. A theory has been advanced to account for the decrease in optical reflectance of a metal in the neighborhood of the surface plasmon energy. A revised formulation of the macroscopic Maxwell theory has been made. The concept of energy as it enters kinetic plasma theory has been reexamined, and a revised version of the theory has been postulated.

9. Interaction of Radiation with Liquids and Solids

With a Seya-Namioka vacuum ultraviolet monochromator the optical properties of cesium have been measured just above the plasma energy and the data interpreted in terms of a plasmon-assisted interband transition. The recently installed soft-x-ray monochromator has been used to extend measurements of the optical properties of MgF_2 and MgO, previously made with a Seya-Namioka monochromator, up to 66 eV. Further refinements have been made to the ultrahigh vacuum-ellipsometer, and optical constants were obtained for palladium from 3000 to 20,000 Å.

Investigations have been continued of the optical emission spectra from metal films bombarded with high-energy electrons. The radiative decay of volume plasmons in magnesium and beryllium has been used to calculate basic parameters associated with these materials. In addition, the radiative decay of "nonradiative" surface plasmons in aluminum has been confirmed. Experimental confirmation of the theory of radiation damping of surface plasmons from aluminum-coated concave diffraction gratings has been obtained, and the results of diffusion pump oil contamination of diffraction gratings have also been investigated and compared with theory.

Abnormally high exoelectron emission currents from magnesium have been observed on exposure to O_2 or H_2O gas. The emission currents, which achieved maxi-

1147938

mum values in times comparable with times estimated to form monolayer coverages on the surface, are believed to be associated with a lowering of the work function of the magnesium and a formation of unstable chemical bonds on the metal surface.

10. Physics of Tissue Damage

The electron flux in an irradiated semiconductor (^{71}Ge) was measured and compared with that in metal irradiated similarly. When data were reduced to eliminate differences due to high-energy stopping powers, densities, and source strengths, identical spectra were found at the higher energies (~5 keV), but the flux in the semiconductor rose to about twice that in the metal at low energies (10 eV), possibly due to reduced semiconductor stopping power near the band gap energy.

An attempt was made to see if the electron flux in an irradiated medium is enhanced substantially by absorption of photons released in the medium by deexcitation, x-ray production, and bremsstrahlung. Thin and thick (compared with most photon attenuation lengths) sources of ^{185}W were examined with the Keplertron (electrostatic spectrometer), but no differences in electron spectra were found. The possibility remains, however, that extremely low-energy photons (less than 1 keV) may be important, and still thinner sources will have to be studied to check this.

The optical constants of the organic liquids CCl_4, C_6H_{14}, C_6H_{12}, C_6H_{10}, C_6H_8, and C_6H_6 have been measured in the energy range from 4.0 to 10.7 eV using the closed-cell semicylinder method. In the course of this work satisfactory techniques were developed for cleaning the semicylinder cell windows, enabling consistent data to be obtained. The data have been interpreted in terms of $\pi \rightarrow \pi^*$, $n \rightarrow \sigma^*$, and $\sigma \rightarrow \sigma^*$ molecular electronic excitations.

11. Electron and Ion Collision Physics

The cross-section behavior for the production of slow electrons (0 to 0.5 eV) upon electron impact ionization of the rare gases, water vapor, and benzene has been studied for the first time using the SF_6 scavenger technique and the trapped-electron method. For the rare gases the cross section for the production of slow electrons abruptly rises at the ionization potential and remains relatively constant up to an energy in excess of 100 eV. The cross sections for water vapor and benzene are found to steadily increase beginning at their ionization potentials in contrast to the flatness exhibited by the rare gases. Absolute cross-section measurements of these inelastic scattering processes will be helpful in interpreting electron-slowing-down spectra in gases.

Negative-ion formation in a large number of organic and inorganic molecules has been studied in considerable depth with both electron swarm and electron beam techniques. The major part of our effort has been devoted to the study of (1) negative-ion lifetimes, (2) temporary negative-ion resonances, (3) dissociative attachment cross sections, (4) thermal energy electron attachment rates, (5) negative-ion mobilities, and (6) mass analysis of negative ions formed in electron swarm experiments. Input data from all these experiments provide a quite detailed description of electron attachment mechanisms.

An apparatus has been constructed to mass identify the positive- and negative-ion products resulting from collisions of fast neutral cesium atoms with molecules. Measurements of the threshold for ion pair production in collisions of cesium atoms with electronegative molecules afford a determination of the lower limit to the electron affinity of molecules. Using this technique we have shown that the electron affinity of nitrogen dioxide is greater than or equal to 2.2 ± 0.2 eV. Mass analysis of ions formed in collisions of high-energy cesium atoms (~30 eV) with Br_2 shows that both Br_2^- and Br^- are produced. Mass analysis of ions formed in collisions of cesium with molecules is providing a wealth of new information about the formation of negative ions due to the complex adiabatic nature of the collision.

Reaction products and rates of reaction of low-energy (0–2 eV) O^- ions with acetylene, ethylene, ethane, and benzene (and their deuterated analogs) have been investigated. The absolute magnitudes of the ion-molecule reaction cross sections, their dependence on O^- energy, and branching ratios and isotope effects have been compared with existing theory.

12. Atomic and Molecular Radiation Physics

The scattering of thermal electrons by highly polar molecules has continued. The dependence of the drift velocity of thermal electrons traveling through polar gases has been investigated, and the data have been used to determine the magnitude and the velocity dependence of the momentum transfer cross section. The data have been discussed within the Born approximation and with relevance to a number of factors which can distinctly affect the scattering. Measurements have been made also of electron diffusion coefficients and mobilities in hydrocarbon vapors. These yielded stopping

1147939

powers of electrons less than ~2 eV which were remarkably insensitive to structural variations.

An accurate and exhaustive experimental test has been made of electron swarm energy distribution functions $f(\epsilon, E/P)$ for the carrier gases C_2H_4, N_2, and Ar used in electron attachment studies. A standard set of $f(\epsilon, E/P)$ has been established and recommended. A method has been developed whereby both the magnitude and the energy dependence of thermal-peaking electron attachment resonances is obtained from electron swarm data alone. The method has been applied successfully to many molecules (e.g., CCl_4, SF_6, anthracene, 1,2-benzanthracene). Lifetimes and cross sections for long-lived polyatomic negative ions have been measured and have been related to electronic and geometrical structure. Estimates of electron affinities were obtained for some molecules.

Electron capture by an organic molecule with simultaneous excitation of one of the orbiting electrons resulting in a long-lived parent negative ion has been observed for the first time. Also, the first energy dependence of the autoionization lifetime of long-lived negative ions has been found for both nuclear- and electron-excited Feshbach resonances, and it clearly showed the effect of increase in internal energy of the ion on the autodetachment rate. A systematic study has been made of electron attachment to molecules of the form $C_nH_{2n+1}Br$ (n = 1 to 10) which allowed a deeper understanding of the energetics and quantitative aspects of dissociative electron attachment to polyatomic molecules. A new high-resolution experimental arrangement has been constructed and built which enables threshold-electron and compound negative-ion excitation studies.

New information of great significance has also been obtained on the emission and decay of organic liquids under electron impact, photophysical studies of liquids, transport of resonance radiation in gases, and sensitized ionization of molecules.

13. Graduate Education and Training

The Health Physics Training Program included fellowship students from Vanderbilt University, The University of Tennessee, the University of Kansas, the University of California, and Georgia Institute of Technology. These reported to ORNL for summer on-the-job instruction in applied and research health physics.

Division personnel visited 17 colleges and universities to give seminars on various research problems of current interest and also to help recruit qualified students in the fellowship program.

The Health Physics Division provided research facilities and advisors for 20 Oak Ridge Graduate Fellows, AEC Fellows, and USPHS Fellows who were conducting thesis research. A total of 41 university personnel ranging from undergraduates to professors spent the summer in the Division.

Teaching assistance was given to The University of Tennessee for its program in Radiation Physics and to Vanderbilt University for its course in Radiation Physics. Lectures and tours were given for several university groups visiting ORNL.

Assistance and consultation were given to eight schools that were interested in establishing health physics courses or programs in their science departments.

The Division cooperated with ORAU in the presentation of a ten-week course in Applied Health Physics and in the screening of applicants for AEC Fellowships.

PART III. RADIATION DOSIMETRY RESEARCH

14. Dosimetry for Human Exposures and Radiobiology

Calculations of depth-dose distributions for neutrons were extended into areas of practical application, especially for the use of ^{252}Cf in cancer therapy. Dose and LET distributions for line, point, and disk-shaped sources of neutrons having the energy spectrum of ^{252}Cf were calculated. The calculations of dose and LET distributions due to neutrons were also made for two small cylinders chosen to approximate the size of rats and rabbits respectively. Preliminary calculations were also made for the dose distributions in human fetuses exposed to radiation from the nuclear bombs exploded over Hiroshima and Nagasaki. Close liaison has been maintained with the Atomic Bomb Casualty Commission (ABCC) in Japan. Emphasis this year has been given to computation of the radiation doses received by those persons exposed near the bombs who survived because of the radiation and blast protection afforded by seismic reinforced buildings.

15. Spectrometry Research and Development

Experimental measurements of dose distributions in man-sized tissue-equivalent media were made to test the recently calculated values. A special extrapolation chamber was developed and used for measuring the dose distribution near bone-tissue and tissue-bone interfaces in phantoms irradiated by the Health Physics Research Reactor (HPRR). Other experiments were directed to the measurement of LET in neutron-

1147940

irradiated tissue phantoms utilizing recently developed counters. Measurement of the HPRR spectrum in the energy range below 0.5 MeV was accomplished. A variety of electronic instruments related to spectrometry research were developed or improved, and zone-refining techniques were used for the purification of detector materials.

16. Applied Dosimetry Research

The emphasis on thermally stimulated exoelectron emission (TSEE) has continued, with minor advances made in the sensitivity and stability of detectors, especially sintered BeO. Initial studies of neutron response characteristics have been completed, and the response per unit dose as a function of photon energy has been measured for several detector types. TSEE techniques were also applied to samples of lunar material with the objective of learning more about the thermal and radiation history of the moon.

Registration of charged-particle tracks in insulating solids has proved to be of increasing practical value, with application in autoradiography with alpha particles and radon monitoring. More basic studies of track registration were made, with emphasis on alpha-particle registration in cellulose nitrate.

17. HPRR and Accelerator Operations

Results from a new target assembly promise greater neutron yields and longer life for tritium targets for accelerators, especially those used for the $T(d,n)^4He$ reaction. The DOSAR Low Energy Accelerator (DLEA) and the 3-MV Van de Graaff are used extensively in these studies and in most other dosimetry research.

The HPRR was operated routinely and without fault. The annual disassembly and inspection revealed no detectable change in the core materials. In July 1970, the seventh intercomparison study in dosimetry was held, using the HPRR as the radiation source, and participants included dosimetrists from four foreign countries.

18. Interaction of Charged Particles with Matter

Transfer of equipment from the University of Kentucky to the 3-MV Van de Graaff was completed, and installation and testing were initiated. Initial studies include the intensities, lifetimes, and wavelengths of the electromagnetic radiations emitted from noble gases irradiated by fast protons as well as the W values of pure gases and gas mixtures.

PART IV. INTERNAL DOSIMETRY

19. Internal Dose Estimation

Estimates of dose to red bone marrow are difficult to obtain because of the complex distribution of red bone marrow within the body. Yet it is a tissue of particular importance, because the dose limits recommended for purposes of radiation protection are lower (5 rems/year for occupational exposure) than for most tissues. The anthropomorphic phantom and Monte Carlo computer program reported here previously for estimation of dose due to photons have been adapted to take account of the distribution of red marrow. Only doses from a monoenergetic photon emitter present in lungs are reported here. As might be expected, the dose is highest for the red marrow in the rib cage and certain portions of the spine. The pelvic region contains a considerable fraction of the total red marrow, and the dose to this portion is much less, often by an order of magnitude.

The Monte Carlo computer program mentioned above has been used to estimate doses in many body organs. However, in some cases the estimates are statistically unreliable, particularly for small organs such as gonads or thyroid when they are far from the source organ. A buildup factor for dose in an infinite medium of water has been reported, and despite the finiteness and heterogeneity of the body, the use of this buildup factor seems to be accurate within a factor of 2 in all cases tested against the Monte Carlo code. This result is being tested further, and if the limit of error is this small, the method may be useful in estimating dose to small organs.

Since many radionuclides are excreted in urine, the bladder wall is irradiated by radiation originating in the urine, which constitutes a pool of variable size. The dose per photon varies markedly as the bladder contents increase, partly because wall thickness is changing and also because of the inverse-square relation of dose and distance. The basic data on dose per photon are estimated for a range of bladder sizes ranging from 0 to 500 ml content.

A compartmental model for metabolism of iodine has been given by Berman, but because of its complexity, it has not been directly compared with more conventional models. This is done here, and for ^{131}I the comparison is rather close. For some compartments and isotopes of iodine, differences by a factor of 2 may occur.

The thorny question of what happens to a radium atom when produced in bone by decay of a thorium parent continues to demand attention, because the estimate of dose to bone will vary greatly depending on

1147941

the model assumed. Last year's report contained calculations corresponding to some hypotheses, and these are supplemented here by further cases ranging from immediate transfer of the radium atom to blood to the assumption that it remains fixed in situ until its decay.

Although immersion in an infinite cloud of radioactive emitter has been a standard case considered in the past, no good estimates of the energy spectrum produced in such a case have been available. Due to this fact, no reliable estimates of dose at various depths within the body have been produced. The energy spectrum resulting from a monoenergetic photon source distributed uniformly in an infinite space of air is given here. It is expected that a correction for ground effect will be forthcoming in next year's report.

20. Stable Element Metabolism

The elemental balance for intake and excretion of certain elements commonly present in diets is reported here for two adult subjects who ate ad libitum. The study is almost unique in that these individuals were studied over a period of several years, and many minor fluctuations appear to "cancel out" over such a period of study.

The gross compositions of bone and cartilage are reported here. The data on cartilage are essentially new and help fill one sizable gap in our knowledge of the composition of the body.

1147942

Part IV. Internal Dosimetry

W. S. Snyder

19. Internal Dose Estimation

ESTIMATES OF DOSE TO RED BONE MARROW FROM MONOENERGETIC SOURCES OF PHOTONS IN LUNGS AND OTHER ORGANS

M. J. Cook W. S. Snyder
G. G. Warner[1]

The International Commission on Radiological Protection (ICRP) has recommended lower dose limits for blood-forming organs than for the majority of other body organs – for radiation workers, 5 rems/year and for members of the public, 0.5 rem/year.[2] In view of the special category into which the ICRP has put the red bone marrow, it is important to have an accurate estimate of the dose to this tissue. Because of the complexity of the skeletal system and the red marrow, this is not an easy problem.

Two types of bone marrow may be distinguished in the adult, namely, red and yellow; however, the demarcation between the two is not sharply defined. Red bone marrow is hematopoietically active, while yellow marrow does not have any hematopoietic activity, being composed mostly of fat.

In the newborn, all of the bone marrow is red. An almost identical amount of red bone marrow is found in a child weighing 15 kg as in an adult weighing 70 kg. Although between the ages of 6 and 20 years there is a gradual replacement of red marrow by yellow marrow, the absolute quantity of red marrow remains essentially unchanged.[3] In this study only the adult is considered, although we plan to make similar studies for individuals of other ages.

Red bone marrow in the adult is located principally in the cavities of the ribs, sternum, skull, clavicles, vertebrae, and the proximal epiphyses of the femur and humerus. Because red bone marrow is scattered throughout the body, its weight has been difficult to obtain. For a 70-kg adult, ~1500 g has been assigned as the weight for the red bone marrow.[4]

A mathematical phantom has been designed which has the approximate form of the human body with 22 internal organs which are mathematical constructs of those in the living body.[5] The exterior form and some of the principal internal organs are shown in Fig. 19.1. For this study the phantom has been changed slightly to include scapulae and clavicles. These "bones" are specified by the following loci.

Clavicles – The clavicles are represented as two portions of a torus. The torus lies along the circular arc $x^2 + (y - 11.1)^2 = 20^2$, $z = 68.25$, and the smaller radius of the torus is 0.7883 cm. The clavicles include only the portion of the torus between the planes $11.1 - y = |x| \tan\theta$ with $8° 5.5' \leqslant \theta \leqslant 48° 12'$. The absolute value sign on x allows for both the right and left

[1] Mathematics Division.

[2] *Recommendations of the International Commission on Radiological Protection* (adopted Sept. 17, 1965), ICRP Publication 9, Pergamon, New York, 1966.

[3] Howard R. Bierman, "Homeostasis of the Blood Cell Elements," chap. 8, pp. 349–418 in *Functions of the Blood*, ed. by Robert G. MacFarlane and A. H. T. Robb-Smith, Academic, New York and London, 1961.

[4] William Bloom and Don W. Fawcett, *A Textbook of Histology*, 9th ed., p. 184, W. B. Saunders, Philadelphia, 1968.

[5] H. L. Fisher, Jr., and W. S. Snyder, "Distribution of Dose in the Body from a Source of Gamma Rays Distributed Uniformly in an Organ," *Health Phys. Div. Ann. Progr. Rept. July 31, 1967*, ORNL-4168, pp. 245–47.

1147943

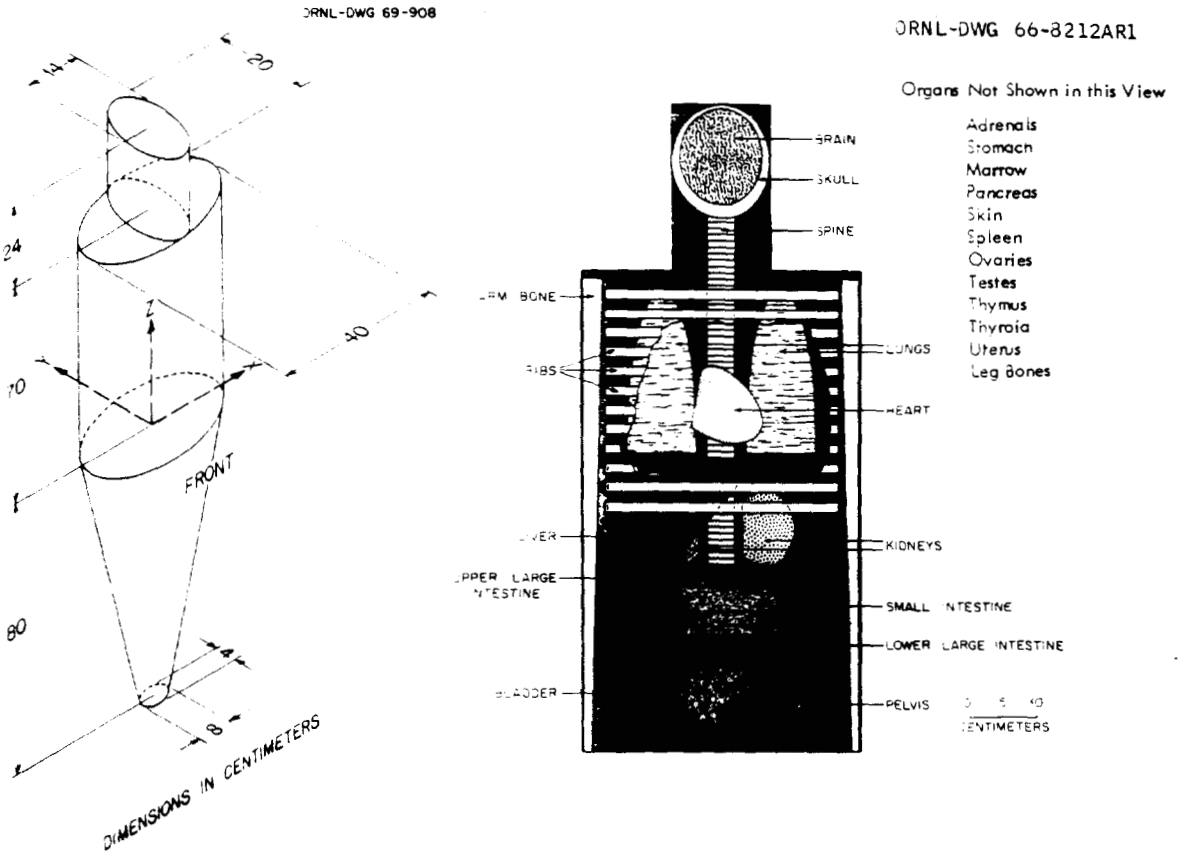

Fig. 19.1. The Adult Human Phantom, Showing an Anterior View of the Principal Organs in the Head and Trunk of the Phantom.

clavicles. The volume of both clavicles is 54.7 cm^3 and the mass is ~82 g.

Scapulae – The scapulae extend from the top of the 12th rib (z = 67.3 cm) to z = 50.9 cm. They lie between two elliptical cylinders,

$$\frac{x^2}{17^2} + \frac{y^2}{9.8^2} = 1 \text{ (outer surface of the rib cage)}$$

and

$$\frac{x^2}{19^2} + \frac{y^2}{9.8^2} = 1 \text{ (a somewhat larger cylinder)}.$$

The tapering shape of the scapulae has been ignored, and they are specified further as the volume between the above cylinders bounded by the planes $y = 0.25x$, $y = 0.80x$, and $50.9 \leqslant z \leqslant 67.3$. The volume of both scapulae is 100.7 cm^3, and the mass is taken as 151 g.

A computer code has been designed to compute random histories of photons which originate in one organ (the source organ) and to estimate the fraction of the photon's initial energy absorbed in each of the 22 target organs. This is essentially an application of the well-known Monte Carlo technique. In a previous report[6] estimates of the absorbed energy have been published for these 22 target organs when a monoenergetic source of photons is distributed uniformly in 16 different source organs. However, "marrow" as reported there includes both red and yellow. For this report the phantom and the computer code have been modified so that absorbed fractions for the red bone marrow are obtained.

In Fig 19.2 the stippled areas represent the red bone marrow in the phantom skeleton and in the drawing of an actual skeleton. Of the total 1500 g of red bone marrow, 13.1% is in the skull, 28.4% in the vertebrae,

[6] W. S. Snyder *et al.*, "Estimates of Absorbed Fractions for Monoenergetic Photon Sources Uniformly Distributed in Various Organs of a Heterogeneous Phantom," MIRD Pamphlet No. 5, Suppl. No. 3, *J. Nucl. Med.*, 7–52 (August 1969).

1147944

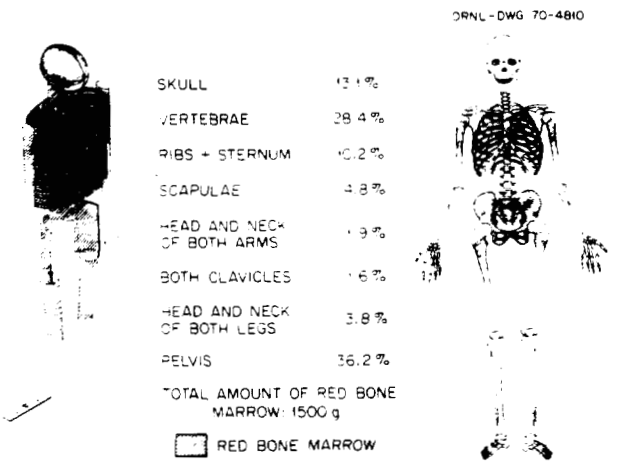

Fig. 19.2. Idealized Model for the Computer (Left) Showing Distribution of Red Bone Marrow in a Normal Adult (Right).

10.2% in the ribs and sternum, 4.8% in the scapulae, 1.6% in the clavicles, 36.2% in the pelvis, 1.9% in the proximal epiphyses of the humerus, and 3.8% in the proximal epiphyses of the femur. These data have been selected from Ellis,[7] although Hashimoto,[8] Russell *et al.*,[9] and others have given similar data. If the red marrow constitutes a fraction f of the total weight of a bone plus marrow, then the energy absorbed in the red marrow of that bone is taken as $f \times$ (energy absorbed in that bone plus marrow). Thus red marrow is assumed to absorb energy as efficiently per gram as do the other constituents of bone. One may use the code to compute the absorbed fraction with the source in any location, but for this study we are only reporting dose to the red bone marrow from a monoenergetic source of photons in the lung. We plan to obtain similar estimates with the source in other organs. The lung was chosen for these first calculations, because a considerable fraction of the red bone marrow is located close to these organs and inhalation is a frequent mode of exposure.

For this study 30,000 photons were programmed for each photon energy. The code provides estimates of average dose to the total red bone marrow, but since this dose would not be expected to be nearly constant, the code also provides separate estimates of dose for red bone marrow in ribs, three sections of the vertebral column, pelvis, arm bones, leg bones, clavicles, scapulae, and skull. A standard deviation and coefficient of variation are provided for each estimate.

As examples, in Fig. 19.3 are presented the dose to the total red bone marrow, three regions of the vertebral column (upper, mid, and lower), ribs and sternum, and pelvis. If [illegible] ficient of variation was greater than 60%, the e[illegible] was not included in this figure. The estimate plus or minus one standard deviation is shown unless the standard deviation was less than 10% of the estimate. The 12 different energies selected are 0.010, 0.015, 0.02, 0.03, 0.05, 0.1, 0.2, 0.5, 1.0, 1.5, 2.0, and 4.0 MeV. For 0.010 MeV the standard deviation of the estimate was always greater than 60%; therefore these data are not included in the figure.

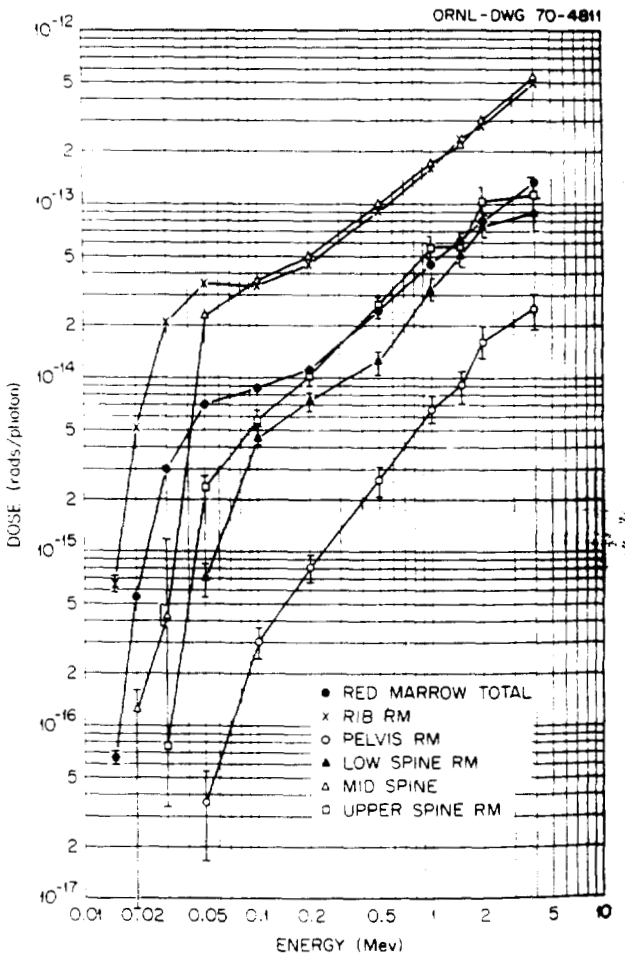

Fig. 19.3. Mean Dose per Photon to Red Bone Marrow and Portions of Red Bone Marrow from a Monoenergetic Source Uniformly Distributed in Lungs.

[7] R. E. Ellis, "The Distribution of Active Bone Marrow in the Adult," *Phys. Med. Biol.* 5, 255–58 (1961).

[8] Michio Hashimoto, "The Distribution of Active Marrow in the Bones of Normal Adult," *Kyushu J. Med. Sci.* 11, 103–11 (1960).

[9] Walter J. Russell *et al.*, "Active Bone Marrow Distribution in the Adult," *Brit. J. Radiol.* 39, 735–39 (1966).

1147945

With the source in the lungs, the ribs and sternum receive the highest dose. The midregion of the vertebral column receives almost the same dose as the ribs and sternum at the higher energies but less at energies below 0.1 MeV. Of the regions shown here, the red bone marrow of the pelvis receives the lowest dose, which is expected as it is farthest from the source in the lungs. The dose to the total red marrow falls about midway between these high and low values, as would be expected. In particular, the red bone marrow of the ribs and midvertebral column receives almost four times the average dose to the total red bone marrow. Of course, dose to the red bone marrow in the pelvis and leg bones is similarly low.

In this report the dose to various regions of the red bone marrow has been calculated when the source is distributed uniformly in the lungs of adults. Plans are under way to calculate the dose to these regions of red bone marrow when the source is in other organs such as the gastrointestinal tract, urinary bladder, etc., and to study the problem for various age groups.

ESTIMATION OF DOSE TO GONADS FROM GAMMA EMITTERS PRESENT IN THE BODY

W. S. Snyder Mary R. Ford
G. G. Warner[10]

The author and colleagues[11] have developed a Monte Carlo type computer code for estimating the specific absorbed fraction of photon energy $\Phi(X \rightarrow Y)$, that is, fraction of energy absorbed in Y per gram of that released in X, where X is an organ of the body containing a source of photons distributed uniformly therein and Y is a target organ. The code involves a mathematical anthropomorphic phantom whose organs approximate those of their prototypes in size, shape, composition, and density. Although results have been published[11] for 16 source organs X and some 20 target organs Y, the estimate is inaccurate sometimes because of poor statistics. This is likely to be the case when Y is a small organ and far from the source. In particular, the estimate of the specific absorbed fraction for the gonads frequently is found to have a large coefficient of variation. For this reason no estimates of the absorbed fraction for gonads were included in ref. 11 except when the gonads are a source organ. The present note is a first attempt to supply an approximate estimate of the specific absorbed fraction for the gonads.

Berger[12] has computed the buildup factor $B(\mu x)$ for photons emanating from a point source in an infinite medium of water, giving values for photon energies from 0.02 to 2 MeV and for $\mu X \leqslant 20$, μ being the mass attenuation coefficient for the photons. The specific absorbed fraction at distance x cm from a point source in the water is then given by

$$\Phi(X) = \frac{\mu_{ab} e^{-\mu x} B(\mu x)}{4\pi x^2}, \qquad (1)$$

where x represents the distance of the infinitesimal target volume from the point source and μ_{ab} is the mass absorption coefficient for the photons. If $\Phi(X)$ is used to estimate the fraction of energy absorbed per gram in the gonads at distance x from a point source in the body, one might expect the result to be an overestimate since $B(\mu x)$ was computed for an infinite medium so that buildup would be maximized. On the other hand, it is not easy to foresee what effect the differences in composition and density of the body might have in comparing buildup in the body with that in a homogeneous medium. Moreover, even if one suspects Eq. (1) will provide an overestimate of the specific absorbed fraction for distances in the body, it is desirable to know approximately the extent of the overestimate.

In an attempt to answer some of the questions raised, $\Phi(X)$ has been computed by the Monte Carlo methods of ref. 11 for certain subregions of the body much larger than the gonads, so that the statistical accuracy, while not always good, is nevertheless much better than for the gonads. These regions are "slices" shown in Fig. 19.4 and are numbered 1 to 5. The source has been placed in the thyroid, so that the distance from source to target is as large as can be attained in the trunk. Distance has been taken from a central point of the thyroid to the center of each slice. Clearly distance from the source to a point of the slice varies significantly at different portions of the slice, and thus a high degree of accuracy cannot be expected from the comparison. Figures 19.5–19.10 show the results for $\Phi(X)$ for photons of energies 2, 1, 0.5, 0.2, 0.1, 0.05 MeV as computed by the Monte Carlo calculation of ref. 11. For comparison, formula (1) with $B(\mu x)$ as

[10] Mathematics Division.

[11] W. S. Snyder *et al.*, "Estimates of Absorbed Fractions for Monoenergetic Photon Sources Uniformly Distributed in Various Organs of a Heterogeneous Phantom," MIRD Pamphlet No. 5, Suppl. No. 3, *J. Nucl. Med.*, 5 (1969).

[12] Martin J. Berger, "Energy Deposition in Water by Photons from Point Isotropic Sources," MIRD Pamphlet No. 2, Suppl. No. 1, *J. Nucl. Med.*, 15 (1968).

1147946

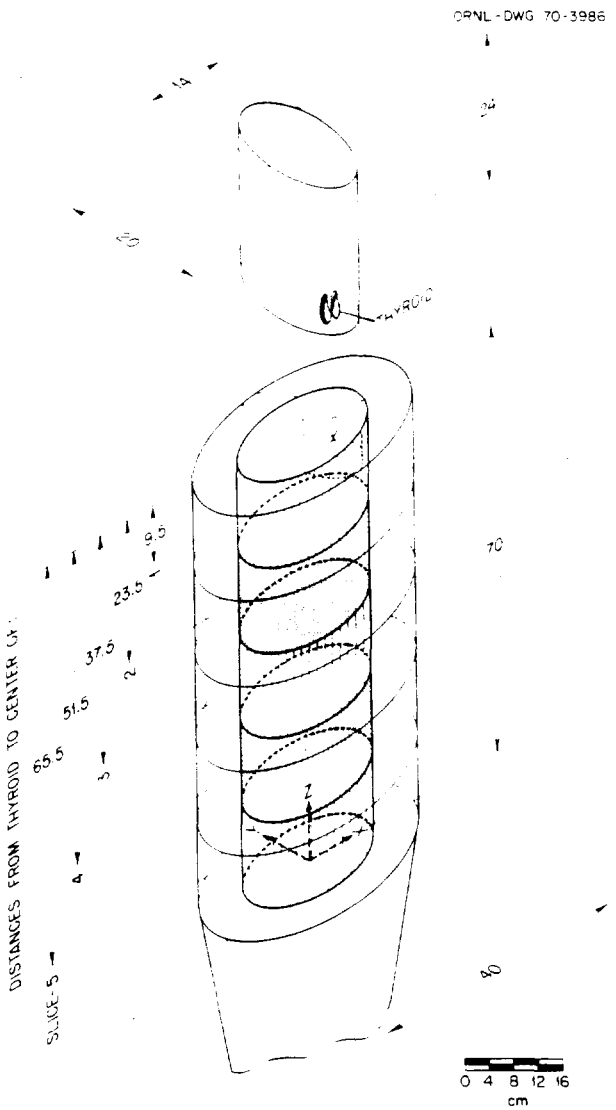

Fig. 19.4. The Human Phantom.

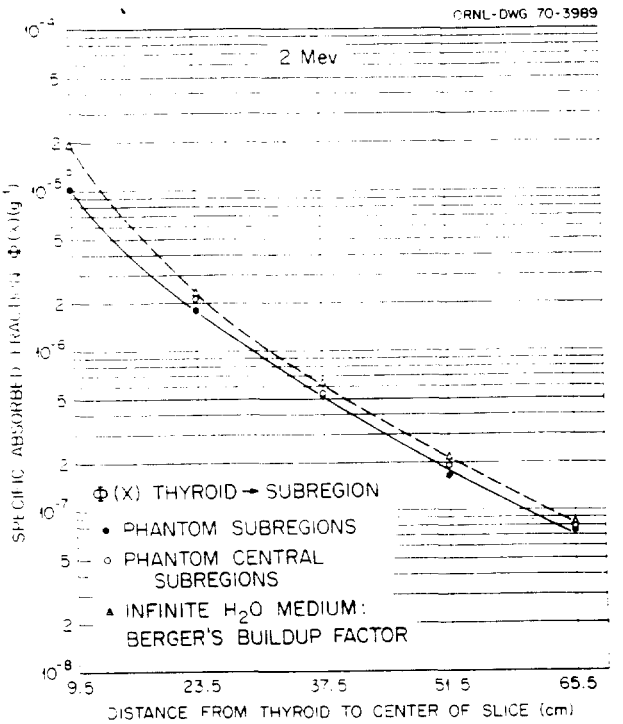

Fig. 19.5. Estimates of Specific Absorbed Fraction Φ for an Infinite Medium of Water and for Subregions of an Anthropomorphic Phantom. 2 MeV.

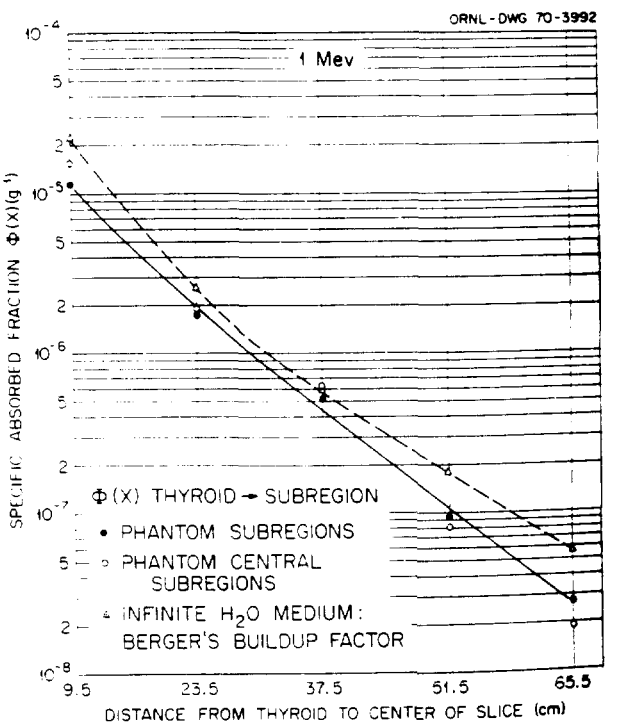

Fig. 19.6. Estimates of Specific Absorbed Fraction Φ for an Infinite Medium of Water and for Subregions of an Anthropomorphic Phantom. 1 MeV.

tabulated by Berger is shown also. It is seen that generally formula (1) is higher, as expected, and the cases when this does not hold might plausibly be due to either poor statistics or to the rather inaccurate characterization of the distance x. To test the influence of this distance factor, the value of $\Phi(X)$ has been computed also for the central portion of the slice (see Fig. 19.4), and it is evident that this generally improves the agreement of the estimate provided by this Monte Carlo calculation and that provided by Berger.

On the basis of the evidence presented here, it seems likely that the use of the buildup factor as given by Berger[12] and of formula (1) given here will generally overestimate $\Phi(X)$ but not by more than about a factor

1147947

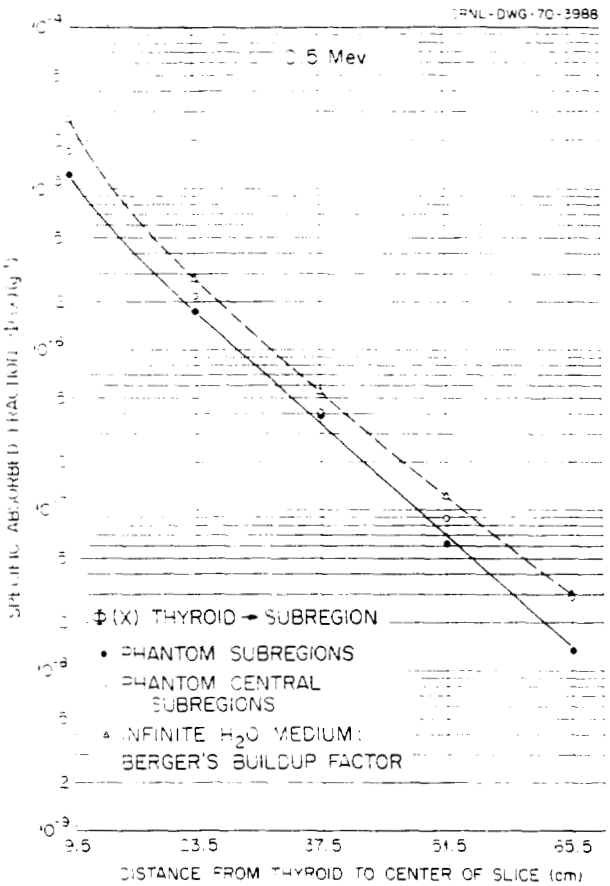

Fig. 19.7. Estimates of Specific Absorbed Fraction Φ for an Infinite Medium of Water and for Subregions of an Anthropomorphic Phantom. 0.5 MeV.

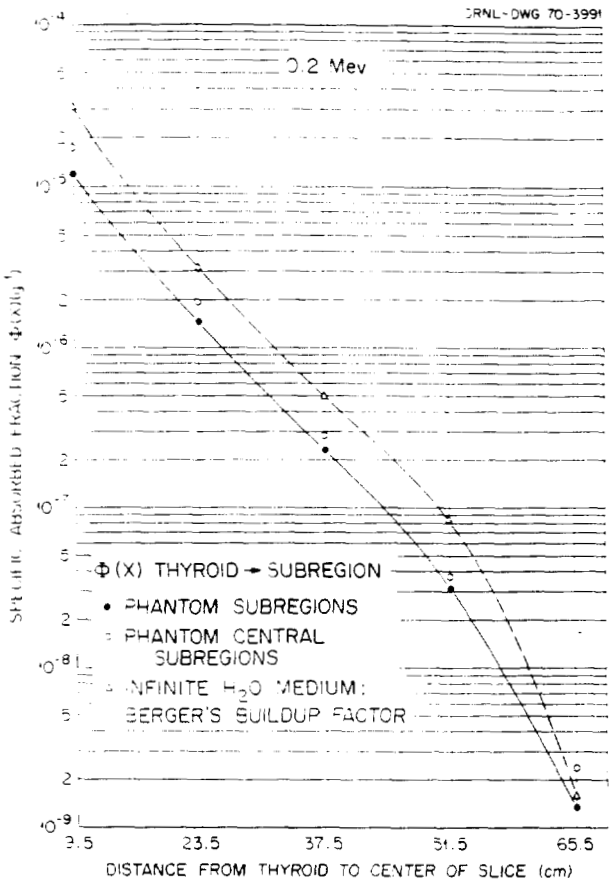

Fig. 19.8. Estimates of Specific Absorbed Fraction Φ for an Infinite Medium of Water and for Subregions of an Anthropomorphic Phantom. 0.2 MeV.

of 2. Such a margin of error is acceptable in view of the fact that alternative methods involve uncertainties of at least as much and are frequently much more difficult. It should be noted that the degree of accuracy obtained for formula (1) is roughly the same as can be attained by use of the reciprocity theorem (see ref. 13), namely, a factor of about 2.

It should be emphasized that the above comments apply only to the "point-source" formula. When the source is much more extended, for example, the lungs or stomach or liver, one should perform an integration over the source region and only then should one expect accuracy as indicated above. The use of a "representative point" for such large organs, say, a central point, will add an additional uncertainty. Moreover, when lungs are the source organ, the distance to the target organ probably should be taken in mass units. The influence of such corrections for the variable density of the body and the choice of "representative points" for source organs are matters which the author hopes to explore further in future studies.

Acknowledgment

The author owes much to his colleagues Gordon Warner, who has coded all these calculations for the computer; Mary Rose Ford, who has assisted in designing the code as well as in evaluating and analyzing the data; and James Hickey, who did the sometimes tedious tabulations necessary for this paper and for preparing the figures.

[13] W. S. Snyder, "Estimation of Absorbed Fraction of Energy from Photon Sources in Body Organs," *Proc. ORAU Symposium on Medical Radionuclides: Radiation Dose and Effects, December 8–11, 1969, Oak Ridge, Tennessee* (in press).

1147948

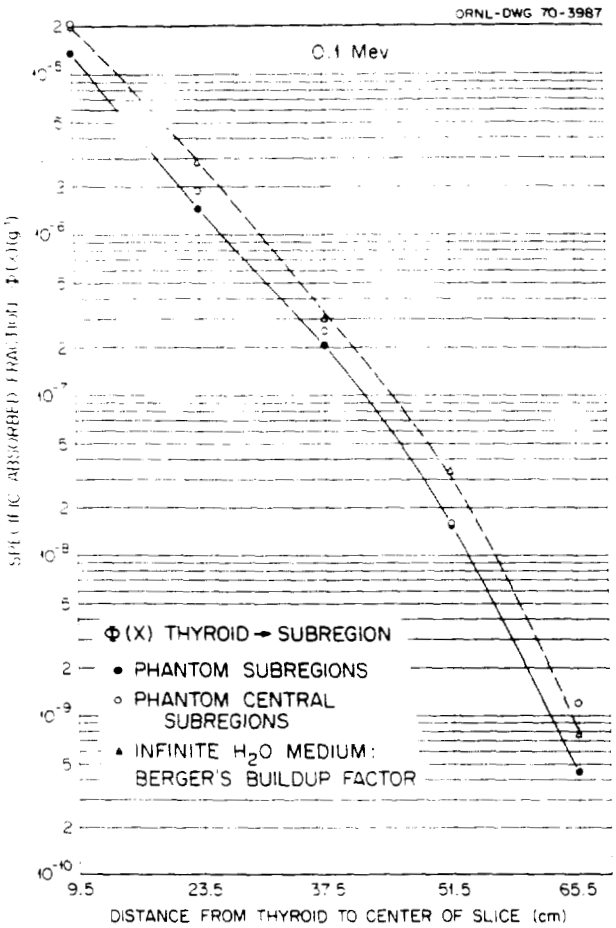

Fig. 19.9. Estimates of Specific Absorbed Fraction Φ for an Infinite Medium of Water and for Subregions of an Anthropomorphic Phantom. 0.1 MeV.

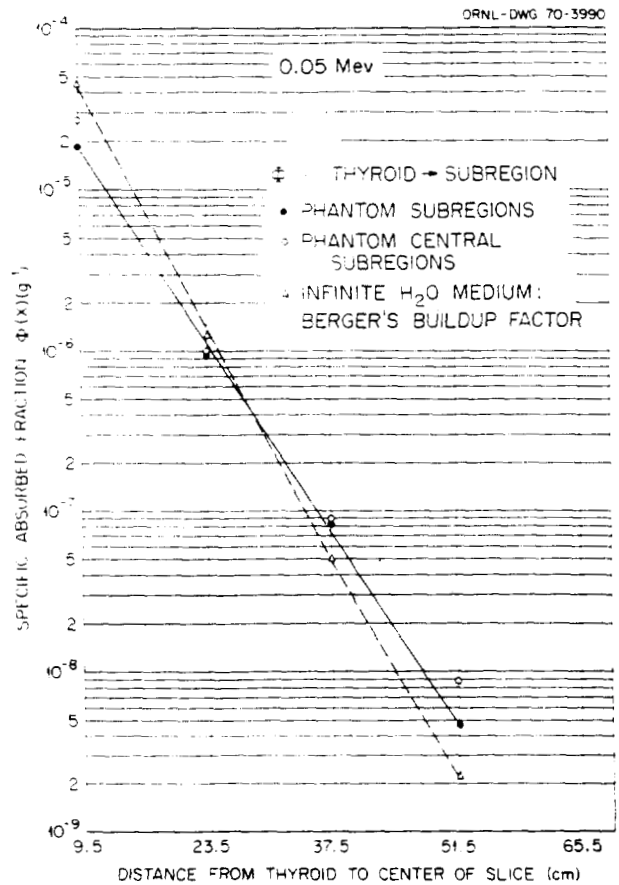

Fig. 19.10. Estimates of Specific Absorbed Fraction Φ for an Infinite Medium of Water and for Subregions of an Anthropomorphic Phantom. 0.05 MeV.

ESTIMATION OF DOSE AND DOSE COMMITMENT TO BLADDER WALL FROM A RADIONUCLIDE PRESENT IN URINE[14]

W. S. Snyder Mary R. Ford
G. G. Warner[10]

Estimation of dose to the bladder wall from a p[illegible]on emitter present in urine is more complicated than [illegible] the case of most organs, because the dose per photon varies by almost an order of magnitude as the bladder fills, being largest for a nearly empty bladder.[15] This large variability implies that a dose estimate will depend significantly on the schedule of bladder voiding. Moreover, if some compartment is present which has an elimination half-time that is short compared with the time for a bladder filling, then the dose estimate will be influenced by whether this activity enters the bladder when it is nearly empty or nearly full. It is the purpose of this study to provide a basis for estimating the extent of the variability of dose to the bladder wall. The present study is concerned only with the dosimetric aspects of the problem. In a later study we hope to take into account certain patterns of urinary excretion which may be regarded as "typical" to provide bounds [illegible] variability of dose to the bladder wall as a consequence of other patterns.

The bladder is considered to be an oblate spheroid,

$$\left(\frac{x-x_0}{a}\right)^2 + \left(\frac{y-y_0}{b}\right)^2 + \left(\frac{z-z_0}{c}\right)^2 = 1 ,$$

[14] Presented at Health Physics Society Meeting, June 28–July 2, 1970, Chicago, Ill.

[15] W. S. Snyder, "Estimation of Absorbed Fraction of Energy from Photon Sources in Body Organs," *Medical Radionuclides: Radiation Dose and Effects*, p. 33, USAEC-DTI, Oak Ridge, June 1970.

1147949

where $(x_0, y_0, z_0) = (0, -4.5, 8)$ are the coordinates of the center in a Cartesian system of coordinates as chosen in MIRD Pamphlet 5,[16] that is, positive x axis to the left, positive y axis pointing toward the back, and positive z axis directed upward along the center line of the trunk with the origin at the base of the trunk. The semiaxes of the ellipsoid have the ratio $a:b:c = 4:3:3$, and this ratio is assumed to remain fixed as the bladder fills. The above equation may be considered to represent the inner wall of the bladder, and the exterior surface is represented by

$$\left(\frac{x - x_0}{\rho a}\right)^2 + \left(\frac{y - y_0}{\rho b}\right)^2 + \left(\frac{z - z_0}{\rho c}\right)^2 = 1 , \quad (2)$$

where ρ is chosen so that

$$\frac{4}{3}\pi abc(\rho^3 - 1) = 45 \text{ g} \quad (3)$$

is the mass of the bladder wall. For different volumes of urine present in the bladder, the mass remains unchanged, and the value of 45 g has been chosen as typical.[17] In Fig. 19.11, a schematic diagram of the bladder is shown for three different situations, namely, empty and for content of 100 and 400 ml.

Define now a function $D_r(V)$ to be the average dose rate to the bladder wall, rads/μCi-hr, when the bladder content (urine content) is V ml. No mathematical formula for $D_r(V)$ is available; rather, its values may be obtained by use of the Monte Carlo method described in MIRD Pamphlet 5,[16] the only change being that the bladder content here is V ml and dose is estimated to the wall rather than averaged over wall and contents.

If one considers $D_r(V)$ as known, then formulas for the dose under any conditions of filling are easily written. Thus if $f(t)\,dt$ ml of urine enter the bladder in time interval dt (hr) and if $s(t)\,dt$ μCi of activity enter the bladder in time dt (hr), then the total dose (rads) from time 0 (commencement of bladder filling) to time T is given by

$$D(T) = \int_0^T dt \int_0^t d\tau\, s(\tau)\, e^{-\lambda_r(t-\tau)} \times D_r\left[\int_0^t d\tau\, f(\tau)\right] . \quad (4)$$

Formula (4) includes the special case where activity begins entering the bladder when it is partly filled; one need only assign $s(t) \equiv 0$ during this period.

Consider now a more special situation where

$$f(t) = \alpha , \quad s(t) = ua\lambda e^{-(\lambda+\lambda_r)t} . \quad (5)$$

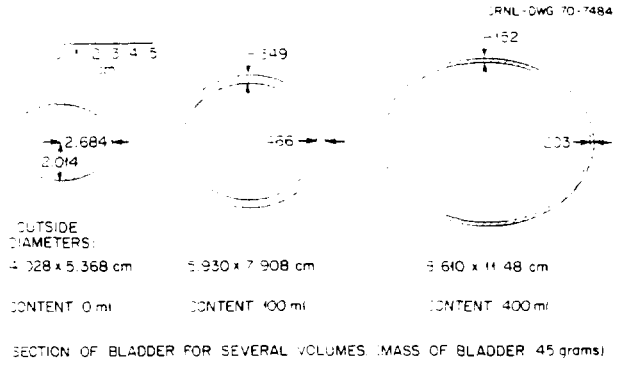

Fig. 19.11. Section of Bladder for Several Volumes.

Equations (5) represent the special, but unusual, case where bladder filling occurs at a constant rate, say, α ml/hr, and excretion is exponential in character [i.e., $a\lambda e^{-(\lambda+\lambda_r)t}$] with only a portion of the material excreted passing through the bladder. With this specialization, Eq. (4) becomes

$$D(T) = au \int_0^T dt\, e^{-\lambda_r t}(1 - e^{-\lambda t})\, D_r(\alpha t)$$

$$= \frac{au}{\alpha}\left[\int_0^{\alpha T} dx\, e^{-(\lambda r/\alpha)x}\, D_r(x) - \int_0^{\alpha T} dx\, e^{-(\lambda+\lambda_r)x/\alpha}\, D_r(x)\right] . \quad (6)$$

The latter integral of Eq. (6) is obtained by substituting $x = \alpha t$ as a new variable of integration.

The function $D_r(V)$ has been computed for $V = 0$, 50, 100, 200, 300, 400, 500 ml and for the same 12 monoenergetic sources of photons given in MIRD Pamphlet 5,[16] namely, 0.01, 0.015, 0.02, 0.03, 0.05, 0.1, 0.2, 0.5, 1, 1.5, 2, 4 MeV. The results are displayed in Fig. 19.12*a* for the four lowest energies and in Fig. 19.12*b* for the others. As will be noted the curves cross, and they are separated here to facilitate their use. This complex behavior seems to be due to the interplay of a number of factors, (1) amount of energy released, (2) changes in the mass absorption and mass attenuation coefficients with energy, and (3) thickness of the wall.

[16] W. S. Snyder, Mary R. Ford, G. G. Warner, and H. L. Fisher, Jr., "Estimates of Absorbed Fractions for Monoenergetic Photon Sources Uniformly Distributed in Various Organs of a Heterogeneous Phantom," MIRD Pamphlet No. 5, Suppl. No. 3, *J. Nucl. Med.* **10**, 7 (1969).

[17] M. M. Nold, R. L. Hayes, and C. L. Comar, *Health Phys.* **4**, 86 (1960).

1147950

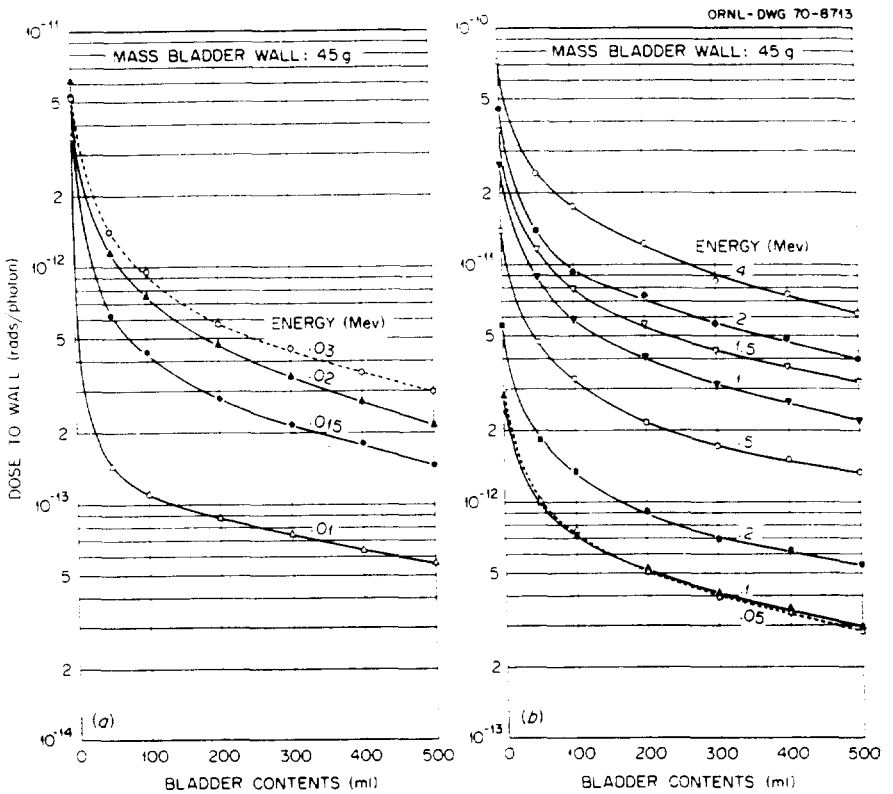

Fig. 19.12. Variation of Dose to Bladder Wall of a Photon Emitter in Urine as a Function of Photon Energy and Mass of Bladder Content. (*a*) Lower energies; (*b*) higher energies.

Where the mass absorption coefficient varies slowly (e.g., 0.1–4 MeV) the $D_r(V)$ decreases as photon energy decreases, but at still lower energies the increase in the mass absorption coefficient causes $D_r(V)$ to increase for small values of V; but for large V, attenuation predominates and $D_r(V)$ continues to decrease, although not regularly, as energy decreases. Also, the numerical values obtained by the Monte Carlo calculation are listed in Table 19.1 together with the coefficient of variation of each estimate, that is, coV = 100 (standard deviation)/estimate.

The data in Figs. 19.12*a*,*b* suggest a multiexponential form for $D_r(V)$. A two-exponential formula,

$$D_r(V) \approx ae^{-\lambda V} + be^{-\mu V} , \qquad (7)$$

has been found to fit the data with sufficient accuracy for practical purposes. The values of the parameters do change with photon energy sufficiently that no single formula applicable for the entire energy range is practical. The errors are not significantly less for a three-exponential form than for formula (7). The values of a, b, λ, and μ and the maximum percent deviation of the formula from the estimated value of $D_r(V)$ are given in Table 19.2. An average percent deviation and a maximum deviation are also given for each energy.

The development of formula (7) is due to P. Brindza, ORAU summer student from Marquette University on assignment to the Health Physics Division.

APPLICATION OF BERMAN'S TEN-COMPARTMENT MODEL FOR HUMAN IODINE METABOLISM TO ESTIMATION OF MICROCURIE-DAYS RESIDENCE OF ^{123}I, ^{124}I, ^{125}I, ^{126}I, AND ^{131}I

S. R. Bernard

A computer code for solving systems of linear differential equations (written by J. A. Carpenter, ORNL Mathematics Division) was employed to obtain the equations for retention and the residence times in the ten compartments of the model for iodine kinetics proposed by Berman.[18]

[18] M. Berman, *J. Clin. Endocrinol. Metab.* 28, 1 (1968).

1147951

Table 19.1. Dose to Bladder Wall from a Source in the Contents

Energy (MeV)	Dose (rads/μCi-hr) for Volume of Contents of													
	0 ml		50 ml		100 ml		200 ml		300 ml		400 ml		500 ml	
	Dose	Coefficient of Variation (%)	Dose	Coefficient of Variation (%)	Dose	Coefficient of Variation (%)	Dose	Coefficient of Variation (%)	Dose	Coefficient of Variation (%)	Dose	Coefficient of Variation (%)	Dose	Coefficient of Variation (%)
0.01	4.72×10^{-4}	0.027	1.90×10^{-5}	2.8	1.45×10^{-5}	3.2	1.18×10^{-5}	3.6	9.78×10^{-6}	3.9	8.43×10^{-6}	4.2	7.55×10^{-6}	4.5
0.015	7.04×10^{-4}	0.053	8.29×10^{-5}	1.5	5.83×10^{-5}	1.8	3.69×10^{-5}	2.3	2.99×10^{-5}	2.6	2.39×10^{-5}	2.9	1.92×10^{-5}	3.2
0.02	8.30×10^{-4}	0.20	1.51×10^{-4}	1.1	1.00×10^{-4}	1.4	6.25×10^{-5}	1.9	4.57×10^{-5}	2.2	3.60×10^{-5}	2.4	3.02×10^{-5}	2.7
0.03	6.93×10^{-4}	0.46	1.87×10^{-4}	1.0	1.27×10^{-4}	1.3	7.66×10^{-5}	1.6	6.01×10^{-5}	1.8	4.74×10^{-5}	2.1	3.94×10^{-5}	2.2
0.05	3.99×10^{-4}	0.77	1.32×10^{-4}	1.3	1.01×10^{-4}	1.4	6.77×10^{-5}	1.7	5.19×10^{-5}	1.9	4.56×10^{-5}	1.9	3.73×10^{-5}	2.1
0.1	3.71×10^{-4}	0.99	1.31×10^{-4}	1.6	9.52×10^{-5}	1.8	6.86×10^{-5}	2.1	5.41×10^{-5}	2.3	4.75×10^{-5}	2.4	3.97×10^{-5}	2.6
0.2	7.37×10^{-4}	1.1	2.43×10^{-4}	1.9	1.77×10^{-4}	2.2	1.22×10^{-4}	2.6	9.22×10^{-5}	2.9	8.30×10^{-5}	3.1	7.18×10^{-5}	3.3
0.5	1.84×10^{-3}	1.4	6.25×10^{-4}	2.4	4.41×10^{-4}	2.8	3.05×10^{-4}	3.3	2.28×10^{-4}	3.8	2.00×10^{-4}	4.1	1.77×10^{-4}	4.2
1.0	3.51×10^{-3}	1.6	1.18×10^{-3}	2.7	7.81×10^{-4}	3.3	5.35×10^{-4}	3.9	4.11×10^{-4}	4.5	3.49×10^{-4}	4.9	3.11×10^{-4}	5.2
1.5	4.86×10^{-3}	1.7	1.55×10^{-3}	3.1	1.05×10^{-3}	3.7	7.45×10^{-4}	4.3	5.75×10^{-4}	5.0	4.92×10^{-4}	5.3	4.26×10^{-4}	5.7
2.0	6.02×10^{-3}	1.8	1.86×10^{-3}	3.3	1.24×10^{-3}	4.0	9.79×10^{-4}	4.6	7.48×10^{-4}	5.2	6.46×10^{-4}	5.6	5.31×10^{-4}	6.2
4.0	9.70×10^{-3}	2.1	3.20×10^{-3}	3.7	2.34×10^{-3}	4.4	1.62×10^{-3}	5.2	1.13×10^{-3}	6.1	1.00×10^{-3}	6.7	8.28×10^{-4}	7.3

1147952

This model proposed by Berman is shown in Fig. 19.13. In all, 12 compartments, ten of them "body" compartments and two excretion compartments, are implied. The two excretion compartments are numbered 0 and 6. Note that there are six compartments (2, 5, 12, 13, 10, and 11) representing the thyroid. The remaining compartments (1, 8, 9, and 4) are not given a clearly defined anatomical location. In this report we take these compartments (1, 4, 8, and 9) as total-body (TB) compartments, while compartments 2, 5, 10, 11, 12, and 13 are taken as thyroid (T) compartments. We have computed microcurie-days residence at 50 years for each of the compartments of Berman's model except those for excretion. The sum of

Table 19.2. Parameter Values for Dose to Bladder Wall: $D_r(V) = ae^{-\lambda V} + be^{-\mu V}$ (rads/photon)

E (MeV)	a	λ	b	μ	Deviation of Function and Data (%)	
					Average	Maximum
	$\times 10^{-12}$		$\times 10^{-12}$			
0.01	0.126	0.00168	3.474	0.0953	±2.51	+4.8
0.015	0.479	0.00252	4.811	0.0631	±4.28	+8.9
0.02	0.872	0.00292	5.301	0.0507	±4.44	+8.7
0.03	0.977	0.00248	4.162	0.0388	±3.83	+10.7
0.05	0.807	0.00218	2.172	0.0390	±3.65	+8.6
0.1	0.766	0.00195	2.022	0.0378	±2.30	−5.4
0.2	1.311	0.00187	4.124	0.0344	±4.04	+9.0
0.5	3.284	0.00192	10.471	0.0342	±3.66	−7.8
1.0	6.137	0.00213	19.916	0.0349	±2.56	−4.6
1.5	8.274	0.00199	28.293	0.0377	±3.03	−6.0
2.0	10.587	0.00198	34.723	0.0414	±2.04	−4.6
4.0	19.086	0.00235	53.210	0.0380	±5.08	−10.9

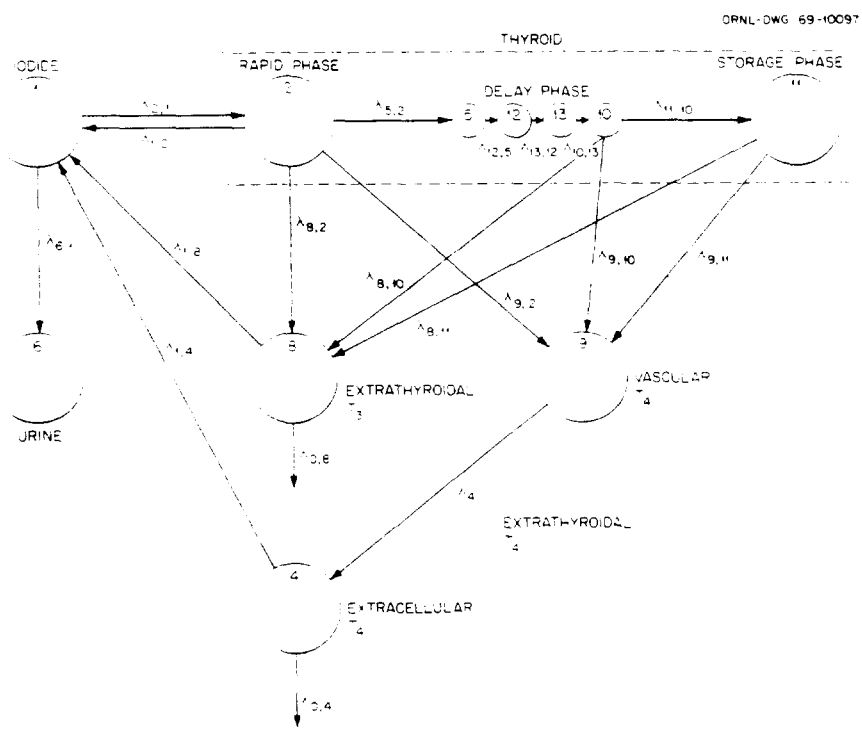

Fig. 19.13. Berman's Compartment Model for Iodine Metabolism.

1147953

the residence times for these compartments present in the thyroid (here designated by T) and the sum of the extrathyroidal compartments (here designated by TB) are given.

The equations for the amounts of iodine present in each compartment of the model, written in matrix notation, are

$$\dot{Y}(t) = -\Lambda\, Y(t)\,. \tag{1}$$

Here $Y(t)$ is a column vector of ten elements $y_j(t)$ (j = 1, ..., 10) corresponding to the amount of iodine in the jth compartment at time t; $\dot{Y}(t)$ is the derivative of the column vector $Y(t)$; $\Lambda = (\lambda_{jk})$ is a 10 by 10 matrix of transfer coefficients λ_{jk} (j, k = 1, ..., 10), and the values for a normal man have been specified by Berman. We do not list these here. They may be found in ref. 18. We do list the solution vectors we have obtained in our application of the computer code. It is unfortunate that these cannot be compared with those of Berman. In Table 19.3 are listed the eigenvalues corresponding to metabolism of stable iodine. Note these are generally complex numbers.

In order to explain the solutions which follow we have to discuss the solution of the differential equations (1). The computer is instructed to diagonalize the matrix Λ, that is, find P and D, where

$$\Lambda = P^{-1} D P \tag{2}$$

and where P is the matrix whose column vectors are left eigenvectors and D is a diagonal matrix whose diagonal elements are the eigenvalues and P^{-1} is just the inverse of P or the matrix of right eigenvectors. Now the solution can be shown to be

$$Y(t) = (P^{-1} e^{-Dt} P)\, Y(0)\,, \tag{3}$$

where

$$e^{-Dt} = \begin{pmatrix} e^{-d_1 t} & 0 \ldots 0 \\ 0 & e^{-d_2 t} \ldots 0 \\ \vdots & \\ 0 & 0 \ldots e^{-d_n t} \end{pmatrix} \tag{4}$$

and d_j is the eigenvalue. Here $Y(0)$ is the column vector of initial values. Now consider the special case where $Y(0)$ represents a vector with all elements equal to 0 except the first, that is, unit amount is present in compartment 1 at time $t = 0$. It is seen from Eq. (3) that the elements of the vector $Y(t)$, that is, the solutions for the amounts present in the various compartments, are linear combinations of the exponentials $e^{-d_j t}$ (j = 1, ..., n). If a vector E is defined to have its jth element equal to $e^{-d_j t}$ and if a diagonal matrix B is defined by $b_{jj} = p_{j1}$, then

$$Y(t) = P^{-1} BE = CE\,,$$

where $C = P^{-1} B$.

Let $R(C)$ and $I(C)$ be matrices formed of the real and imaginary parts of C and similarly let $R(E)$ and $I(E)$ be the vectors composed of the real and imaginary parts of E. Then the $R[Y(t)]$, the real part of $Y(t)$, is given by

$$R[Y(t)] = R(C)\, R(E) - I(C)\, I(E)\,. \tag{5}$$

Since $I[Y(0)] = 0$ and the differential equation is linear, this implies that $Y(t) = R[Y(t)]$. In Table 19.4 the elements of $R(C)$ and $I(C)$ are displayed. In our notation E is the vector with jth component $e^{-d_j t} = e^{-R(d_j)t}[\cos I(-d_j)t + i \sin I(-d_j)t]$. Explicit solutions

Table 19.3. Eigenvalues of the 10 × 10 Matrix of λ_{jk} for Stable Iodine

Compartment No. (This Paper)	Compartment No. (Berman's Paper)	$R(d_j)$	$I(d_j)$	$R(E_j)$	$I(E_j)$
1	1	+0.588	0.0	$e^{-0.588t}$	0
2	2	+0.134	0.0	$e^{-0.134t}$	0
3	4	+0.00720	0.0	$e^{-0.00720t}$	0
4	5	+1.71	0.0	$e^{-1.71t}$	0
5	8	+1.82	0.0	$e^{-1.82t}$	0
6	9	+2.43	0.0	$e^{-2.43t}$	0
7	10	+2.88	−0.585	$e^{-2.88t} \cos 0.585t$	$e^{-2.88t} \sin 0.585t$
8	11	+2.88	+0.585	$e^{-2.88t} \cos 0.585t$	$-e^{-2.88t} \sin 0.585t$
9	12	+3.47	−0.307	$e^{-3.47t} \cos 0.307t$	$-e^{-3.47t} \sin 0.307t$
10	13	+3.47	+0.307	$e^{-3.47t} \cos 0.307t$	$e^{-3.47t} \sin 0.307t$

1147954

Table 19.4. Real and Imaginary Parts of the Coefficient Matrix.

RL PT COEFFICIENT MATRIX

ROW	COLUMN 1	COLUMN 2	COLUMN 3	COLUMN 4	COLUMN 5
1	0.220290363062178 4D-02	-0.262873991049847 9D-03	0.941413749431955 7D-03	-0.177691695990473 0D 00	0.261430721599605 6D 00
2	0.215482754292203 8D-02	-0.179069901699730 0D-03	0.587354954545275 5D-03	0.184769986551398 1D 01	-0.124137579387542 5D 01
3	-0.154234291672819 7D-03	-0.751047572678371 4D-02	0.126830720973423 5D-01	-0.149020752876525 4D 01	0.219099931767977 9D 01
4	0.133989418529766 7D-02	-0.931899670004644 2D-04	0.294383793169503 2D-03	0.214212681977256 2D 01	-0.157891961093259 4D 01
5	0.932459006515074 0D-02	0.115910758845579 4D-04	0.271391008581050 5D-02	-0.398405788036520 1D 00	0.270180155552482 3D 00
6	0.350643275720492 4D-04	0.285230709021402 6D-05	0.797778496450412 7D-03	0.117217424376689 2D 01	-0.184876255862226 2D 01
7	0.253508305990339 4D-02	-0.105284354440119 1D-03	0.292602203879539 5D-03	0.259031848365923 5D 02	-0.251318917373685 4D 02
8	-0.131649512670684 0D-01	0.255457499901757 0D-02	0.313268392668067 1D 00	-0.458147439141441 2D 02	0.416413214052159 3D 02
9	0.166632028970631 5D-02	-0.975388863210768 6D-04	0.295091807807913 6D-03	0.496694313744754 4D 01	-0.401598196789934 D 01
10	0.207227058550902 8D-02	-0.102090757730065 9D-03	0.295801525273517 1D-03	0.115168224874784 9D 02	-0.102152966456613 7D 02

RL PT COEFFICIENT MATRIX

ROW	COLUMN 6	COLUMN 7	COLUMN 8	COLUMN 9	COLUMN 10
1	0.140096785787557 4D 00	0.196533630338678 1D 00	0.196533630308675 6D 00	0.190107742298476 8D 00	0.190107742298476 7D 00
2	-0.170568992728327 2D 00	-0.120616259649290 2D 00	-0.120616259649289 9D 00	-0.995433361037082 0D-01	-0.995433361037082 0D-01
3	-0.172932184534298 3D 01	0.259570998942139 6D 00	0.259570998942138 7D 00	0.252184848232646 9D 00	0.252184848232646 5D 00
4	-0.449931135752975 4D 00	-0.246807527372045 3D 00	-0.246807527372044 6D 00	0.189349946822815 0D 00	0.189349946822815 3D 00
5	0.466297710222495 1D 00	-0.176070511188010 1D-01	-0.176070511188009 0D-01	-0.201954033749997 8D 00	-0.201954033749997 4D 00
6	0.198729314576641 4D 01	-0.247399686613056 2D 00	-0.247399686613055 3D 00	-0.408370576408023 9D 00	-0.408370576408023 3D 00
7	-0.617236155916491 0D 02	-0.512384085891381 8D 01	-0.512384085891381 2D 01	0.355986409546211 7D 02	0.355986409546211 0D 02
8	0.764742280369268 6D 02	-0.389358765860916 7D 01	-0.389358765860915 0D 01	-0.324081441135902 1D 02	-0.324081441135901 5D 02
9	-0.237367910406077 7D 01	0.100702048308439 3D 01	0.100702048308439 0D 01	-0.296591982989840 2D 00	-0.296591982989840 7D 00
10	-0.125226996785307 7D 02	0.831752727217422 2D 01	0.831752727217419 7D 01	-0.270807334449391 6D 01	-0.270807334449389 9D 01

IM PT COEFFICIENT MATRIX

ROW	COLUMN 1	COLUMN 2	COLUMN 3	COLUMN 4	COLUMN 5
1	0.594478908643318 6D-15	-0.943426048266470 9D-16	0.156701953999787 9D-16	0.974307771928535 7D-16	0.0
2	0.581505022836285 6D-15	-0.639073432121775 5D-16	0.977675003411127 6D-17	-0.101311894743517 7D-14	0.0
3	-0.416218994396739 5D-16	-0.269542772460026 1D-14	0.211114632813995 0D-15	0.817121040573341 9D-15	0.0
4	0.361585873254227 3D-15	-0.334448615301235 3D-16	0.490013191791234 4D-17	-0.117455724783137 0D-14	0.0
5	0.251634799108870 7D-14	0.415991056142623 6D-17	0.451740942495169 3D-16	0.169651398556242 9D-15	0.0
6	0.946251252101301 5D-17	0.102366186773220 2D-17	0.132793311472479 6D-16	-0.642719068278023 0D-15	0.0
7	0.684121352301806 6D-15	-0.379212940205642 3D-16	0.487047667619414 4D-17	-0.142037682829600 0D-13	0.0
8	-0.355271367880050 1D-14	0.916809071410362 4D-15	0.521447336913014 8D-14	0.251298467328777 0D-13	0.0
9	0.449675715952779 8D-15	-0.350056411847020 D-16	0.491191709497888 9D-17	-0.272344078050554 3D-14	0.0
10	0.559226077329283 8D-15	-0.366392581303460 4D-16	0.492373061626163 5D-17	-0.631493328912857 6D-14	0.0

IM PT COEFFICIENT MATRIX

ROW	COLUMN 6	COLUMN 7	COLUMN 8	COLUMN 9	COLUMN 10
1	-0.187758758737209 8D-15	0.243961864473512 4D-01	-0.243961864479511 5D-01	0.915048473603162 0D-02	-0.915048473603122 0D-02
2	0.228597838085242 0D-15	-0.749454562133551 0D-01	0.749454562133549 0D-01	-0.211329514811206 3D-01	0.211329514811206 0D-01
3	0.231765005394989 8D-14	-0.371698666946786 8D 00	0.371698666946785 7D 00	-0.836363630333557 0D-01	0.836363630333562 0D-01
4	0.603001068806138 2D-15	0.257267164442534 8D 00	-0.257267164442534 1D 00	0.189657684693451 2D 00	-0.189657684693451 7D 00
5	-0.624935674157020 2D-15	0.283594436700161 1D 00	-0.283594436700160 3D 00	0.113222801947167 0D 00	-0.113222801947167 1D 00
6	-0.266338511764205 1D-14	0.585687380106463 9D 00	-0.585687380106462 2D 00	0.178268563962328 1D 00	-0.178268563962328 9D 00
7	0.827224506480434 0D-13	-0.441253331369811 4D 02	0.441253331369810 1D 02	-0.238107654929703 3D 02	0.238107654929703 0D 02
8	-0.102491331623933 5D-12	0.453907865685225 9D 02	-0.453907865685224 6D 02	0.177545342813947 6D 02	-0.177545342813947 8D 02
9	0.318122244490025 2D-14	0.147998821805634 8D 01	-0.147998821805634 7D 01	-0.139408784865444 8D 01	0.139408784865444 6D 01
10	0.167830136449530 6D-13	-0.2[illegible]6187260 01	0.340720646561871 8D 01	0.707982538047136 7D 01	-0.707982538047136 9D 01

1147955

for the retention function $Y_j(t)$ for the jth compartment are displayed below.

$$
\begin{aligned}
Y_1(t) = {} & 0.220 \times 10^{-2} e^{-0.588t} - 0.263 \times 10^{-2} e^{-0.134t} \\
& + 0.941 \times 10^{-3} e^{-0.00720t} - 0.178 \times 10^{0} e^{-1.71t} \\
& + 0.394 \times 10^{0} e^{-2.88t} \cos 0.585t \\
& + 0.380 \times 10^{0} e^{-3.47t} \cos 0.307t \\
& + 0.488 \times 10^{-1} e^{-2.88t} \sin 0.585t \\
& + 1.830 \times 10^{-2} e^{-3.47t} \sin 0.307t \,. \qquad (6a)
\end{aligned}
$$

$$
\begin{aligned}
Y_2(t) = {} & 0.215 \times 10^{-2} e^{-0.588t} - 0.178 \times 10^{-3} e^{-0.134t} \\
& + 0.587 \times 10^{-3} e^{-0.00720t} + 0.185 \times 10^{1} e^{-1.71t} \\
& - 0.124 \times 10^{1} e^{-0.82t} - 0.171 \times 10^{0} e^{-2.45t} \\
& - 0.242 \times 10^{0} e^{-2.88t} \cos 0.585t \\
& - 1.970 \times 10^{-1} e^{-3.47t} \cos 0.307t \\
& - 1.498 \times 10^{-1} e^{-2.88t} \sin 0.585t \\
& - 1.830 \times 10^{-2} e^{-3.47t} \sin 0.307t \,. \qquad (6b)
\end{aligned}
$$

$$
\begin{aligned}
Y_3(t) = {} & -0.154 \times 10^{-3} e^{-0.588t} - 0.751 \times 10^{-2} e^{-0.134t} \\
& + 0.127 \times 10^{-1} e^{-0.00720t} - 0.149 \times 10^{1} e^{-1.71t} \\
& + 0.219 \times 10^{1} e^{-1.82t} - 0.173 \times 10^{1} e^{-2.45t} \\
& + 0.520 \times 10^{0} e^{-2.88t} \cos 0.585t \\
& + 0.504 \times 10^{0} e^{-3.47t} \cos 0.307t \\
& - 0.744 \times 10^{0} e^{-2.88t} \sin 0.585t \\
& - 1.672 \times 10^{-1} e^{-3.47t} \sin 0.307t \qquad (6c)
\end{aligned}
$$

$$
\begin{aligned}
Y_4(t) = {} & 0.134 \times 10^{-2} e^{-0.588t} - 0.932 \times 10^{-4} e^{-0.134t} \\
& + 0.294 \times 10^{-3} e^{-0.00720t} + 0.214 \times 10^{1} e^{-1.71t} \\
& - 0.158 \times 10^{1} e^{-1.82t} - 0.450 \times 10^{0} e^{-2.45t} \\
& - 0.494 \times 10^{0} e^{-2.88t} \cos 0.585t \\
& + 0.504 \times 10^{0} e^{-3.47t} \cos 0.307t \\
& + 0.514 \times 10^{0} e^{-2.88t} \sin 0.585t \\
& + 0.380 \times 10^{0} e^{-3.47t} \sin 0.307t \,. \qquad (6d)
\end{aligned}
$$

$$
\begin{aligned}
Y_5(t) = {} & 0.932 \times 10^{-2} e^{-0.588t} + 0.116 \times 10^{-4} e^{-0.134t} \\
& + 0.271 \times 10^{-2} e^{-0.00720t} - 0.309 \times 10^{0} e^{-1.71t} \\
& + 0.270 \times 10^{0} e^{-1.82t} + 0.466 \times 10^{0} e^{-2.45t} \\
& - 0.352 \times 10^{-1} e^{-2.88t} \cos 0.585t \\
& - 0.404 \times 10^{0} e^{-3.47t} \cos 0.307t \\
& + 0.570 \times 10^{0} e^{-2.88t} \sin 0.585t \\
& + 0.226 \times 10^{0} e^{-3.47t} \sin 0.307t \,. \qquad (6e)
\end{aligned}
$$

$$
\begin{aligned}
Y_6(t) = {} & 0.351 \times 10^{-4} e^{-0.588t} + 0.285 \times 10^{-5} e^{-0.134t} \\
& + 0.798 \times 10^{-3} e^{-0.00720t} + 0.117 \times 10^{0} e^{-1.71t} \\
& - 0.185 \times 10^{1} e^{-1.82t} + 0.199 \times 10^{1} e^{-2.45t} \\
& - 0.494 \times 10^{0} e^{-2.88t} \cos 0.585t \\
& - 0.816 \times 10^{0} e^{-3.47t} \cos 0.307t \\
& + 1.172 \times 10^{0} e^{-2.88t} \sin 0.585t \\
& + 0.356 \times 10^{0} e^{-3.47t} \sin 0.307t \,. \qquad (6f)
\end{aligned}
$$

$$
\begin{aligned}
Y_7(t) = {} & 0.254 \times 10^{-2} e^{-0.588t} - 0.105 \times 10^{-3} e^{-0.134t} \\
& + 0.293 \times 10^{-3} e^{-0.00720t} + 0.259 \times 10^{2} e^{-1.71t} \\
& - 0.251 \times 10^{2} e^{-1.82t} + 0.199 \times 10^{1} e^{-2.45t} \\
& - 0.494 \times 10^{0} e^{-2.88t} \cos 0.585t \\
& - 0.816 \times 10^{0} e^{-3.47t} \cos 0.307t \\
& - 0.882 \times 10^{2} e^{-2.88t} \sin 0.585t \\
& - 0.476 \times 10^{2} e^{-3.47t} \sin 0.307t \,. \qquad (6g)
\end{aligned}
$$

$$
\begin{aligned}
Y_8(t) = {} & -0.132 \times 10^{-1} e^{-0.588t} + 0.255 \times 10^{-2} e^{-0.134t} \\
& + 0.313 \times 10^{0} e^{-0.00720t} - 0.458 \times 10^{2} e^{-1.71t} \\
& + 0.416 \times 10^{2} e^{-1.82t} + 0.765 \times 10^{2} e^{-2.45t} \\
& - 0.778 \times 10^{1} e^{-2.88t} \cos 0.585t \\
& - 0.648 \times 10^{2} e^{-3.47t} \cos 0.307t \\
& + 0.908 \times 10^{2} e^{-2.88t} \sin 0.585t \\
& + 0.356 \times 10^{2} e^{-3.47t} \sin 0.307t \,. \qquad (6h)
\end{aligned}
$$

$$
\begin{aligned}
Y_9(t) = {} & 0.167 \times 10^{-2} e^{-0.588t} - 0.975 \times 10^{-4} e^{-0.134t} \\
& + 0.295 \times 10^{-3} e^{-0.00720t} + 0.497 \times 10^{1} e^{-1.71t} \\
& - 0.402 \times 10^{1} e^{-1.71t} - 0.237 \times 10^{1} e^{-1.82t} \\
& + 0.202 \times 10^{1} e^{-2.88t} \cos 0.585t \\
& - 0.594 \times 10^{0} e^{-3.47t} \cos 0.307t \\
& + 0.296 \times 10^{1} e^{-2.88t} \sin 0.585t \\
& - 0.278 \times 10^{1} e^{-3.47t} \sin 0.307t \,. \qquad (6i)
\end{aligned}
$$

$$
\begin{aligned}
Y_{10}(t) = {} & 0.207 \times 10^{-2} e^{-0.588t} - 0.102 \times 10^{-3} e^{-0.134t} \\
& + 0.296 \times 10^{-3} e^{-0.00720t} + 0.115 \times 10^{2} e^{-1.71t} \\
& - 0.102 \times 10^{2} e^{-1.82t} - 0.125 \times 10^{2} e^{-2.45t} \\
& + 0.832 \times 10^{1} e^{-2.88t} \cos 0.585t \\
& - 0.542 \times 10^{1} e^{-3.47t} \cos 0.307t \\
& - 0.682 \times 10^{1} e^{-2.88t} \sin 0.585t \\
& + 1.416 \times 10^{1} e^{-3.47t} \sin 0.307t \,. \qquad (6j)
\end{aligned}
$$

1147956

Table 19.7. Microcurie-Days at 50 Years for ^{232}Th, ^{228}Ra-^{228}Ac, ^{224}Th, and ^{224}Ra Chain in Man for Cases of No Recycling, 20% Recycling to Blood of the Two Ra Daughters, and 100% Recycling

Radionuclide	Compartment	Microcurie-Days at 50 Years		
		0% Recycling	20% Recycling	100% Recycling
^{232}Th	Blood	1.267×10^{1}	1.267×10^{1}	1.267×10^{1}
	Bone, long term	1.014×10^{4}	1.014×10^{4}	1.014×10^{4}
	Bone, short term	1.425×10^{3}	1.425×10^{3}	1.425×10^{3}
	Soft tissues	6.229×10^{2}	6.229×10^{2}	6.229×10^{2}
^{228}Ra-^{228}Ac	Blood	3.642×10^{1}	5.406×10^{1}	1.195×10^{2}
	Bone, long term	6.962×10^{3}	5.513×10^{3}	1.331×10^{2}
	Bone, short term	1.382×10^{2}	1.148×10^{1}	2.792×10^{1}
	Soft tissues	6.085×10^{1}	5.086×10^{1}	1.375×10^{1}
^{228}Th	Blood	1.699×10^{0}	1.487×10^{0}	1.362×10^{0}
	Bone, long term	6.433×10^{3}	5.104×10^{3}	8.609×10^{1}
	Bone, short term	1.732×10^{2}	1.497×10^{2}	1.043×10^{2}
	Soft tissues	7.569×10^{1}	6.551×10^{1}	4.550×10^{1}
^{224}Ra	Blood	7.487×10^{0}	8.998×10^{2}	2.006×10^{2}
	Bone, long term	6.416×10^{3}	4.080×10^{3}	5.531×10^{-1}
	Bone, short term	1.702×10^{2}	1.218×10^{2}	8.825×10^{-1}
	Soft tissues	7.441×10^{1}	5.353×10^{1}	4.346×10^{-1}

recycling is assumed. The reason for this is that the shortest half-life for radium in blood is 20 days (see ORNL-4446, Tables 24.5 and 24.6), and hence ^{224}Ra with its 3.6-day half-life undergoes decay in the blood before reentering bone. This is the price one pays for approximating the power function with a sum of only three exponentials. Further study of this problem is indicated.

SCATTERED ENERGY SPECTRUM FOR A MONOENERGETIC GAMMA EMITTER UNIFORMLY DISTRIBUTED IN AN INFINITE CLOUD

L. T. Dillman[21]

Introduction

A basic problem in assessing the radiation dose received by various parts of the human body due to an external source of radiation distributed in a cloud is first of all to determine the spectrum of radiations incident upon the body. It is obvious that for a monoenergetic gamma emitter uniformly distributed in an infinite cloud there will be a continuous spectrum of scattered photons ranging in energy up to that of the initial photon. This spectrum results from Compton events in the scattering medium and also from the annihilation photons associated with pair production when this process is energetically possible. In addition, there will be a continuous spectrum of scattered electrons as a result of the photoelectric, Compton, and pair production events. For the case of an infinite unbounded medium it is clear from symmetry that there will be no angular dependence of the scattered photon and electron spectra but only energy dependence. This fact considerably reduces the complexity of the analysis of the problem, but a residual core of moderately complex equations remains. This report discusses analytic procedures which may be used to determine the scattered photon and electron spectra for the case of a monoenergetic gamma emitter uniformly distributed in an infinite unbounded cloud of air.

Several calculations of scattered photon spectra similar to those reported here have been made previously for the case of a water medium,[22] but the

[21] Consultant to ORNL from Ohio Wesleyan University.

[22] U. Fano, L. V. Spencer, and M. J. Berger, "Penetration and Diffusion of X-Rays," *Handbuch Der Physik*, S. Flugge, ed., vol. XXXVIII/2, pp. 660–817, Springer-Verlag, 1959.

1147959

Table 19.6. Comparison of Microcurie-Days Residence at 50 Years in Thyroid (T) Compartments and Total Body (TB) Compartments from Berman's Model and Riggs' Model

Lumped Compartment	^{123}I		^{124}I		^{125}I		^{126}I		^{131}I	
	Berman	Riggs	Berman	Riggs	Berman	Riggs	Berman	Riggs	Berman	Riggs
T	0.181	0.184	1.74	1.79	16.7	18.0	5.15	5.30	3.29	3.39
TB	0.240	0.277	0.387	0.416	1.19	2.60	0.596	0.786	0.471	0.567

formed by decay of the thorium parent was cycled to blood, where it was eliminated as would be the case with freshly injected radium. We tested these models against data of Stover *et al.*[20] on retention of ^{228}Th and ^{224}Ra in beagle dogs. They defined the fraction of radium daughter undergoing translocation in the body by

$$F_T(t) = \frac{1 - (^{224}Ra/^{228}Th)\ \text{body}}{0.3}$$

and reported that $F_T(t)$ decreased with time after injection (see Fig. 19.14). The fraction $F_T(t)$ was computed for the extreme cases of no recycling and for 100% recycling of the ^{224}Ra daughter using parameters appropriate for the beagle dog (see ORNL-4446), and results are plotted in Fig. 19.14. As can be seen the assumption of 0% recycling produces a lower estimate of $F_T(t)$ than the data of Stover *et al.* This lower $F_T(t)$ would correspond to higher estimates of dose commitment than the other case.

In this report we have made additional calculations corresponding to the cases of 50% recycling and 20% recycling, and the results are also plotted in Fig. 19.14. Here it can be seen that the case of 20% recycling of ^{224}Ra daughter corresponds to an $F_T(t)$ which more closely agrees with the experimental findings than the other cases shown in the figure. The case of 50% recycling overshoots the data at all times. Since the agreement with the dog data is better when 20% recycling is assumed, we shall assume in the following that this fraction also applies to man and compute corresponding estimates of microcurie-days residence in the various compartments of the mammillary model. In order to estimate microcurie-days residence in man, we use the data for the mammillary model given in the previous report. There we showed how to operate on total-body-retention equations to estimate parameters for the mammillary model. We only present here the final results in microcurie-days residence employing the parameters derived before for man.

Table 19.7 presents estimates of microcurie-days residence for ^{232}Th, ^{228}Ra-^{228}Ac, ^{228}Th, and ^{224}Ra following entry of ^{232}Th to blood. For comparison, estimates of microcurie-days residence are given using these assumptions: 0% recycling of all daughters, 20% recycling of the two radium daughters, and 100% recycling of all daughters. As can be noted, the long-term bone compartment has the highest microcurie-days, and the estimates of residence using 20% recycling of radium daughters is not much different than that using 0% recycling. Also, it can be noted that in the case of 100% recycling of all daughters the residence in blood is higher than it is in the other cases. Note too the microcurie-days residence in blood of ^{224}Ra is higher than the residence in bone when 100%

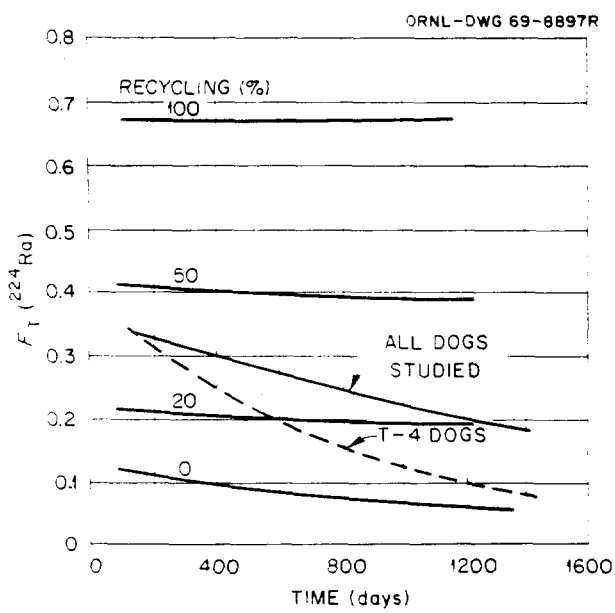

Fig. 19.14. Stover *et al.* Estimate of Fraction of ^{224}Ra Formed in the Dog Which Translocates Compared with Estimates Made with Model in Text.

[20] B. J. Stover *et al.*, "The ^{228}Th Decay Series in Adult Beagles: ^{224}Ra, ^{212}Pb, and ^{212}Bi in Blood and Excretion," *Radiation Res.* **26**, 226 (1965).

1147958

It will be noted in Table 19.4 that certain elements of the matrix C are exceedingly small, less than 10^{-10}, and these have been interpreted to be 0. These occur in the imaginary parts of columns 1 through 6. Also, column 7 is the negative of column 8, and similarly for columns 9 and 10. It is also noted that only three digits have been used in the solutions $Y_1(t)$, ...,$Y_{10}(t)$. If additional digits (accuracy) are needed, then these can be obtained from Table 19.4.

The microcurie-days residence at 50 years were also computed in each of the ten compartments for injection of 1 μCi of ^{123}I, ^{124}I, ^{125}I, ^{126}I, and ^{131}I into compartment 1 and appear in Table 19.5. We mention that the correspondence between rows of the vector and Berman's compartment system is as follows:

Row No.	Berman's Compartment No.
1	1
2	2
3	4
4	5
5	8
6	9
7	10
8	11
9	12
10	13

Now the microcurie-days residence in the T and TB compartments mentioned earlier for each of these isotopes are shown in Table 19.6. Also shown are the estimates obtained by Snyder and Ford (unpublished data) in application of Riggs' three-compartment (*Pharmacol. Rev.* 4, 284, 1952) model as studied by Snyder, Fisher, and Boyd (ORNL-4007, p. 228). Here the inorganic and organic compartments are combined into the TB compartment. The point to note in this table is that there is only a slight difference in the microcurie-days residence given by either model. It is seen that the two models yield about the same residence times for these two compartments, namely, thyroid and total body, but in one case differ by a factor of about 2. This suggests that the three-compartment model of Riggs might be adequate for internal dose estimation for various isotopes of iodine injected into man.

APPLICATION OF A MAMMILLARY COMPARTMENT MODEL TO ESTIMATION OF MICROCURIE-DAYS RESIDENCE OF ^{232}Th, ^{228}Ra-^{228}Ac, ^{228}Th, AND ^{224}Ra IN MAN

S. R. Bernard C. F. Holoway

In a previous annual report[19] a mammillary model for distribution of thorium and radium in organs and tissues of man was presented, and the residence times for ^{232}Th and ^{228}Ra were estimated with this model. Two sets of residence times were computed. One calculation corresponded to the assumption of no recycling of radium daughter born in each of the compartments by decay of the thorium parent. Thus the radium daughter was assumed to be eliminated only by radioactive decay in situ. Another estimate of residence times was computed by the use of the other extreme assumption; namely, all of the radium daughter

[19] S. R. Bernard and C. F. Holoway, "Application of a Mammillary Compartment Model to the Estimation of Microcurie-Days Residence of ^{232}Th Parent and ^{228}Ra Daughter in Man," *Health Phys. Div. Ann. Progr. Rept. July 31, 1969*, ORNL-4446, p. 285.

Table 19.5. Microcurie-Days Residence at 50 Years in Each Compartment for Different Radionuclides per Microcurie Administered

Compartment No.	Microcurie-Days Residence for Isotope –				
	^{123}I	^{124}I	^{125}I	^{126}I	^{131}I
1	0.236×10^{0}	0.323×10^{0}	0.383×10^{0}	0.345×10^{0}	0.336×10^{0}
2	0.827×10^{-1}	0.182×10^{0}	0.237×10^{0}	0.207×10^{0}	0.198×10^{0}
3	0.125×10^{-2}	0.407×10^{-1}	0.614×10^{0}	0.162×10^{0}	0.933×10^{-1}
4	0.292×10^{-1}	0.863×10^{-1}	0.118×10^{0}	0.102×10^{0}	0.863×10^{-1}
5	0.152×10^{-2}	0.173×10^{-1}	0.148×10^{0}	0.478×10^{-1}	0.314×10^{-1}
6	0.863×10^{-3}	0.607×10^{-2}	0.444×10^{-1}	0.150×10^{-1}	0.102×10^{-1}
7	0.102×10^{-1}	0.726×10^{-1}	0.115×10^{0}	0.955×10^{0}	0.873×10^{-1}
8	0.242×10^{-1}	0.124×10^{1}	0.160×10^{2}	0.455×10^{1}	0.273×10^{1}
9	0.206×10^{-1}	0.818×10^{-1}	0.117×10^{0}	0.100×10^{0}	0.936×10^{-1}
10	0.145×10^{-1}	0.775×10^{-1}	0.117×10^{0}	0.984×10^{-1}	0.910×10^{-1}

1147957

technique employed was numerical solution of the moment equations rather than direct numerical integration of the integral equation, which is discussed in this report. Calculations of the scattered electron spectrum have not been reported previously in the literature.

Calculation of the Differential Photon and Electron Density Functions

The principal mathematical symbols used in this report are defined below.

E_0 = energy of initial photons in MeV,

$f(E')$ = differential photon density at energy E' (photons per initial photon per unit energy interval),

$\alpha_0 = E_0/m_0c^2$, the initial photon energy in terms of rest-mass energy units,

$K_p(E', E)\,dE'$ = probability that a photon of energy E will give rise to a Compton-scattered *photon* in the range of energy between E' and $E' + dE'$,

$K_e(E', E)\,dE'$ = probability that a photon of energy E will give rise to a Compton-scattered *electron* in the range of energy between E' and $E' + dE'$,

$P(E', E)\,dE'$ = probability that a photon of energy E will give rise to a pair-production electron *or* positron in the range of energy between E' and $E' + dE'$,

$\tau(E)$ = photoelectric cross section at energy E,

$\sigma(E)$ = Compton cross section at energy E,

$\kappa(E)$ = pair-production cross section at energy E,

$\mu(E) = \tau(E) + \sigma(E) + \kappa(E)$ = total cross section at energy E,

$g(E')$ = differential electron density at energy E' (electrons per initial photon per unit energy interval),

$\alpha = E/mc^2$, the energy E in terms of rest-mass energy units.

With these definitions the function $f(E')$ is determined from

$$f(E') = K_p(E', E_0) + \int_{E'}^{E_0} f(E)\,K_p(E', E)\,dE\,. \quad (1)$$

The first term on the right-hand side of Eq. (1) is the contribution to $f(E')$ due to the initial photons, and the second term is the contribution to $f(E')$ from the scattered radiation of energy higher than E'. The integral in the second term is required since all radiation of energy higher than E' has a finite probability of scattering with a resultant scattered photon energy of E'. Of course, the Compton scattering equations imply that $K_p(E', E) = 0$ if $E' < E/(1 + 2\alpha)$, and this discontinuity must be taken into account.

In this integral equation for $f(E')$, which is of the Volterra type, function $K_p(E', E)$ for an air medium, using MeV as the energy unit and all cross sections in cm^2/g, is given by

$$K_p(E', E) = 0.0755829 \left[1 + (1 - x)^2 + \frac{\alpha^2 x^2}{1 + \alpha x}\right] \frac{1}{\alpha E\,\mu(E)}\,, \quad (2)$$

where

$$x = \frac{E - E'}{\alpha E'}\,,$$

for

$$E' \geqslant \frac{E}{1 + 2\alpha}$$

and

$$K_p(E', E) = 0.0$$

if

$$E' < \frac{E}{1 + 2\alpha}\,.$$

The integral equation has been solved numerically using an iterative technique. This iterative technique makes use of the fact that the solution is given exactly by $K_p(E_0, E_0)$ when $E' = E$. One uses this result as a trial solution at E' slightly less than E_0 and performs the integration of the second term on the right-hand side to obtain a better approximation to the solution. This second approximation is then used in the integral on the right-hand side to obtain a still better approximation to the solution, etc., until the iterative procedure is terminated when the change in the iterated solution is less than 0.1% from the previous iteration. By this process one can work gradually downward in energy to obtain $f(E')$ at all desired energies.

In the computer implementation of Eq. (1), $f(E')$ was determined for 100 uniformly spaced energy increments between zero energy and the initial photon

1147960

energy, E_0. The numerical integration of the second term on the right-hand side of Eq. (1) was performed by quadrature using Simpson's rule, and the integration was terminated when the approximation to the integral changed by less than 0.1% in consecutive quadratures.

$$g(E') = f(E')\frac{\tau(E')}{\mu(E')} + K_e(E', E_0) + \int_{E'}^{E_0} f(E)\, K_e(E', E)\, dE + 2\left[P(E', E_0) + \int_{E'+2m_0c^2}^{E_0} f(E)\, P(E', E)\, dE\right] . \quad (3)$$

The first term on the right-hand side of Eq. (3) is due to photoelectric absorption of photons of energy E', the second term is due to Compton scattering of the initial photons which give rise to electrons of energy E', the third term is due to scattered photons which give rise to electrons of energy E', and the fourth and last term is due to pair-production events which give rise to electrons of energy E'. The factor of 2 in the fourth term is present because a positron and an electron are created with each pair-production event, and statistically over many such events the number of positrons of energy E' is the same as the number of electrons of energy E'. The fourth term has been separated into two parts, the first term being the contribution due to the initial photons and the second term being due to the scattered photons.

In Eq. (3) the function $K_e(E', E)$ for an air medium, using MeV as the energy unit and all cross sections in cm^2/g, is given by

$$K_e(E', E) = 0.0755829\left[1 + (1-x)^2 + \frac{\alpha^2 x^2}{1+\alpha x}\right]\frac{1}{\alpha E\, \mu(E)} , \quad (4)$$

where

$$x = \frac{E'}{\alpha(E - E')} ,$$

for

$$E' \leqslant \frac{2\alpha E}{1+2\alpha}$$

and

$$K_e(E', E) = 0.0$$

if

$$E' > \frac{2\alpha E}{1+2\alpha} .$$

Similarly the function $P(E', E)$ is given by

$$P(E', E) = 0.0012925TZ(1-Q)\, K(E)/\mu(E) , \quad (5)$$

where $Q = 0.135(T - 0.52)Z(1 - Z^2)$, with the restriction that Q is set equal to zero if this expression for Q is negative, and where

$$Z = 2[x(1-x)]^{1/2} ,$$

where

$$x = \frac{E'}{E - 2m_0c^2} ,$$

and

$$T = \frac{P^2}{2E_h^3}\left\{-\frac{1}{3} - \frac{E_h^2}{P^2} + \frac{m_0^2c^4E_h}{P^3}\epsilon - \frac{m_0^2c^4}{P^2}\epsilon^2 + 2\ln\left(\frac{E_h}{m_0c^2}\right)\left[\frac{E_h^2(E_h^4+P^4)}{P^6} - \frac{2E_h^2}{3P^2} - \frac{m_0^2c^4E_h}{P^2}\left(\frac{m_0^2c^4\epsilon}{P^3} + \frac{E_h^3}{P^4}\right)\right]\right\} .$$

where

$$\epsilon = \ln\left(\frac{E_h + P}{m_0c^2}\right) ,$$

$$P = (E_h^2 - m_0^2c^4)^{1/2} ,$$

$$E_h = E/2 .$$

In addition to the above expressions for $f(E')$ and $g(E')$ the probability of obtaining annihilation radiation per initial photon, P_a, is

$$P_a = 2\left[\frac{K(E_0)}{\mu(E_0)} + \int_{2m_0c^2}^{E_0} f(E)\frac{K(E)}{\mu(E)}\, dE\right] . \quad (6)$$

where the integral is, of course, zero if $E_0 \leqslant 2m_0c^2$. The probability of obtaining photoelectrons of energy equal to the initial photon energy, P_e, is

$$P_e = \frac{\tau(E_0)}{\mu(E_0)} . \quad (7)$$

The probability of obtaining photoelectrons of energy equal to the annihilation radiation energy, P_{ae}, is

$$P_{ae} = P_a\frac{\tau(m_0c^2)}{\mu(m_0c^2)} . \quad (8)$$

These equations have been applied to find the differential photon and electron densities for a source

1147961

of monoenergetic photons uniformly distributed in an infinite homogeneous cloud of *air*. The generated table of terms of $f(E')$ as a function of E' from Eq. (1) is used to evaluate $g(E')$. The integrals on the right-hand side of Eqs. (1), (3), and (6) must, in general, be evaluated by dividing the range of the integration into several smaller subranges of integration because of discontinuities in the functions $f(E)$, $K_p(E', E)$, and $K_e(E', E)$. For example, $f(E)$ is discontinuous at $E = E_0/(1 + 2\alpha_0)$, $K_p(E', E)$ is discontinuous at $E' = E/(1 + 2\alpha)$, and $K_e(E', E)$ is discontinuous at $E' = 2\alpha E/(1 + 2\alpha)$. The cross sections used in this work were computed from theoretical expressions given in Chap. 2 of *Alpha-, Beta- and Gamma-Ray Spectroscopy*,[23] but interpolation from National Bureau of Standards or comparable tables[24,25] would work equally well and provide greater speed.

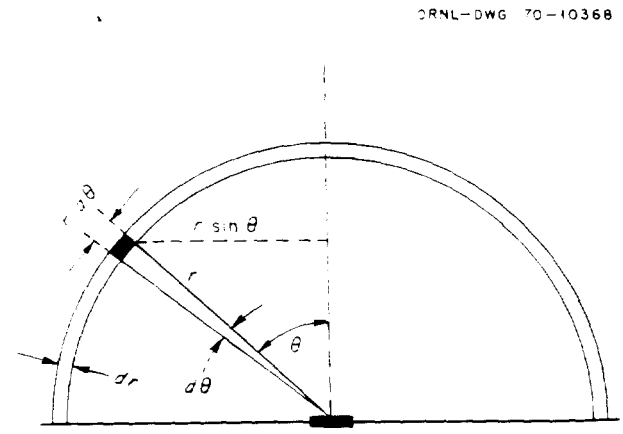

Fig. 19.15. Illustration of Geometric Parameters Involved in the Calculation of the Photon Flux.

Calculation of the Photon and Electron Fluxes

The equations discussed above may in turn be used to find the photon and electron fluxes which pass through any given cross-sectional area of the infinite cloud. Consider the volume element of the cloud, $r^2\, dr \sin\theta\, d\theta$, which is illustrated in Fig. 19.15. The number of disintegrations per second in this volume element, dV, is $3.7 \times 10^4\, C\rho\, dV$, where $dV = \text{cm}^3$, 3.7×10^4 = dis sec^{-1} μCi^{-1}, C = μCi per gram of air, and ρ = the density of air = 1.2929×10^{-3} g/cm^3. Thus disintegrations per second in volume $dV = 47.84C\, dV$. Now the solid angle subtended by an infinitesimal area dA as shown, for a point at dV is

$$d\Omega = \frac{dA \cos\theta}{r^2} ,$$

and so the fraction of radiations emitted from dV which start out in a direction such that they would pass through dA if undeflected or unabsorbed is

$$\text{fraction} = \frac{dA \cos\theta}{4\pi r^2} .$$

But the probability that the gamma rays survived to distance r is $e^{-\mu r}$, where μ is the linear absorption coefficient. Thus the number of gamma rays from volume element dV which pass through dA per second is

$$\frac{47.84C\, dV\, F\, dA \cos\theta\, e^{-\mu r}}{4\pi r^2} = \frac{3.807CF \cos\theta\, dA\, dV\, e^{-\mu r}}{r^2} ,$$

where F is the number of initial gamma rays per disintegration. Integrating over the half space which can contribute to photons passing through dA in one direction (i.e., integrating over the ranges $0 \leqslant \phi \leqslant 2\pi$, $0 \leqslant \theta \leqslant \pi/2$, and $0 \leqslant r \leqslant \infty$), we have

initial photons per second passing through dA in one sense

$$= 3.807CF\, dA \int_0^{2\pi} d\phi \int_0^{\pi/2} \cos\theta \sin\theta\, d\theta \int_0^{\infty} e^{-\mu r}\, dr = \frac{11.96CF}{\mu}\, dA .$$

Thus the number of initial photons per second per square centimeter of area is obtained by dividing this result by dA; so we have

$$\text{initial photons sec}^{-1}\ \text{cm}^{-2} = \frac{11.96CF}{\mu(E_0)} . \qquad (9)$$

Since we are dealing with an infinite medium, there are scattered photons associated with each initial photon. Let $f(E)$ represent the number of scattered

[23] C. M. Davisson, "Interaction of Gamma Radiation with Matter," *Alpha-, Beta- and Gamma-Ray Spectroscopy*, K. Siegbahn, ed., chap. 2, North-Holland, Amsterdam, 1966.

[24] G. W. Grodstein, "X-Ray Attenuation Coefficients for 10 keV to 100 MeV," *NBS Circular 583*, 1957; and R. T. McGinnis, *Supplement to NBS Circular 583*, 1959.

[25] J. H. Hubbell, "Photon Cross Sections, Attenuation Coefficients, and Energy Absorption Coefficients from 10 keV to 100 GeV," NSRDS-NBS 29, 1969.

1147962

photons per initial photon per MeV at energy E [see Eq. (1)]. Then the number of scattered photons sec^{-1} cm^{-2} MeV^{-1} at energy E is

$$\text{scattered photons sec}^{-1}\ \text{cm}^{-2}\ \text{MeV}^{-1} = \frac{11.96CF\,f(E)}{\mu(E)}\,. \quad (10)$$

In Eqs. (9) and (10), $\mu(E)$ = linear absorption coefficient in cm^{-1} rather than in cm^2/g as used previously. In addition, if the initial photon energy is above $2m_0c^2$, pair production will give rise to annihilation quanta. Let P_a be the probability of obtaining annihilation radiation per initial photon [see Eq. (6)]. Then the number of annihilation photons sec^{-1} cm^{-2} will be given by

$$\text{annihilation photons sec}^{-1}\ \text{cm}^{-2} = \frac{11.96CFP_a}{\mu(m_0c^2)}\,. \quad (11)$$

Next we shall calculate the number of electrons sec^{-1} cm^{-2} MeV^{-1} which cross a unit cross-sectional area in one sense in the medium of air. The number of disintegrations per second per cubic centimeter of air is $3.7 \times 10^4\ \rho C = 47.84C$, where the units are as given previously. Thus the number of electrons per unit volume per second associated with a particular gamma ray and of energy equal to that of the gamma ray is

$$\text{initial photoelectrons sec}^{-1}\ \text{cm}^{-3} = 47.84CFP_e\,,$$

where F is the number of gamma rays per disintegration and P_e is the probability of obtaining photoelectrons of the energy equal to the initial photon energy as given by Eq. (7). Consider a volume of cross-sectional area A and thickness dr. The number of initial photoelectrons emitted per second by such a volume is $47.84CFP_eA\ dr$. Now $dE = S(E)\ dr$, where $S(E)$ is the stopping power; that is, $S(E) = dE/dr$ by definition. Hence the number of initial photoelectrons emitted per second by such a volume may be written as $47.84CFP_eA\ dE/S(E)$.

Half of these photoelectrons will pass through one surface of area A and the other half through the other surface. The number of photoelectrons which pass through surface A in one sense per second is $23.92CFP_eA\ dE/S(E)$. The number of initial photoelectrons per square centimeter per MeV is simply obtained by dividing this result by $A\ dE$. Letting $N(E)_p$ represent the number of initial photoelectrons per square centimeter per MeV in one sense we have

$$N(E)_p = \frac{23.92CFP_e}{S(E)}\,. \quad (12)$$

Because of scattering there will be a continuous distribution of Compton-scattered electrons and photoelectrons of energy lower than the initial gamma-ray energy. Now $g(E')$ in Eq. (3) represents the number of such electrons per initial photon per MeV. Any such electrons which initially start out with an energy greater than E will pass through energy E in the slowing-down process and thus contribute to the flux at energy E. Therefore the number of scattered electrons cm^{-2} sec^{-1} MeV^{-1}, $N(E)_c$, is

$$N(E)_c = \frac{23.92CF \int_E^{E_0} g(E')\,dE'}{S(E)}\,. \quad (13)$$

The total number of electrons cm^{-2} sec^{-1} MeV^{-1}, $N(E)$, is thus

$$N(E) = \frac{23.92CF}{S(E)}\left[P_e + \int_E^{E_0} g(E')\,dE'\right]\,. \quad (14)$$

This expression neglects the probability of obtaining photoelectrons of energy equal to the annihilation radiation energy, P_{ae}, which is negligible for air. To include this effect in the above equation one would merely add the term P_{ae} to the two terms in the brackets.

In Eqs. (12), (13), and (14), $S(E)$ is in units of MeV/cm. $S(E)$ was determined from the relativistic Bethe-Block equation.[26]

Discussion of the Results

The calculated photon and electron fluxes for initial photon energies of 0.1, 0.5, and 4.0 MeV are shown in Figs. 19.16, 19.17, and 19.18 respectively. The results are for a source intensity of 1 μCi per gram of air and assuming 1 photon per disintegration. The discontinuities in the photon flux curves occur at an energy corresponding to the fact that there is a minimum energy of the scattered photon equal to $E_0/(1 + 2\alpha_0)$ when the *initial* photon scatters. The discontinuity in the case of the 0.1-MeV initial energy photon curve is sufficiently severe that a small bump in the curve occurs at an energy value of approximately $E/(1 + 2\alpha)$, where $E = E_0/(1 + 2\alpha_0)$. This is precisely what one would expect.

The discontinuities in the slope of the electron flux curves occur at an energy complementary to that of the

[26] G. Knop and W. Paul, "Interaction of Electrons and Alpha Particles with Matter," *Alpha-, Beta- and Gamma-Ray Spectroscopy*, K. Siegbahn, ed., chap. 1, p. 12, North-Holland, Amsterdam, 1966.

1147963

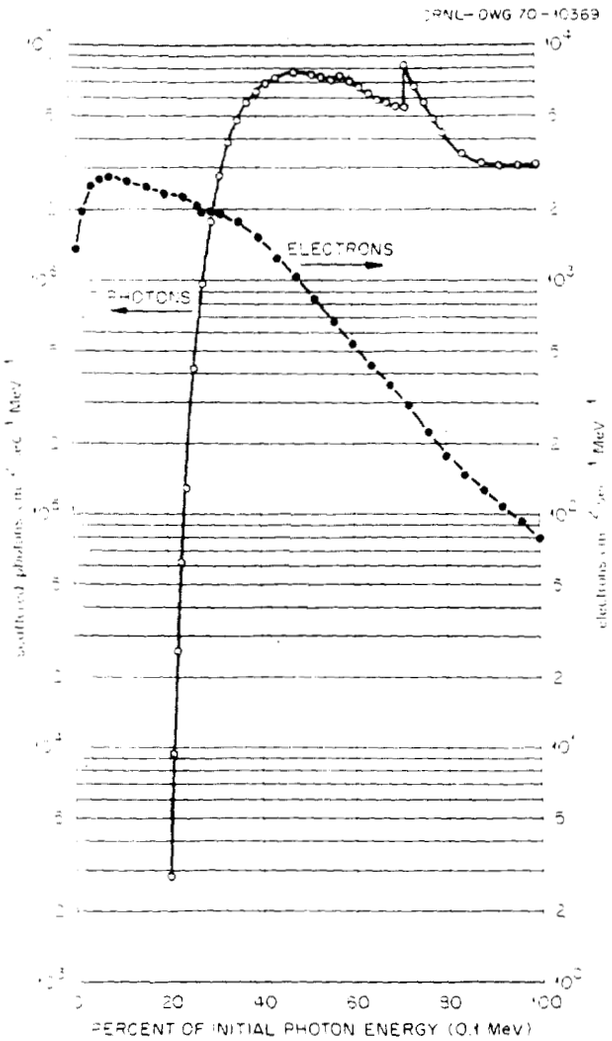

Fig. 19.16. Photon and Electron Fluxes in an Infinite Cloud of Air for a 0.1-MeV Photon Emitter Uniformly Distributed in the Cloud. Source intensity is 1 μCi per gram of air.

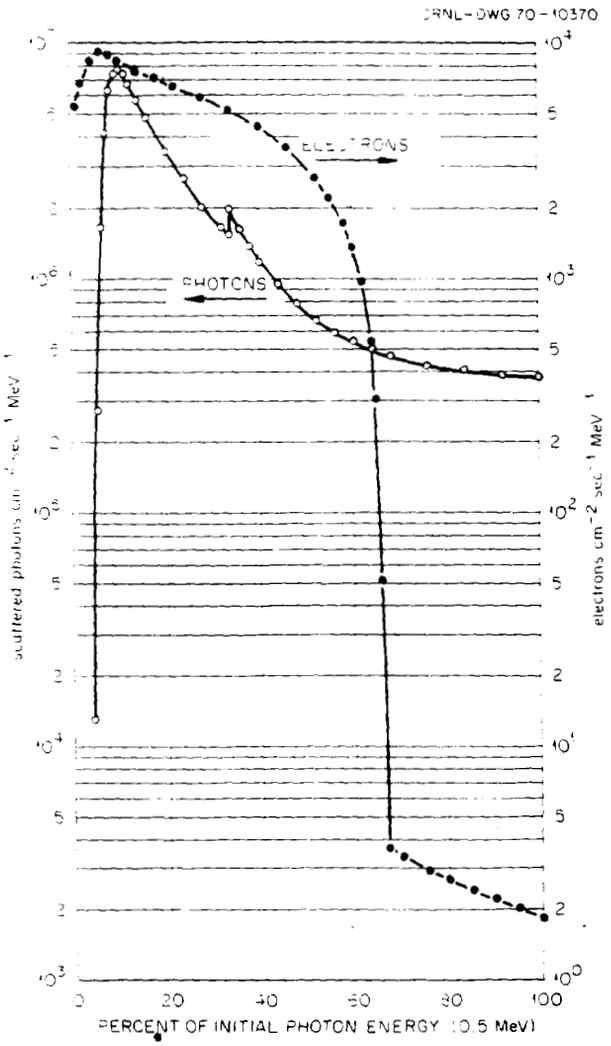

Fig. 19.17. Photon and Electron Fluxes in an Infinite Cloud of Air for a 0.5-MeV Photon Emitter Uniformly Distributed in the Cloud. Source intensity is 1 μCi per gram of air.

photon flux discontinuity, namely, at an energy value of $E_0 - E_0/(1 + 2\alpha_0)$.

The curves illustrated have been tested in several ways. The energy integral of the function $g(E)$ determined by Eq. (3) plus the energy associated with initial photoelectrons should equal the initial photon energy, since all of the photon energy is eventually delivered to electrons. The observed error increases slowly as the initial photon energy increases and amounts to 1.2% at 4.0 MeV, the highest energy used. At 0.5 MeV the error is 0.3%. One expects the error to increase with increasing initial photon energy because of the rapid variation of $g(E)$ at low energy values when the initial photon energy is high. The numerical integration of the function $g(E)$ over energy thus becomes less accurate.

Another test of the accuracy of the results presented here has been to obtain the curves by an alternate procedure.[27] The alternate procedure is only expected to be accurate at energies greater than approximately 20% of the initial photon energy, and the two methods agree to better than 1% in this region.

[27] L. T. Dillman, unpublished data, 1969.

1147964

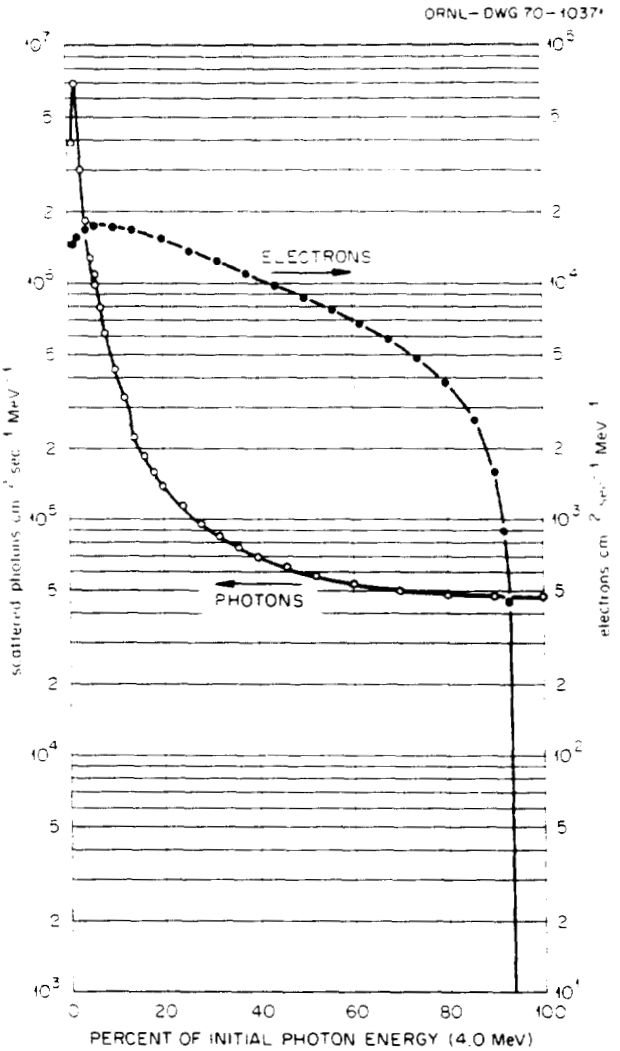

Fig. 19.18. Photon and Electron Fluxes in an Infinite Cloud of Air for a 4.0-MeV Photon Emitter Uniformly Distributed in the Cloud. Source intensity is 1 μCi per gram of air.

It is important to note that the photon fluxes illustrated in Figs. 19.16–19.18 are only for *scattered* photons. In addition, there are initial photon fluxes of 6.098×10^4, 1.055×10^5, and 2.997×10^5 photons cm^{-2} sec^{-1} for the 0.1-, 0.5-, and 4.0-MeV initial photon energy cases respectively. Furthermore, there is an annihilation quanta flux of 1.500×10^4 photons cm^{-2} sec^{-1} in the case of the 4.0-MeV initial photon energy case, where pair production is possible.

Work is presently in progress to apply these results to immersion dose problems. The most obvious application is to program the Monte Carlo gamma-ray code developed by Snyder and Fisher[28,29] for a source uniformly distributed on the surface of the phantom they use to represent standard man. Then if one picks initial photon energies according to the probability distribution implied by the photon fluxes calculated in this report and runs the Monte Carlo code for many photons, one may calculate the relative dose distribution to various organs of the body. A number of modifications must be considered so that photon and electron fluxes associated with finite and bounded clouds may be determined.

[28] H. L. Fisher, Jr., and W. S. Snyder, *Health Phys. Div. Ann. Progr. Rept. July 31, 1966*, ORNL-4007, p. 221.

[29] H. L. Fisher, Jr., and W. S. Snyder, *Health Phys. Div. Ann. Progr. Rept. July 31, 1967*, ORNL-4168, p. 245.

1147965

20. Stable Element Metabolism

ELEMENTAL INTAKE AND EXCRETION IN LONG-TERM BALANCE STUDIES

Isabel H. Tipton[1] Peggy L. Stewart[1]

This final year of the program for the study of trace elements in normal human beings has been spent for the most part in analyzing duplicates of the self-chosen daily diet and all excreta of a fourth adult male, subject F, for the period November 6, 1967, to November 14, 1968. This material has been ashed, and values for the concentrations of Cd, Ca, Mg, P, K, Na, and Zn have been determined by atomic absorption or flame photometry. Ashed samples have been excited in a dc arc, and photographic records of spectra have been made. Transmissions of appropriate lines of 16 elements (Al, Ba, Be, B, Cr, Co, Cu, Fe, Mn, Mo, Ni, Sr, Sn, Ti, V, and Zn) on the resulting films have been measured with a densitometer. Unfortunately there has not been time to convert these raw data into concentrations nor to calculate the daily intake and excretion from the concentrations already determined.

Descriptive statistics for a full year's data for subject E [see annual report 1969 (ORNL-4446)] have been prepared, and multiple regressions of diets and feces and diets and urine have been carried out [see annual report 1968 (ORNL-4316)]. Table 20.1 includes the mean daily elemental intake by ingestion and fecal and urinary excretion and Table 20.2 gives the mean daily gross dietary intake and gross fecal and urinary excretion.

Plots of daily intake and excretion (Fig. 20.1) brought to light an interesting circumstance for this subject. A marked elevation in the intake of magnesium, which began on the 148th day of the period and continued for 14 days, was followed by a similar elevation in fecal excretion on the 174th day which lasted for 17 days.

Regressions were run on fecal excretion over a 4-day period and intake over the same period, the previous 4-day period, 2 periods previous, and so on through 12 periods previous or covering a total of 48 days before excretion for the three subjects C, D, and E. For subjects C and D no significant relation between fecal excretion and intake by ingestion of magnesium was brought out by this statistical treatment. For subject E, however, this treatment indicated a high correlation between the 4-day amount of magnesium excreted in feces and the intake by ingestion during the two 4-day periods that included the 29th to 36th days previous. In fact, the multiple correlation coefficient R for this subject was 0.91, indicating that 83% (R^2) of the variability of magnesium in feces was due to the intake 29 to 36 days previously. The correlation coefficients for the periods 29–32 and 33–36 days previous were 0.43 and 0.26, indicating that for this subject 69% of magnesium ingested during an 8-day period was excreted after an elapse of about 4 to 5 weeks.

GROSS COMPOSITION OF BONE AND CARTILAGE

Isabel H. Tipton[1] Cyrus Feldman[2]
Mary Jane Cook

Samples of bone and cartilage, carefully collected by Alfred P. Stoholski, M.D., of the New York Medical Examiner's office, were analyzed at ORNL, and the results of the analyses were used to calculate the gross composition shown in Table 20.3.

The same rib and vertebra and a portion from the same region of costal cartilage, skull, and sternum were taken at autopsy, placed in polyethylene bags, and transported frozen to ORNL, where they were kept frozen until analysis.

Specific gravity was determined by the method of water displacement on thawed bone. Dry weight was determined first after the sample had been in a freeze-drying apparatus overnight at 50 μ pressure and

[1] Department of Physics, University of Tennessee.
[2] Analytical Chemistry Division.

1147966

Table 20.1. Mean Daily Intake by Ingestion and Fecal and Urinary Excretion

Subject E: October 5, 1964–October 5, 1965 (365 days)
All values except ratio in milligrams per day

Element	Diet, Mean (±S.E.)	Feces, Mean (±S.E.)	Urine, Mean (±S.E.)	Excreta, Sum of Feces plus Urine (±S.E.)	Balance (±95% Confidence Interval), Difference, Diet Minus Excreta (±2S.E.)	Urine/Excreta, F_u
Al	21(2)	13.(0.6)	6(0.03)	14(0.6)	7.(4.2)	0.040
Ba	1.0(0.1)	0.96(0.02)	.021(0.007)	0.98(0.02)	0.02(0.13)	0.021
Be	0.043(0.003)	0.00034(0.0001)	0.00058(0.0003)	0.00092(0.0003)	0.042(0.006)	0.63
B	13.(1.)	0.30(0.006)	2.2(0.4)	2.5(0.4)	10.5(2.)	0.88
Ca	1100.(23.)	790.(17.)	230(5.1)	1000(18)	80.(60.)	0.23
Cd	0.14(0.004)	0.047(0.001)	0.075(0.004)	0.12(0.004)	0.02(0.01)	0.62
Cr	0.51(0.07)	0.12(0.001)	0.33(0.04)	0.45(0.04)	0.06(0.08)	0.62
Co	0.24(0.02)	0.047(0.003)	0.16(0.02)	0.21(0.02)	0.03(0.06)	0.76
Cu	4.1(0.2)	2.5(0.1)	0.031(0.004)	2.8(0.08)	1.3(0.4)	0.011
Fe	25.(0.8)	18.(0.4)	1.6(0.13)	20(0.4)	5(2)	0.080
Mg	380.(19.)	320.(14.)	70.(2)	330(14)	50(50.)	0.21
Mn	7.9(0.8)	2.5(0.1)	0.006(0.002)	2.5(0.1)	5.4(2)	0.0024
Mo	0.11(0.01)	0.052(0.001)	0.053(0.015)	0.11(0.01)	0.0(0.03)	0.48
Ni	0.88(0.25)	0.29(0.01)	0.084(0.016)	0.37(0.02)	0.51(0.5)	0.23
P	1900.(32.)	550.(14.)	1100.(25.)	1700(28)	200.(90)	0.65
K	3100(35.)	420(10)	2500(48.)	2900.(50)	200.(120)	0.86
Ag	0.095(0.008)	0.0037(0.0005)	0.010(0.002)	0.014(0.002)	0.081(0.02)	0.71
Na	4500.(63.)	210.(7.)	4300.(71.)	4500(72)	0(190)	0.96
Sr	2.2(0.1)	3.4(0.1)	0.21(0.011)	3.6(0.1)	−1.4(0.4)	0.058
Sn	15(0.8)	2.7(0.1)	0.066(0.018)	2.8(0.1)	12.(2.)	0.024
Ti	0.18(0.02)	0.26(0.01)	0.14(0.01)	0.40(0.02)	−0.22(0.06)	0.35
V	0.071(0.004)	0.053(0.002)	0.010(0.001)	0.063(0.003)	0.01(0.02)	0.16
Zn	14.0(0.3)	15.0(0.4)	0.52(0.02)	16.0(0.4)	2.0(0.3)	0.032
Zr	0.045(0.004)	0.032(0.002)	0.058(0.019)	0.090(0.02)	−0.045(0.04)	0.64

Table 20.2. Gross Daily Intake and Excretion (g/day)

Subject E: October 5, 1964–October 5, 1965
Mean ± standard deviation

Total daily intake by ingestion	3200 ± 520
Water content	2700 ± 580
Total daily fecal excretion	220 ± 72
Total daily urinary excretion	1100 ± 200

Table 20.3. Gross Composition of Bone and Cartilage

Number of subjects included in each determination indicated in parentheses

Tissue	Water (% ± S.D.)	Ash (% ± S.D.)	Fat (% ± S.D.)	Protein (% ± S.D.)	Specific Gravity
Cartilage (costal)	54.7 ± 6.2 (4)	2.1 ± 0.2 (4)	3.4 ± 0.9 (4)	32.1 ± 3.3 (4)	1.13 ± 0.001 (4)
Rib	25.9 ± 10.8 (4)	38.8 ± 6.6 (5)	9.0 ± 4.7 (4)	22.6 ± 6.9 (4)	1.40 ± 0.08 (4)
Skull	15.6 ± 6.8 (7)	50.2 ± 5.4 (7)	7.2 ± 4.1 (7)	20.4 ± 3.8 (7)	1.66 ± 0.116 (7)
Sternum	46.4 ± 8.2 (8)	13.0 ± 2.7 (8)	10.1 ± 3.0 (8)	27.4 ± 5.1 (8)	1.14 ± 0.028 (8)
Vertebra	45.3 ± 4.8 (4)	17.2 ± 3.8 (4)	22.2 ± 2.9 (4)	10.1 ± 2.0 (4)	1.17 ± 0.030 (4)
Rib plus vertebra	33.0 (1)	N.D.	10.8	24.1	1.25

1147967

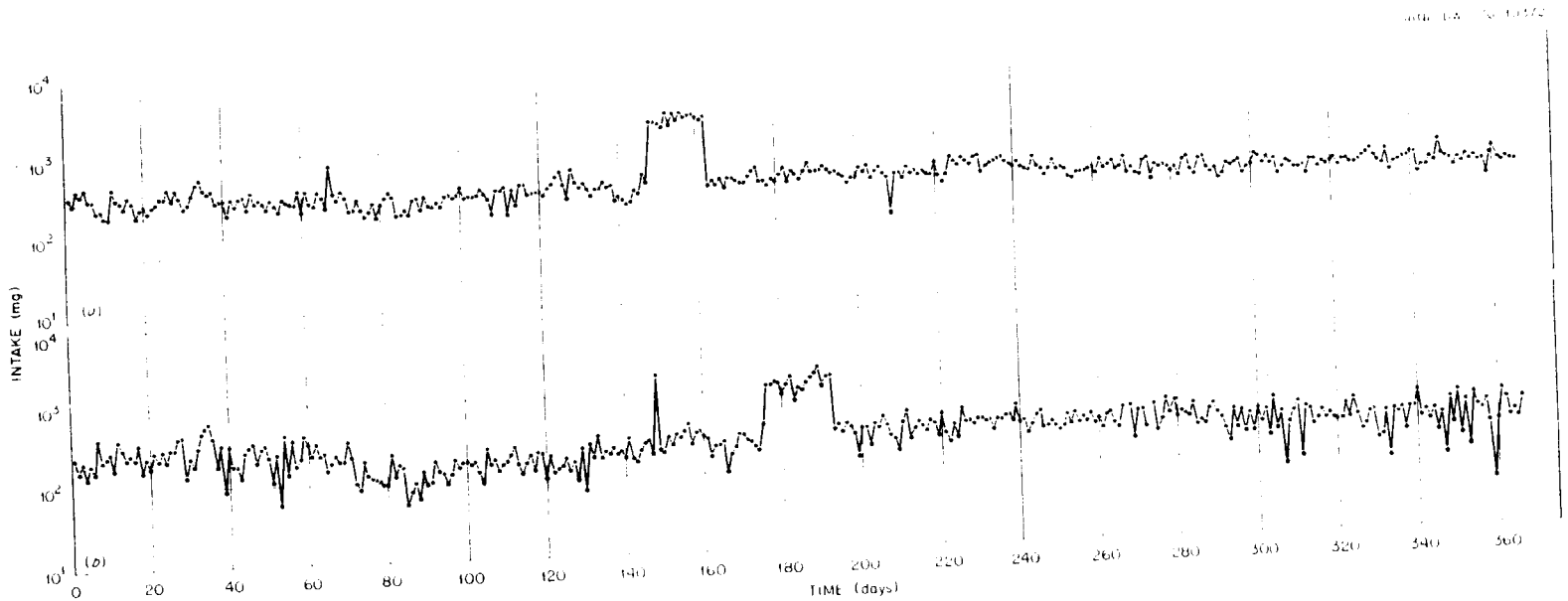

Fig. 20.1. (*a*) Daily Dietary Intake of Magnesium in Milligrams, Subject E, October 5, 1964–October 5, 1965; (*b*) Daily Fecal Excretion of Magnesium in Milligrams, Subject E, October 5, 1964–October 5, 1965.

1147968

again after the freeze-dried sample had been in a drying oven at 110° for 18 hr. The water content was determined on the basis of the weight after this final drying, An aliquot of the freeze-dried material was ashed in a muffle furnace at 450°C, and the weight of ash was related back to wet weight to determine ash percent of wet weight.

Each freeze-dried sample was finely divided in a special apparatus. Aliquots of this mealy material were taken for fat extraction by the Folch procedure [(*J. Biol. Chem.* **226**, 479–509 (1967)] and total nitrogen determination by the Kjeldahl method. Total nitrogen values were used in calculating the protein in the total sample.

1147969

Theses, Papers, Publications, and Lectures

Theses

A. J. Braundmeier, Jr.
Plasmon Radiation from Electron Bombarded Aluminum Foils, ORNL-TM-2612 (December 1969).

A. J. Braundmeier, Jr.
Radiative Decay of Coulomb-Stimulated Plasmons in Al, Mg, and Be (in preparation).

Barbara Brooks
The Application of the Technique of Ellipsometry in the Determination of the Optical Constants of Sodium (in preparation).

E. L. Chaney
Electron Attachment to Polyatomic Molecules, ORNL-TM-2613 (January 1970).

A. A. Christodoulides
Resonant Electron Attachment Processes in Polyatomic Molecules (in preparation).

P. M. Collins
Investigation of Negative Ions with Electron Beams, ORNL-TM-2614 (in preparation).

J. J. Cowan
Surface Plasmon Resonance Effects in Grating Diffraction, ORNL-TM-2615 (November 1969).

C. E. Easterly
Study of Aromatic Hydrocarbons in Relation to Carcinogenesis, ORNL-TM-2616 (in preparation).

J. M. Elson
Collective Excitations in Inhomogeneous Plasmas (in preparation).

T. F. Gesell
Photoelectric Properties of Magnesium in the Vacuum Ultraviolet, ORNL-TM-2617 (in preparation).

J. T. Grissom
Electron Impact Excitation and Ionization Studies of the Rare Gases, ORNL-TM-2618 (March 1970).

W. F. Hanson
Optical Properties of Solids in the Extreme Ultraviolet (in preparation).

D. L. McCorkle
Interactions of Low-Energy Electrons with Polyatomic Systems (in preparation).

W. T. Naff
Transient Negative Ion States and Electron Excitation in Cyclic Molecules (in preparation).

S. J. Nalley
Charge Exchange Between Fast Atoms and Molecules, ORNL-TM-2620 (in preparation).

1147970

M. N. Pisanias
Inelastic Scattering of Slow Electrons by Organic Molecules (in preparation).

B. L. Sowers
Optical Properties of Organic Liquids in the Vacuum Ultraviolet (in preparation).

R. B. Vora
Stopping Power of Matter at Extreme Relativistic Energies, ORNL-TM-2621 (in preparation).

U. S. Whang
Optical Constants of Cesium for Photons of Energy 5 to 9.6 eV, ORNL-TM-2622 (March 1970).

Papers

E. T. Arakawa
Optical and Electronic Properties of Liquids in the Vacuum UV, Symposium on Recent Developments in Radiation Dosimetry, March 4, 1970, Dallas, Texas.

E. T. Arakawa and T. Gesell
High Current Exo-Electron Emission from Mg, American Physical Society, September 2–4, 1969, Honolulu, Hawaii.

J. A. Auxier, T. D. Jones, and H. H. Hubbell, Jr.
Review of Depth Dose Calculation and Experimentation, Symposium on Neutrons in Radiobiology, November 11–14, 1969, Oak Ridge, Tennessee.

K. Becker
New Imaging Techniques for Ionizing Radiation, Second International Conference on Medical Physics, August 11–15, 1969, Boston, Massachusetts.

Recent Progress in Solid-State Dosimetry, Symposium on Neutrons in Radiobiology, November 11–14, 1969, Oak Ridge, Tennessee.

Recent Progress in Solid-State Dosimetry (Refresher Course), 55th Scientific Assembly of the Radiological Society of North America, November 30–December 5, 1969, Chicago, Illinois.

Thermal Fading in TSEE Dosimeters, Radiation Research Society, March 2–5, 1970, Dallas, Texas.

Solid-State Microdosimetry, IVth International Congress of Radiation Research, June 28–July 4, 1970, Evian, France.

Klaus Becker, J. S. Cheka, and R. B. Gammage
Progress in Exoelectron Dosimetry, International Symposium on Exoelectrons, July 6–8, 1970, Braunschweig, Germany.

Klaus Becker and K. W. Crase
Gamma and Fast Neutron Response of Ceramic TSEE Dosimeters, Health Physics Society, June 28–July 2, 1970, Chicago, Illinois (presented by K. Becker).

K. Becker and D. R. Johnson
Some Dosimetric Applications of Nuclear Track Registration in Polymers, Radiation Research Society, March 2–5, 1970, Dallas, Texas.

S. R. Bernard
Use of Mathematics in Interpreting Bioassay Data, Health Physics Society Annual Meeting, June 28–July 2, 1970, Chicago, Illinois.

1147971

S. R. Bernard (and R. L. Hayes)
Dose to Various Segments of the Gastrointestinal Tract, ORAU Symposium on Medical Radionuclides: Radiation Dose and Effects. December 8–11, 1969, Oak Ridge, Tennessee.

R. D. Birkhoff
The Electron Flux Spectra and Radiation Yields in Solids Irradiated by Nuclear Radiation, IEEE Conference on Nuclear and Space Radiation Effects, July 7–11, 1969, University Park, Pennsylvania.

W. P. Bonner
Pollution of an Underground Aquifer in Florida, Annual Meeting of Florida Pollution Control Association and Florida Section of American Water Works Association, November 2–6, 1969, Miami Beach, Florida.

R. H. Boyett, D. R. Johnson, and K. Becker
On the Oxygen Enhancement of Alpha Particle Track Registration in Polymers, Second International Conference on Medical Physics, August 11–15, 1969, Boston, Massachusetts.

R. L. Bradshaw
Disposal of Solidified Power Reactor Wastes in Salt Mines, American Nuclear Society Meeting, December 2–4, 1969, San Francisco, California.

A. J. Braundmeier, Jr., and E. T. Arakawa
Emission of Photons by Nonradiative Surface Plasmons, American Physical Society, Southeastern Section, November 6–9, 1969, Gainesville, Florida.

Zolin G. Burson
Energy and Angular Distribution of Neutrons Emerging from the HENRE Targets, American Nuclear Society, June 28–July 2, 1970, Los Angeles, California.

E. L. Chaney and L. G. Christophorou
Electron Attachment to N_2O, Sixth International Conference on the Physics of Electronic and Atomic Collisions, July 26–August 2, 1969, Cambridge, Massachusetts.

E. L. Chaney, L. G. Christophorou, P. M. Collins, and J. G. Carter
Electron Attachment in the Field of the Ground and Excited Electronic States of the Azulene Molecules, 22nd Annual Gaseous Electronics Conference, October 29–31, 1969, Gatlinburg, Tennessee.

L. G. Christophorou
Electron Molecule Interactions, IBM Corporation Research Center, April 6, 1970, York Town Heights, New York.

Resonance Electron Attachment Processes in Polyatomic Molecules, Symposium on the Chemistry of Ions in the Gas State, May 24–29, 1970, Toronto, Canada.

Criteria for Scientific Research, Nuclear Research Center "Democritus," June 5, 1970, Athens, Greece.

Cross Section Functions for Slow-Electron Molecule Collision Processes, International Discussion on Progress and Problems in Contemporary Radiation Chemistry, June 22–25, 1970, Marianské Lázné, Czechoslovakia.

L. G. Christophorou, J. G. Carter, E. L. Chaney, and P. M. Collins
Long-Lived Parent Negative Ions Formed by Capture of Low-Energy Electrons (0–3 eV) in the Field of the Ground and Excited Electronic States of Organic Molecules, IVth International Congress of Radiation Research, June 28–July 4, 1970, Evian, France.

P. M. Collins, L. G. Christophorou, E. L. Chaney, and J. G. Carter
Electron Attachment Cross Sections and Negative-Ion Lifetimes for p-Benzoquinone and 1,4-Naphthoquinone, 22nd Annual Gaseous Electronics Conference, October 29–31, 1969, Gatlinburg, Tennessee.

Mary Jane Cook (W. S. Snyder, and G. G. Warner)
Estimates of Dose to Red Bone Marrow from Monoenergetic Sources of Photons in Lung and Other Organs, Second Congress of the International Radiation Protection Association, May 3–8, 1970, Brighton, England.

1147972

R. N. Compton

Mass Identification of Negative Ions Formed in Electron Swarm Experiments, Annual Conference on Mass Spectrometry and Allied Topics, June 14–19, 1970, San Francisco, California.

R. N. Compton, J. A. D. Stockdale, and H. C. Schweinler

Negative Ion Formation in Selected Hexafluoride Molecules, Sixth International Conference on the Physics of Electronic and Atomic Collisions, July 26–August 2, 1969, Cambridge, Massachusetts.

J. J. Cowan and E. T. Arakawa

Dispersion of Surface Plasmons in Dielectric-Metal Coatings on Concave Diffraction Gratings, American Physical Society, Southeastern Section, November 6–8, 1969, Gainesville, Florida.

K. E. Cowser and E. G. Struxness

Methods of Estimating Potential Dose Equivalents to Population Groups, 1969 Winter Meeting of American Nuclear Society, November 30–December 4, 1969, San Francisco, California.

Wallace de Laguna

Radioactive Waste Disposal by Hydraulic Fracturing, Third Annual National Pollution Control Conference, April 1–3, 1970, San Francisco, California.

Radioactive Waste Disposal by Hydraulic Fracturing, American Gas Association Conference on Underground Storage, April 13–15, Denver, Colorado.

Waste Disposal by Hydraulic Fracturing, American Institute of Chemical Engineers, August 26–28, 1969, Portland, Oregon.

Radioactive Waste Disposal by Hydraulic Fracturing, 25th Industrial Waste Disposal Conference, Purdue University, May 5–7, 1970, Lafayette, Indiana.

B. R. Fish

Particle-Particle and Particle-Surface Adhesion and Removal Forces and *Parametric Sampling of Gasborne Particles*, U.S.–Japan Seminar on Particulate Technology, October 5–11, 1969, Kyoto, Japan.

Mary Rose Ford (W. S. Snyder and)

Energy Absorbed in Body Organs from Internal Emitters, Health Physics Society Annual Meeting, June 28–July 2, 1970, Chicago, Illinois.

C. W. Francis

Soil Mineral Segregation Using Isopycnic Zonal Centrifugation, Annual Meeting of the American Society of Agronomy, November 9–13, 1970, Detroit, Michigan.

W. R. Garrett

Variational Method for Long Range Scattering Interactions, Sixth International Conference on the Physics of Electronic and Atomic Collisions, July 26–August 2, 1969, Cambridge, Massachusetts.

W. R. Garrett and V. E. Anderson

Electron Scattering by Polar Molecules, 22nd Annual Gaseous Electronics Conference, October 29–31, 1969, Gatlinburg, Tennessee.

T. F. Gesell

Contamination Effects on the Photoelectric Properties of Magnesium Films in the Vacuum Ultraviolet, Optical Contamination in Space, August 13–15, 1969, Aspen, Colorado.

J. T. Grissom, R. N. Compton, and W. R. Garrett

Electron Impact Excitation and Ionization Studies of He, Ne, and Ar, 22nd Annual Gaseous Electronics Conference, October 29–31, 1969, Gatlinburg, Tennessee.

R. N. Hamm, M. W. Williams, and E. T. Arakawa

Optical Properties of Organic Liquids in the Vacuum Ultraviolet. I. Analysis of Optical Data, American Physical Society, Southeastern Section, November 6–8, 1969, Gainesville, Florida.

1147973

W. F. Hanson and E. T. Arakawa
Optical Properties of MgO and MgF_2 in the XUV, American Physical Society, April 27–30, 1970, Washington, D.C.

S. Jablon, S. Fujita, K. Fukushima, T. Ishimaru, and J. A. Auxier
RBE of Neutrons in Japanese Survivors, Symposium on Neutrons in Radiobiology, November 11–14, 1969, Oak Ridge, Tennessee (presented by J. A. Auxier).

D. G. Jacobs
Consideration of the Radiological Impact from the Hypothetical Use of Contaminated Natural Gas from Nuclearly Stimulated Reservoirs, Second International Congress of the International Radiation Protection Association, May 3–8, 1970, Brighton, England.

A Preliminary Assessment of the Radiological Implications of Commercial Utilization of Natural Gas from a Nuclearly Stimulated Well, Fourth Plowshare Symposium, January 14–16, 1970, Las Vegas, Nevada.

T. D. Jones and J. A. Auxier
Dose, Dose Equivalent, and Linear Energy Transfer Distributions from Several Configurations of ^{252}Cf Sources of Neutrons, Health Physics Society, June 28–July 2, 1970, Chicago, Illinois.

C. E. Klots
Photosensitized Ionization of Molecules, 2nd U.S.–Japan Conference on Fundamental Processes of Radiation Chemistry, November 10–13, 1969, Hakone, Japan.

Fundamental Processes in Gas-Phase Radiolysis, Gordon Conference on Radiation Chemistry, July 14–18, 1969, New Hampton, New Hampshire.

Comparison of Photoabsorption and Resonance Energy Transfer Processes, IVth International Congress of Radiation Research, June 28–July 4, 1970, Evian, France.

C. E. Klots and D. R. Nelson
The Ratio of Transverse and Longitudinal Diffusion Coefficients, 22nd Annual Gaseous Electronics Conference, October 29–31, 1969, Gatlinburg, Tennessee.

W. T. Naff, R. N. Compton, and C. D. Cooper
Electron Attachment in Substituted Aromatic Hydrocarbons, 18th Annual Conference on Mass Spectrometry and Allied Topics, June 14–19, 1970, San Francisco, California.

S. J. Nalley, J. A. D. Stockdale, and R. N. Compton
Charge Transfer from Negative Halogen Ions to NO_2, 22nd Annual Gaseous Electronics Conference, October 29–31, 1969, Gatlinburg, Tennessee.

D. R. Nelson and F. J. Davis
Thermal Electron Attachment Rates of SF_6 for Different Carrier Gas Dilutants, Sixth International Conference on the Physics of Electronic and Atomic Collisions, July 26–August 2, 1969, Cambridge, Massachusetts.

Jacob Neufeld
An Alternative Approach to the Formulation of Quality Factor, Second International Congress of IRPA, May 3–8, 1970, Brighton, England.

Ambiguity of the Term "Quality Factor," Second International Conference on Medical Physics, August 11–15, 1969, Boston, Massachusetts.

R. H. Ritchie
Surface Plasmons in Solids, American Physical Society, September 2–4, 1969, Honolulu, Hawaii.

Surface Collective Modes in Solids, 4th Thin Films and Surface Conference, April 6–8, 1970, Reading, United Kingdom.

S. Y. Shieh and R. H. Ritchie
Simultaneous Generation of Transition Radiation and Bremsstrahlung from a Thin Foil, American Physical Society, January 26–29, 1970, Chicago, Illinois.

1147974

W. S. Snyder

The Use of the Reciprocity Theorem for Estimation of Dose, Second International Conference on Medical Physics, August 11–15, 1969, Boston, Massachusetts.

The Relation of Intake to Blood, Blood Activity, and Excretion of Plutonium at Early Times Post Exposure, 15th Annual Bioassay and Analytical Chemistry Meeting, October 9–10, 1969, Los Alamos, New Mexico.

Estimation of Absorbed Fraction of Energy from Photon Sources in Body Organs, ORAU Symposium on Medical Radionuclides: Radiation Dose and Effects, December 8–11, 1969, Oak Ridge, Tennessee.

Estimation of Dose to Gonads from Gamma Emitters Present in the Body, Second Congress of the International Radiation Protection Association, May 3–8, 1970, Brighton, England.

Estimation of Dose and Dose Commitment to the Bladder Wall from a Radionuclide Present in Urine, Health Physics Society Annual Meeting, June 28–July 2, 1970, Chicago, Illinois.

B. L. Sowers, R. N. Hamm, M. W. Williams, and E. T. Arakawa

Optical Properties of Organic Liquids in the Vacuum Ultraviolet. II. Saturated Hydrocarbons, American Physical Society, Southeastern Section, November 6–8, 1969, Gainesville, Florida.

J. A. D. Stockdale, R. N. Compton, and P. W. Reinhardt

Reactions of Low Energy O^- with Hydrocarbons, IVth International Congress of Radiation Research, June 28–July 4, 1970, Evian, France.

E. G. Struxness and P. S. Rohwer

An Approach to the Development of Guidelines for Plowshare, presented at 2nd Session of U.S.-U.S.S.R. Exchange Talks, Moscow, February 10–18, 1970.

Tsuneo Tamura

Soil Mineral Segregation Using Isopycnic Zonal Centrifugation, Annual Meeting of American Society of Agronomy, November 10–14, 1969, Detroit, Michigan.

J. E. Turner

Determination of Dose Equivalent for Monte Carlo Analysis of Pulse Height Spectra, Second International Conference on Medical Physics, August 11–15, 1969, Boston, Massachusetts.

J. E. Turner, R. D. Birkhoff, V. E. Anderson, E. B. Wagner, and H. A. Wright

Monte Carlo Method of Determining LET Spectra from Pulse-Height Measurements, Second Symposium on Microdosimetry, October 20–24, 1969, Ispra, Italy.

J. E. Turner, J. Dutrannois, H. A. Wright, J. Baarli, R. N. Hamm, and A. H. Sullivan

Calculation of Pion Depth-Dose Curves and Comparison with Experiment, IVth International Congress of Radiation Research, June 28–July 4, 1970, Evian, France.

J. E. Turner and H. A. Wright

Calculation of Dose from High-Energy Nucleons, Second International Conference on Accelerator Dosimetry and Experience, November 5–7, 1969, Stanford, California.

R. B. Vora and J. E. Turner

Stopping Power of Matter for Deuterons at Extreme Relativistic Energies, American Physical Society, Southeastern Section, November 6–8, 1969, Gainesville, Florida.

U. S. Whang, E. T. Arakawa, and T. A. Callcott

Optical Constants of Cesium for Photons of Energy 5 to 9.6 eV, American Physical Society, March 23–26, 1970, Dallas, Texas.

M. W. Williams, B. L. Sowers, R. N. Hamm, R. D. Birkhoff, and E. T. Arakawa

Optical Properties of Organic Liquids in the Vacuum Ultraviolet. III. Silicone Pump Oils, American Physical Society, Southeastern Section, November 6–8, 1969, Gainesville, Florida.

Harvel Wright and W. S. Snyder

Summability of the Derivates of Arbitrary Real-Valued Set Functions, 76th Annual Meeting of the American Mathematical Society, January 22–26, 1970, San Antonio, Texas.

1147975

H. A. Wright and J. E. Turner
Free-Nucleon Target Model Applied to Nucleon Penetration Through Matter, American Nuclear Society, November 30–December 4, 1969, San Francisco, California.

Publications

J. C. Ashley and R. H. Ritchie
"Double-Plasmon Excitation in a Free Electron Gas," *Phys. Status Solidi* **38**, 425–34 (1970).

"The Mean Free Path of Relativistic Electrons for Plasmon Excitation," submitted for publication in *Physica Status Solidi.*

J. A. Auxier, J. S. Cheka, and T. D. Jones
Report of Trip to Japan During Period August 17 Through September 19, 1969, October 29, 1969 (internal memorandum).

K. Becker
Report of Trip to Germany, Belgium, and France April 28 Through May 13, 1969, July 11, 1969 (internal memorandum).

Thermally Stimulated Exoelectron Emission from Terrestrial and Lunar Materials, ORNL-TM-2869 (February 1970).

"Radiophotoluminescence Dosimetry Bibliography II," *Health Phys.* **17**, 631–36 (1969).

"Application of the Track Etching Process in Radiation Protection," *Proceedings of International Topical Conference on Nuclear Track Registration in Insulating Solids, May 6–9, 1969*, Clermont-Ferrand, France (to be published).

"Recent Progress in Neutron Solid-State Dosimetry," *Proceedings of the Symposium on Neutrons in Radiobiology, November 11–14, 1969*, Oak Ridge, Tennessee (to be published).

"Principles of Thermally Stimulated Exoelectron Emission (TSEE) Dosimetry," to be published in *Atomic Energy Review.*

"Solid-State Dosimetry," to be published in *Critical Reviews in Radiological Sciences.*

K. Becker and N. Chantanakom
"On the Thermal Fading Characteristics of Some TSEE Dosimetry Materials," *Atompraxis* **16**(1), 31–36 (1970).

Klaus Becker and K. W. Crase
"A Sensitive Integrating Fast Neutron Dosimeter Based on TSEE," to be published in *Nuclear Instruments and Methods.*

K. Becker and D. R. Johnson
"Non-Photographic Alpha-Autoradiography and Neutron-Induced Autoradiography," *Science* **167**, 1370–72 (1970).

K. Becker, M. Oberhofer, and J. S. Cheka
"Thermally Stimulated Exoelectron Emission, Thermoluminescence, and Impurities in LiF and BeO," to be published in *Health Physics.*

G. M. Begun and R. N. Compton
"Threshold Electron Impact Excitation and Negative Ion Formation in XeF_6 and XeF_4," *J. Chem. Phys.* **51**, 2367–70 (1969).

S. R. Bernard and R. L. Hayes
"Dose to Various Segments of the Gastrointestinal Tract," p. 295 in *Medical Radionuclides: Radiation Dose and Effects*, USAEC-DTIE, Oak Ridge, Tenn., June 1970.

1147976

R. D. Birkhoff
"Electron Flux Spectra and Radiation Yields in Solids Irradiated by Beta Rays," *IEEE Trans. Nucl. Sci.* **16**(6), 233–41 (1969).

"Electron Flux Spectra and Radiation Yields in Solids Irradiated by Beta Rays," submitted for publication to *National Academy of Sciences–National Research Council.*

R. D. Birkhoff, J. E. Turner, V. E. Anderson, J. M. Feola, and R. N. Hamm
"The Determination of LET Spectra from Energy Proportional Pulse-Height Measurements. I. Track-Length Distributions in Cavities," *Health Phys.* **18**, 1–14 (1970).

W. J. Boegly, Jr., D. G. Jacobs, T. F. Lomenick, and O. M. Sealand
The Feasibility of Deep-Well Injection of Waste Brine from Inland Desalting Plants, Research and Development Progress Report No. 432, U.S. Govt. Printing Office, Washington, D.C. (March 1969).

W. J. Boegly, Jr., W. L. Griffith, O. M. Sealand, and W. E. Baldry
Solid Waste Management Practices: An Annotated Bibliography and Permuted-Title and Key-Word Index, ORNL-HUD-12 (February 1970).

W. P. Bonner and Tsuneo Tamura
Walker Branch Watershed Project: Progress Report for the Period 1968–1969 on Characterization of Soil and Water and Their Possible Interactions (internal memorandum).

R. H. Boyett and K. Becker
"LET Effects on the Chemical Resistance of Irradiated Polymers," to be published in the *Journal of Applied Polymer Science.*

R. H. Boyett, D. R. Johnson, and K. Becker
"Some Studies on the Chemical Damage Mechanism Along Charged Particle Tracks in Polymers," *Radiation Res.* **42**, 1-12 (1970).

R. L. Bradshaw, F. M. Empson, W. C. McClain, and B. L. Houser
"Results of a Demonstration and Other Studies of the Disposal of High Level Solidified, Radioactive Wastes in a Salt Mine," *Health Phys.* **18**, 63–67 (1970).

R. L. Bradshaw, W. C. McClain, and F. M. Empson
"Disposal of Solidified Power Reactor Wastes in Salt Mines," *Transactions of 1969 Winter Meeting of American Nuclear Society, November 30–December 4, 1969, San Francisco, California* **12**(2), 452 (1969).

R. L. Bradshaw and Florentino Sanchez
"Migration of Brine Cavities in Rock Salt," *J. Geophys. Res.* **74**(17), 4209–12 (Aug. 15, 1969).

A. J. Braundmeier, Jr., and E. T. Arakawa
"Observed Radiation from 'Nonradiative' Surface Plasmons in Aluminum," submitted for publication in *Zeitschrift für Physik.*

A. J. Braundmeier, Jr., E. T. Arakawa, and M. W. Williams
"Intrinsic Damping Rate and Volume Plasmon Energy in Mg from Radiative Decay Measurements," submitted for publication in *Physics Letters.*

Daniel G. Brown, Donald F. Johnson, and John A. Auxier
"Unilateral and Bilateral Exposure of Swine to Fission Neutrons," to be published in *Health Physics.*

E. L. Chaney and L. G. Christophorou
"Electron Attachment to N_2O," *J. Chem. Phys.* **51**, 883–93 (1969).

E. L. Chaney, L. G. Christophorou, P. M. Collins, and J. G. Carter
"Electron Attachment in the Field of Ground and Excited Electronic States of the Azulene Molecules," *J. Chem. Phys.* **52**, 4413–17 (1970).

J. S. Cheka
Distribution of Radiation from a 14 MeV Neutron Source in and near Structures, CEX-65.13 (May 1969).

1147977

J. S. Cheka and K. Becker
"High Dose-Level Glass Dosimeters with Low Dependence on Energy," *Nucl. Appl.* **6**, 163–67 (1969).

J. S. Cheka, E. M. Robinson, Leo Wade, Jr., and W. A. Gramly
"The UT-AEC Agricultural Research Laboratory Variable Gamma Dose Rate Facility," to be published in *Health Physics.*

L. G. Christophorou
Atomic and Molecular Radiation Physics, Wiley, Sussex, England, 1970.

L. G. Christophorou, J. G. Carter, E. L. Chaney, and P. M. Collins
"Long-Lived Parent Negative Ions Formed by Capture of Low-Energy Electrons (0 to 3 eV) in the Field of the Ground and Excited Electronic States of Organic Molecules," submitted for publication in *Proc. IVth International Congress of Radiation Research*, Gordon and Breach, Paris.

L. G. Christophorou, J. G. Carter, C. E. Easterly, and D. L. McCorkle
"Anomalous Emission from Liquid Benzene, Toluene, and Ethyl Benzene," submitted for publication in *Chemical Physics Letters.*

L. G. Christophorou and E. L. Chaney
"Electron Attachment to Gaseous Naphthalene," *J. Chem. Phys.* **52**, 2165–66 (1970).

L. G. Christophorou, E. L. Chaney, and A. A. Christodoulides
"Electron Attachment and 'Carrier Gas' Energy Distribution Functions," *Chem. Phys. Letters* **3**, 363–66 (1969).

L. G. Christophorou, D. L. McCorkle, and J. G. Carter
"Cross Sections for Thermal Peaking Electron Attachment Resonances," submitted for publication in the *Journal of Chemical Physics.*

L. G. Christophorou and D. Pittman
"Thermal Electron Scattering by Polar Molecules," submitted for publication in the *Journal of Physics B.*

T. G. Clark, B. R. Fish, W. H. Wilkie, J. L. Thompson, R. H. Boyett, and G. W. Royster
Biohazards of Aerospace Nuclear Systems, Final Report, SC-CR-69-3291 (December 1969).

P. M. Collins, L. G. Christophorou, E. L. Chaney, and J. G. Carter
"Energy Dependence of the Electron Attachment Cross Section and the Transient, Negative-Ion Lifetime for *p*-Benzoquinone and 1,4-Naphthoquinone," *Chem. Phys. Letters* **4**, 646–650 (1970).

R. N. Compton and R. H. Huebner
"Collisions of Low-Energy Electrons with Molecules: Excitation and Negative Ion Formation," in *Advances in Radiation Chemistry* (ed. by J. L. Magee) (in press).

"Temporary Attachment of Electrons to Azulene-h_8 and Azulene-d_8," *J. Chem. Phys.* **51**, 3132–33 (1969).

J. J. Cowan and E. T. Arakawa
"Dispersion of Surface Plasmons in Multiple Metal and Dielectric Layers on Concave Diffraction Gratings," *Phys. Status Solidi* (a) **1**, 695 (1970).

J. J. Cowan, E. T. Arakawa, and L. Robinson Painter
"Time Studies of the Polarization Due to Gratings," *Appl. Opt.* **8**, 1734–35 (1969).

J. J. Cowan, E. T. Arakawa, and R. H. Ritchie
"Dispersion of Surface Plasmons in Dielectric-Metal Coatings on Concave Diffraction Gratings," submitted for publication in *Zeitschrift für Physik.*

K. E. Cowser and E. G. Struxness
"Methods of Estimating Potential Dose Equivalents to Population Groups," *Transactions of 1969 Winter Meeting of American Nuclear Society, November 30–December 4, 1969, San Francisco, California* **12**(2), 814–15 (1969).

1147978

K. E. Cowser, W. S. Snyder, and E. G. Struxness
"Application of ICRP Recommendations Relevant to Internal Dose," *Proceedings for the Symposium on Public Health Aspects of Peaceful Uses of Nuclear Explosives*, sponsored by the Southwestern Radiological Health Laboratory, Las Vegas, Nevada, April 7 through 11, 1969, U.S. Public Health Service (1969).

Julian Crowell and R. H. Ritchie
"Surface Plasmon Effect in the Reflectivity of a Metal," *J. Opt. Soc. Am.* **60**, 794–99 (June 1970).

F. J. Davis and D. R. Nelson
"Attachment Rate of Thermal Electrons to SF_6," to be published in *Chemical Physics Letters* (August 1970).

"Pseudo-First Order Attachment Rates of Thermal Electrons by SF_6 in Different Carrier Gases," *Chem. Phys. Letters* **3**, 461–63 (1969).

Wallace de Laguna
"Control of Pollution from the Generation of Nuclear Power," *IEEE Trans. Geoscience Electronics* GE-7(4), 212–19 (October 1969).

Radioactive Waste Disposal by Hydraulic Fracturing (internal memorandum).

Hydraulic Fracturing Test in New York State (internal memorandum).

"Tracer Aids Interpretation of Pumping Test," *Water Resour. Res.* **6**(1), 172–84 (1970), published by American Geophysical Union.

Wallace de Laguna and W. C. McClain
First Fracturing Test, West Valley, New York, Preliminary Report (internal memorandum).

C. E. Easterly, L. G. Christophorou, R. P. Blaunstein, and J. G. Carter
"Fluorescence from the Second Excited π-Singlet State of 1,2-Benzanthrane and 3,4-Benzopyrene in Solutions," submitted for publication in *Chemical Physics Letters*.

J. M. Elson and R. H. Ritchie
"Photon Surface Plasmon Coupling at a Dielec[illegible] Shield," submitted for publication in *Physics Letters*.

L. C. Emerson
"Induced Radioactivity" (book review), to be published in *Health Physics*.

Chester W. Francis, Gordon Chesters, and Larry A. Haskin
"Determination of ^{210}Pb Mean Residence Time in the Atmosphere," *Environmental Science and Technology* (in press).

C. W. Francis, Tsuneo Tamura, W. P. Bonner, and J. W. Amburgey, Jr.
"Separation of Clay Minerals and Soil Clays Using Isopycnic Zonal Centrifugation," *Soil Sci. Soc. Amer. Proc.* **34**(2), 351–52 (1970).

F. W. Garber, M. Y. Nakai, J. A. Harter, and R. D. Birkhoff
"Low-Energy Electron Beam Studies in Thin Aluminum Foils," submitted for publication in the *Journal of Applied Physics*.

W. R. Garrett
"Critical Binding of an Electron to a Non-Stationary Electric Dipole," *Chem. Phys. Letters* **5**, 393–97 (1970).

"Variational Method for Elastic Scattering Involving Long Range Forces," submitted for publication in the *Journal of Physics B*.

W. R. Garrett, J. E. Turner, and V. E. Anderson
Analysis of Ground-State Energy Eigenfunctions for Finite Dipole in Spherical Coordinate Systems, ORNL-4431 (February 1970).

"Spherical Coordinate Analysis of Ground State Energy Eigenfunctions for an Electron in the Field of a Finite Dipole," *Phys. Rev.* **88**, 513–14 (1969).

T. F. Gesell, E. T. Arakawa, and T. A. Callcott
"Exo-Electron Emission During Oxygen and Water Chemisorption on Fresh Magnesium Surfaces," *Surface Sci.* **20**, 174–78 (1970).

1147979

J. T. Grissom, R. N. Compton, and W. R. Garrett
"Electron Impact Excitation and Ionization of Helium near 60 eV," *Phys. Letters* **30A**, 117–18 (1969).

V. G. Horton, E. T. Arakawa, R. N. Hamm, and M. W. Williams
"A Triple-Reflection Polarizer for Use in the Vacuum Ultraviolet," *Appl. Optics* 8, 667–70 (1969).

S. Jablon, S. Fujita, K. Fukushima, T. Ishimaru, and J. A. Auxier
"RBE of Neutrons in Japanese Survivors," *Proceedings of the Symposium on Neutrons in Radiobiology, November 11–14, 1969, Oak Ridge, Tennessee* (to be published).

D. G. Jacobs
"Isotope and Radiation Techniques in Soil Physics and Irrigation Studies" (book review), *Health Phys.* **18**, 300 (1970).

D. G. Jacobs and M. J. Kelly
Fifth Quarterly Progress Report on the Theoretical Evaluation of Consumer Products from Nuclearly Stimulated Gas Wells, ORNL-TM-2862 (February 1970).

Fourth Quarterly Progress Report on the Theoretical Evaluation of Consumer Products from Project Gasbuggy, ORNL-TM-2721 (October 1969).

D. G. Jacobs, E. G. Struxness, and C. R. Bowman
"A Preliminary Assessment of the Radiological Implications of Commercial Utilization of Natural Gas from a Nuclearly Stimulated Well," p. 83 in *Proceedings of the ANS Topical Meeting, Engineering with Nuclear Explosives, Las Vegas, Nevada, January 1970*, CONF-700101, vol. I (1970).

D. R. Johnson, R. H. Boyett, and K. Becker
"Sensitive Automatic Counting of Alpha Particle Tracks in Polymers and Its Application in Dosimetry," *Health Phys.* **18**, 424–25 (1970).

"Some Studies on the Chemical Damage Mechanism Along Charged Particle Tracks in Polymers," *Proceedings of International Topical Conference on Nuclear Track Registration in Insulating Solids, May 6–9, 1969, Clermont-Ferrand, France* (to be published).

D. R. Johnson, J. H. Thorngate, and P. T. Perdue
"A Sensitive Spectrometer for Fast Neutrons Using LiI(Eu)," *Nucl. Instr. Methods* **75**, 61–65 (1969).

D. R. Johnson, J. A. Auxier, J. W. Poston, D. G. Brown, W. A. Gramly, W. D. Gibbs,
Harold D. Hodges, and D. R. Davy
"'Total' and 'Exchangeable' Sodium Studies in Swine and Sheep Using Activation Analysis and Isotopic Dilution," *Health Phys.* **18**, 729–30 (1970).

Larry D. Johnson
"Molecular Orbitals and Oscillation Strengths for Magnesium Porphin," submitted for publication in the *Journal of Chemical Physics.*

T. D. Jones and J. A. Auxier
"Absorbed Dose and Linear Energy Transfer Distributions from Therapeutic Sources of ^{252}Cf," to be published in *Physics in Medicine and Biology.*

"Neutron Dose, Dose Equivalent, and Linear Energy Transfer from ^{252}Cf Sources," to be published in *Health Physics.*

T. D. Jones, W. S. Snyder, and J. A. Auxier
"Absorbed Dose, Dose Equivalent, and LET Distributions in Cylindrical Phantoms Irradiated by a Collimated Beam of Monoenergetic Neutrons," to be published in *Health Physics.*

S. V. Kaye and P. S. Rohwer
Dose Estimation Studies Related to Proposed Construction of an Atlantic-Pacific Interoceanic Canal with Nuclear Explosives: Phase III, ORNL-4579 (in press).

1147980

C. E. Klots

"Bimolecular Association Reactions and Microscopic Reversibility," to be published in the *Journal of Chemical Physics.*

"Comparison of Direct and Photosensitized Ionization Efficiencies," to be published in *Proceedings IVth International Congress of Radiation Research*, Gordon and Breach, Paris.

C. E. Klots and P. W. Reinhardt

"Energy-Loss Rates of Slow Electrons in Hydrocarbons," *J. Phys. Chem.* (in press).

C. E. Klots and Harvel Wright

"Aspects of Degradation Spectra," *International Journal of Radiation Physics and Chemistry* (in press).

Vinod Krishan and R. H. Ritchie

"Anomalous Damping of Volume Plasmons in Polycrystalline Metals," *Phys. Rev. Letters* **24**, 1117–19 (1970).

T. F. Lomenick and R. L. Bradshaw

"Deformation of Rock Salt in Openings Mined for the Disposal of Radioactive Wastes," *Rock Mechanics* **1**, 5–30 (1969).

T. F. Lomenick and NSIC Staff

Earthquakes and Nuclear Power Plant Design, ORNL-NSIC-28 (July 1970).

W. C. McClain

"Disposal of Radioactive Wastes by Hydraulic Fracturing: Part V. Site Evaluations," *Nucl. Eng. Design* **9**, 315–26 (1969).

W. C. McClain and R. L. Bradshaw

"Radioactive Wastes in Salt Mines," *Mines Mag.* **59**, 11–14 (1969).

"Status of Investigations of Salt Formations for Disposal of Highly Radioactive Power-Reactor Wastes," *Nucl. Safety* **11**(2), 130–41 (March–April 1970).

W. C. McClain and G. A. Cristy

Examination of High Pressure Water Jets for Use in Rock Tunnel Excavation, ORNL-HUD-1 (January 1970).

W. C. McClain and O. H. Myers

Seismic History and Seismicity of the Southeastern Region of the United States, ORNL-4582 (June 1970).

K. Z. Morgan

"Risks from Diagnostic X-Rays," *Amer. Radiography Technologist* **14**(4), 15–22 (Winter 1969).

"History of the Health Physics Society," to be published as part of *The RSNA Symposium on the Critical History of American Radiology* (November 1970).

"History of the International Radiation Protection Association," to be published as part of *The RSNA Symposium on the Critical History of American Radiology* (November 1970).

"Tainted Radiation," *Sci. Technol.* No. 90, 46–50 (June 1969).

"You Can Drastically Cut X-Ray Exposure Below Today's Levels," reprinted from *Consultant*, March–April, 1970.

K. Z. Morgan and J. E. Turner

"Health Physics," submitted for publication in *American Institute of Physics Handbook.*

O. H. Myers

The ORNL Seismograph Station ORT: Operation from September 1, 1968, to February 28, 1969 (internal memorandum).

The ORNL Seismograph Station ORT: Operation from March 1, 1968, to August 31, 1968 (internal memorandum).

W. T. Naff, C. D. Cooper, and R. N. Compton

"Attachment of Electrons to Substituted Benzenes," submitted for publication in the *Journal of Chemical Physics.*

1147981

D. R. Nelson and F. J. Davis
"Determination of Diffusion Coefficients of Thermal Electrons with a Time-of-Flight Swarm Experiment," *J. Chem. Phys.* **51**, 2322–35 (1969).

J. Neufeld
"Comments on Quality Factor," *Health Phys.* **17**, 625–28 (1969).

"Dosimetric Field Quantities in Health Physics," submitted for publication in *Health Physics.*

"Radiation Quantities and Their Significance in Health Physics," *Health Phys.* (in press).

"Revised Formulation of the Macroscopic Maxwell Theory – I. Fundamentals of the Proposed Formulation," *Nuovo Cimento* **65B**, 33–69 (1970).

"Revised Formulation of the Macroscopic Maxwell Theory – II. Propagation of an Electromagnetic Disturbance in Dispersive Media," *Nuovo Cimento* **66B**, 51–76 (1970).

Revised Formulation of the Macroscopic Maxwell Theory. I. Fundamentals of the Proposed Formulation, ORNL-4406, part I (November 1969).

Revised Formulation of the Macroscopic Maxwell Theory. II. Propagation of an Electromagnetic Disturbance in Dispersive Media, ORNL-4406, part II (November 1969).

"Revised Formulation of the Kinetic Plasma Theory," *Intern. J. Electronics* **27**, 301–17 (1969).

Revised Formulation of the Kinetic Plasma Theory, ORNL-4474.

"To Amend Refereeing," *Physics Today*, pp. 9–10 (April 1970).

J. Neufeld, W. S. Snyder, J. E. Turner, Harvel Wright, B. M. Wheatley, and Harold Wyckoff
"Radiation Dose from Neutrons and Protons in the Energy Range from 400 MeV to 2 GeV," *Health Phys.* **17**, 449–57 (1969).

M. Oberhofer and E. M. Robinson
"A TSEE G-M Gasflow Counter," *Kerntechnik* **12**(1), 34–38 (1970).

L. Robinson Painter, R. D. Birkhoff, and E. T. Arakawa
"Optical Measurements of Liquid Water in the Vacuum Ultraviolet," *J. Chem. Phys.* **51**, 243–51 (1969).

P. T. Perdue and J. H. Thorngate
Conversion of the Nuclear Data 130A Pulse-Height Analyzer to ASC 11 Paper Tape with Manual Entry for Data Identification, ORNL-TM-2936 (May 1970).

J. W. Poston
Book review: "Fast Burst Reactors," *AEC Symposium Series 15*, Clearinghouse for Federal Scientific and Technical Information, Springfield, Virginia 22151, 646 pp., 1969, to be published in *Health Physics.*

R. H. Ritchie
"Optical Emission from Surface Plasmons," *Phys. Status Solidi* **39**, 297 (1970).

R. H. Ritchie, F. W. Garber, M. Y. Nakai, and R. D. Birkhoff
"Low-Energy Electron Mean Free Paths in Solids," pp. 1–28 in *Advances in Radiation Biology*, vol. 3 (ed. by Leroy G. Augenstein, Ronald Masson, and Max Zelle), Academic, New York, 1969.

E. M. Robinson and M. Oberhofer
"A Sensitive Ceramic BeO-TSEE-Dosimeter," *Health Phys.* **18**, 434–37 (1970).

A. S. Rogowski and T. Tamura
"Environmental Mobility of Cesium-137," *Radiat. Bot.* **10**, 35–45 (1970).

"Erosional Behavior of Cesium-137," *Health Phys.* **18**, 467–77 (1970).

P. S. Rohwer and E. G. Struxness
Quarterly Progress Report on Radiological Safety of Peaceful Uses of Nuclear Explosives: Development of Transient-Exposure Guides, ORNL-TM-2810 (May 1970).

1 1 1 7 0 8 2

T. Saigusa
"Calculation of Spectra of Energy Deposited by Recoil Heavy Particles," *Health Phys.* **18**, 547–60 (1970).

H. A. Schroeder, A. P. Nason, and I. H. Tipton
"Essential Metals in Man – Magnesium," *J. Chronic Dis.* **21**, 815–41 (1969).

H. C. Schweinler and E. P. Wigner
"Orthogonalization Methods," *J. Math. Phys.* (in press).

S. Y. Shieh and R. H. Ritchie
"Simultaneous Generation of Transition Radiation and Bremsstrahlung from a Thin Foil," submitted for publication in the *Physical Review.*

W. S. Snyder
"Estimation of Absorbed Fraction of Energy from Photon Sources in Body Organs," p. 33 in *Medical Radionuclides: Radiation Dose and Effects*, USAEC-DTIE, Oak Ridge, Tenn., June 1970.

"Estimation of Dose Within the Body on the Basis of Personnel Monitoring Data," p. 255 in *Progress in Nuclear Energy, Series XII, Health Physics*, ed. by F. Duhamel, Pergamon, London, 1969, vol. 2, part I.

J. A. D. Stockdale, R. N. Compton, and P. W. Reinhardt
"Reactions of O^- with Some Hydrocarbons in the Energy Region Between 0 and 2 eV," submitted for publication in the *International Journal of Mass Spectrometry and Ion Physics.*

"Studies of Negative Ion–Molecule Reactions in the Energy Region from Zero to Three Electron Volts," *Phys. Rev.* **184**, 81–93 (1969).

J. A. D. Stockdale, R. N. Compton, and H. C. Schweinler
"Negative Ion Formation in Selected Hexafluoride Molecules," to be published in the *Journal of Chemical Physics.*

D. R. Stone, E. B. Wagner, T. D. Jones, and W. H. Shinpaugh
"Calculated and Experimentally Determined Neutron Dose Conversion Factor for Californium," *Health Phys.* **18**, 69 (1970).

D. R. Stone, J. H. Thorngate, K. W. Crase, M. D. Brown, and D. W. Carver
The Development of a Spectrometer and the Measurement of the Neutron Spectrum from the Health Physics Research Reactor Between 50 keV and 450 keV, ORNL-TM-2707 (November 1969) (Master's thesis).

E. G. Struxness
Trip Report of Second Session of U.S.–U.S.S.R. Technical Talks Concerning Peaceful Nuclear Explosives Held in Moscow, February 10–18, 1970, internal memorandum, Mar. 10, 1970.

J. C. Sutherland, R. N. Hamm, and E. T. Arakawa
"Extinction Coefficient and Imaginary Part of the Dielectric Constant for Sodium and Potassium Above the Plasma Energy," *J. Opt. Soc. Am.* **59**, 1581–83 (1969).

Tsuneo Tamura
"A Review of the Radiosensitivity of the Tissues in Bone" (book review), *Health Phys.* **18**, 299–300 (1970).

Tsuneo Tamura and W. P. Bonner
Phosphorus in Land-Water Systems, ORNL-TM-2913 (1970).

William A. Thomas and Donald G. Jacobs
"Curium Behavior in Plants and Soil," *Soil Sci.* **108**(4), 305–7 (1969).

J. H. Thorngate
"An Experimental Measurement of the High Energy Gamma Rays Produced by the Slowing Down of 14 Mev Neutrons in Air," *Health Phys.* **18**, 339–46 (1970).

An Instrument That Provides Linear Temperature Ramps for Use with TSEE Experiments, ORNL-TM-2687 (October 1969).

1147983

J. H. Thorngate, D. R. Johnson, and P. T. Perdue
Energy and Angular Distribution of Neutrons and Gamma Rays – Operation HENRE, CEX-65.11 (August 1969).

I. H. Tipton
"Trace Elements in Human Tissue – a Need for Standards," *Amer. J. Clin. Nutr.* **23**, 123 (1970).

I. H. Tipton and P. L. Stewart
"Long Term Studies of Elemental Intake and Excretion of Three Adult Male Subjects," *Develop. Appl. Spectros.* 8, 40 (1970).

J. E. Turner
"Calculation of the Penetration of Charged Particles Through Matter at Very High Energies," submitted for publication to National Academy of Sciences–National Research Council.

J. E. Turner and V. E. Anderson
"Relativistic Ground-State Energy Eigenvalues of the Electron-Dipole System," submitted for publication to *Nuovo Cimento.*

J. E. Turner, V. E. Anderson, R. D. Birkhoff, and D. R. Johnson
"The Determination of LET Spectra from Energy Proportional Pulse-Height Measurements. II. A Monte Carlo Unfolding Procedure," *Health Phys.* **18**, 15–24 (1970).

J. E. Turner, R. D. Birkhoff, V. E. Anderson, E. B. Wagner, and H. A. Wright
"Monte Carlo Method of Determining LET Spectra from Pulse-Height Measurements," to be published in *Proceedings Second Symposium on Microdosimetry, Ispra, Italy, October 21–24, 1969.*

J. E. Turner and Hal Hollister
"RBE, LET, z, ν; Some Further Thoughts," *Health Phys.* **17**, 356 (1969).

J. E. Turner, V. N. Neelavathi, R. B. Vora, T. S. Subramanian, and M. A. Prasad
"Contributions of Spin, Anomalous Magnetic Moment, and Form Factors to the Stopping Power of Matter for Protons and Muons at Extreme Relativistic Energies," *Phys. Rev.* **183**, 453–57 (1969).

J. E. Turner, Patricia Dalton Roecklein, and R. B. Vora
"Mean Excitation Energies for Chemical Elements," *Health Phys.* **18**, 159–70 (1970).

J. E. Turner and Harvel Wright
"Calculation of Dose from High Energy Nucleons," to be published in *Proceedings Second International Conference on Accelerator Dosimetry and Experience, Stanford, California, November 5–7, 1969.*

J. E. Turner, H. A. Wright, and J. H. Grossen
"A New Model for Calculation of High-Energy Nucleon Penetration Through Matter," *Health Phys.* **18**, 80–82 (1970).

R. C. Vehse, E. T. Arakawa, and M. W. Williams
"Optical and Photoemissive Properties of Palladium in the Vacuum UV Spectral Region," *Phys. Rev.* B **1**, 517–22 (Jan. 15, 1970).

R. B. Vora, V. N. Neelavathi, T. S. Subramanian, M. A. Prasad, and J. E. Turner
"Semiclassical Calculation of the Effect of Magnetic Moment (Spin) on the Slowing Down of Heavy Particles," submitted for publication in the *American Journal of Physics.*

R. B. Vora and J. E. Turner
"Stopping Power of Matter for Deuterons at Extreme Relativistic Energies," *Phys. Rev.* **1**(5), 2011 (1970).

O. E. Wagner
"On the Temperature Dependence of Ovshinsky Type Devices," *J. Appl. Phys.* **40**, 4212–13 (1969).

O. E. Wagner, L. G. Christophorou, and J. G. Carter
"Lifetimes of Liquid Benzene, Toluene, and Mesitylene Excited by a Pulsed-Electron Beam," *Chem. Phys. Letters* **4**, 224–25 (1969).

1147984

U. S. Whang, E. T. Arakawa, and T. A. Callcott
"Collective Effects in the Optical Properties of Cs Above the Plasma Frequency," submitted for publication in *Physical Review Letters.*

H. A. Wright and J. E. Turner
"Free-Nucleon Target Model Applied to Penetration and Dose Calculations for 200 and 400 MeV Protons and Neutrons," to be published in *Health Physics.*

"Free-Nucleon Target Model Applied to Nucleon Penetration Through Matter," *Trans. Am. Nucl. Soc.* 12, 968–69 (1969).

Donald G. Willhoit and Troyce D. Jones
"Dose and LET Distributions in Small Animal-Sized Geometries for a Fission Neutron Spectrum," to be published in *Radiation Research.*

Lectures

K. Becker

Research on Advanced Neutron Personnel Dosimetry Systems at ORNL, AEC Neutron Personnel Dosimetry Workshop, September 23 and 24, 1969, Bethesda, Maryland.

Recent Progress in Solid-State Dosimetry, University of Texas, Anderson Hospital and Tumor Institute, January 9, 1970, Houston, Texas.

Some Advances in Solid-State Dosimetry, Lawrence Radiation Laboratory, March 23, 1970, Berkeley, California.

The Future of Personnel Radiation Monitoring, North Carolina Chapter, Health Physics Society, April 3, 1970, Chapel Hill, North Carolina.

Some Advances in Solid-State Dosimetry, University of North Carolina, April 3, 1970, Chapel Hill, North Carolina.

Some Advances in Solid-State Dosimetry, National Bureau of Standards, April 6, 1970, Washington, D.C.

Thermally Stimulated Exoelectron Emission, Naval Research Laboratory, April 7, 1970, Washington, D.C.

W. P. Bonner

Phosphorus Fractionation, Using Zonal Centrifugation, Briefing of Conservationists, Oak Ridge National Laboratory, April 29, 1970, Oak Ridge, Tennessee.

R. N. Compton

Autoionizing and Autodetaching Negative Ion States of Atoms and Molecules, Department of Physics, University of Florida, January 23, 1970, Gainesville, Florida.

K. E. Cowser

Permanent Disposal of Radioactive Wastes, Muskingum College Students, New Concord, Ohio, Oak Ridge National Laboratory, Building 3504, January 19, 1970, Oak Ridge, Tennessee.

Long Range Management of Radioactive Waste, American Institute of Chemical Engineers Environmental Pollution Symposium, Oak Ridge Associated Universities Training Building Conference Room W-18, March 26, 1970, Oak Ridge, Tennessee.

Long Range Management of Radioactive Waste, General Engineering Contractors Seminar, Oak Ridge National Laboratory, June 18, 1970, Oak Ridge, Tennessee.

C. W. Francis

Soils: Their Role in Pollution, Muskingum College Students, New Concord, Ohio, Oak Ridge National Laboratory, Building 3504, January 19, 1970, Oak Ridge, Tennessee.

1147985

D. G. Jacobs

Post-Deposition Movements of ^{90}Sr, ^{90}Cs, and ^{131}I in the Soil and into Plants. Trans-Pacific Fallout Seminar, Oak Ridge National Laboratory, February 19 and 20, 1970, Oak Ridge, Tennessee.

Disposal of Radioactive Wastes. Western Illinois University Students' Visit to ORNL and UT-AEC Agricultural Research Laboratories, July 17, 1970, Isotopes Development Auditorium, Building 3047, Oak Ridge National Laboratory, Oak Ridge, Tennessee.

Radioactive Waste Management and Movement of Radionuclides Released to the Environment. Memphis State University, Summer Program on Earth Sciences for Junior High School Teachers, July 28, 1970, Memphis, Tennessee.

Considerations in the Peaceful Application of Nuclear Explosives. Muskingum College Students, New Concord, Ohio, Oak Ridge National Laboratory, Building 3504, January 19, 1970, Oak Ridge, Tennessee.

Global Cycling of Tritium. Nuclear Safety Program Seminar, Building 4500-N, East Auditorium, Oak Ridge National Laboratory, June 18, 1970, Oak Ridge, Tennessee.

Waste Disposal. Oak Ridge Associated Universities Students, Building 3504, Oak Ridge National Laboratory, February 12, 1970, Oak Ridge, Tennessee.

T. F. Lomenick

Earthquakes and Reactor Safety, Muskingum College Students, New Concord, Ohio, Oak Ridge National Laboratory, Building 3504, January 19, 1970, Oak Ridge, Tennessee.

W. C. McClain

Liquid Waste Disposal by Hydraulic Fracturing and Bedded Salt Techniques. 8th Faculty-Student Conference at Argonne National Laboratory, August 25 through August 29, 1969, Argonne, Illinois.

K. Z. Morgan

Health Physics Research Needed to Develop Improved Protective Measures in Case of Massive Fallout in the U.S., Trans-Pacific Fallout Seminar, Oak Ridge National Laboratory, March 13, 1970, Oak Ridge, Tennessee.

Health Physics Considerations in Reactor Siting, Metals and Ceramics Division Seminar, Oak Ridge National Laboratory, March 18, 1970, Oak Ridge, Tennessee.

Cause and Cure of Recent Reactor Siting Controversy, ORAU Ten Week Health Physics Course, March 20, 1970, Oak Ridge, Tennessee.

Cause and Cure of Recent Reactor Siting Controversy, Georgia Institute of Technology, March 30, 1970, Atlanta, Georgia.

Internal Dose Lecture, Vanderbilt University, April 6, 7, 13, 14, 1970, Nashville, Tennessee.

Internal Dose Lecture, University of Tennessee, April 9, 16, 23, 1970, Knoxville, Tennessee.

A Time of Challenge to the Health Physicist, Presidential Address (IRPA), Second International Congress on Radiation Protection, May 8, 1970, Brighton, England.

An Introduction to Radiation: Its Effects, Its Control and General Impact upon the Environment, Public Affairs Workshop on Radiation and Man's Environment, October 5–8, 1969, Gleneden Beach, Oregon.

Acceptable Risk Concepts, University of Florida, Gainesville, Florida, November 4, 1969.

Acceptable Risk Concepts, Pittsburgh Section of the American Nuclear Society, November 18, 1969, Pittsburgh, Pennsylvania.

Why the 1968 Act for Radiation Control for Health and Safety Is Required, Symposium on Radiation Legislation, Its Meaning to the Radiologist, Radiological Society of North America, December 1, 1969, Chicago, Illinois.

Standard Man–Standard Patient, ORAU Symposium on Medical Radionuclides: Radiation Dose and Effects, December 8, 1969, Oak Ridge, Tennessee.

Radiation Standards for Reactor Siting, Testimony Before the Joint Committee on Atomic Energy Hearings on Environmental Effects of Producing Electrical Power, Phase 2, January 27, 1970, Washington, D.C.

1147986

Energy Pollution of the Environment, Health Physics Society Midyear Symposium, January 28, 1970, Louisville, Kentucky.

Acceptable Radiation Risk Concepts, UT-AEC Agricultural Research Laboratory, February 6, 1970, Oak Ridge, Tennessee.

Health Physics Profession – Where Do We Go from Here? East Tennessee Chapter of the Health Physics Society, August 4, 1969, Oak Ridge, Tennessee.

Acceptable Risk Concepts – ICRP, AEC Fellowship Students, ORNL, August 6, 1969, Oak Ridge, Tennessee.

Benefits and Risks of Diagnostic Radiation, Nashville Dental Society, September 23, 1969, Nashville, Tennessee.

O. H. Myers

ORNL Seismograph Station, Muskingum College Students, New Concord, Ohio, Oak Ridge National Laboratory, Building 3504, January 19, 1970, Oak Ridge, Tennessee.

P. S. Rohwer

CUE: A Guide for Transient Radiation Exposure, Seminar for Plowshare Program Personnel, Lawrence Radiation Laboratory, May 18, 1970, Livermore, California.

H. C. Schweinler

Molecular Potential Energy Curves by Klein's Method, Department of Chemistry, University of Tennessee, November 6, 1969, Knoxville, Tennessee.

W. S. Snyder

A Plutonium Exposure – Internal Dose, AEC Fellowship Program, ORNL, August 4, 1969, Oak Ridge, Tennessee.

Estimates of Dose from Photon Sources Within an Anthropomorphic Phantom, Southwestern Radiological Health Laboratory, October 13, 1969, Las Vegas, Nevada.

A Two-Exponential Model for Retention of Tritium and a Speculative Interpretation in Terms of Dose, Radiation Technology Class, University of Nevada, October 14, 1969, Las Vegas, Nevada.

Dose in a Homogeneous Phantom from Monoenergetic Beams of Neutrons with Energy Below 14 Mev, Lake Mead Chapter of the Health Physics Society, October 14, 1969, Las Vegas, Nevada.

Estimation of Dose from Photon Sources in the Body, Societe Francaise de Radioprotection, December 3, 1969, Paris, France.

Emergency Guidelines, Exposure Limits for Personnel, Contamination Guides, Fifth AEC-Sponsored Seminar on Medical Planning and Care in Radiation Accidents, December 16, 1969, Oak Ridge Associated Universities, Oak Ridge, Tennessee.

Health Physics Organizations and Journals, Ten-Week Course in Health Physics, January 16, 1970, Oak Ridge, Tennessee.

Monte Carlo Estimation of the Absorbed Fraction of Photon Energy for Organs in the Body, Comitato Nazionale per L'Energia Nucleare, May 19, 1970, Rome, Italy.

Dosimetry of the ICRP Models of the Lung and Gastrointestinal Tract, Comitato Nazionale per L'Energia Nucleare, May 20, 1970, Rome, Italy.

E. G. Struxness

The Interpretation and Application of ICRP Recommendations, Seminar at Lawrence Radiation Laboratories, June 18, 1970, Livermore, California.

Environmental Monitoring, Exhibits Managers' Training Course, ORAU, August 1969, Oak Ridge, Tennessee.

Environmental Monitoring, Oak Ridge High School, July 1969, Oak Ridge, Tennessee.

Tsuneo Tamura

Mineral Segregation by Zonal Centrifugation, Department of Agronomy, University of Tennessee, August 20, 1969, Knoxville, Tennessee.

Separation of Soils and Sediments by Zonal Centrifugation, 5th Nuclear Engineering Congress, Holiday Inn, April 7, 1970, Oak Ridge, Tennessee.

1147987

HEALTH PHYSICS DIVISION

SEPTEMBER 1, 1970

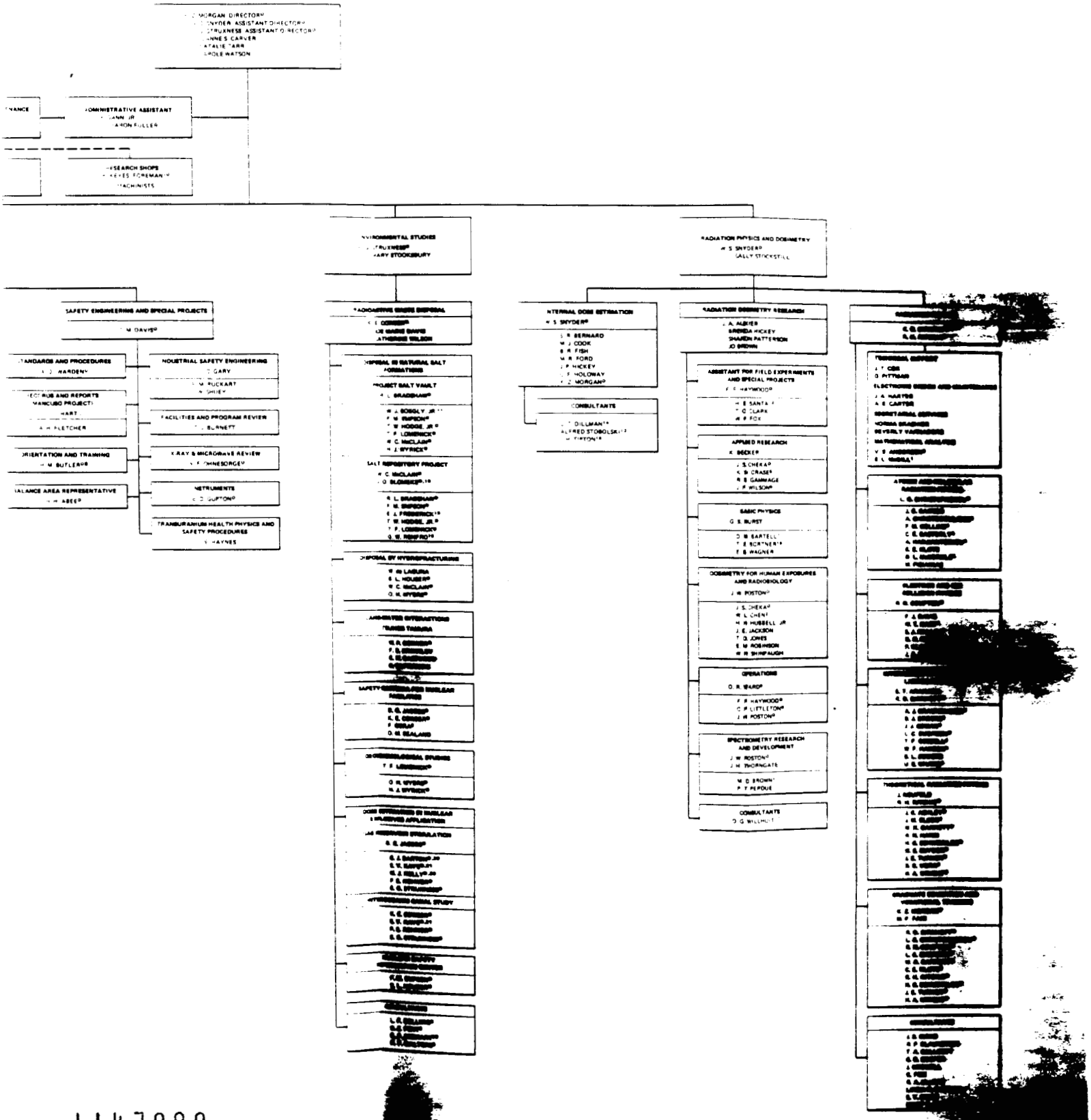

1147989

HEALTH PHYSICS DIVISION

SEPTEMBER 1, 1970

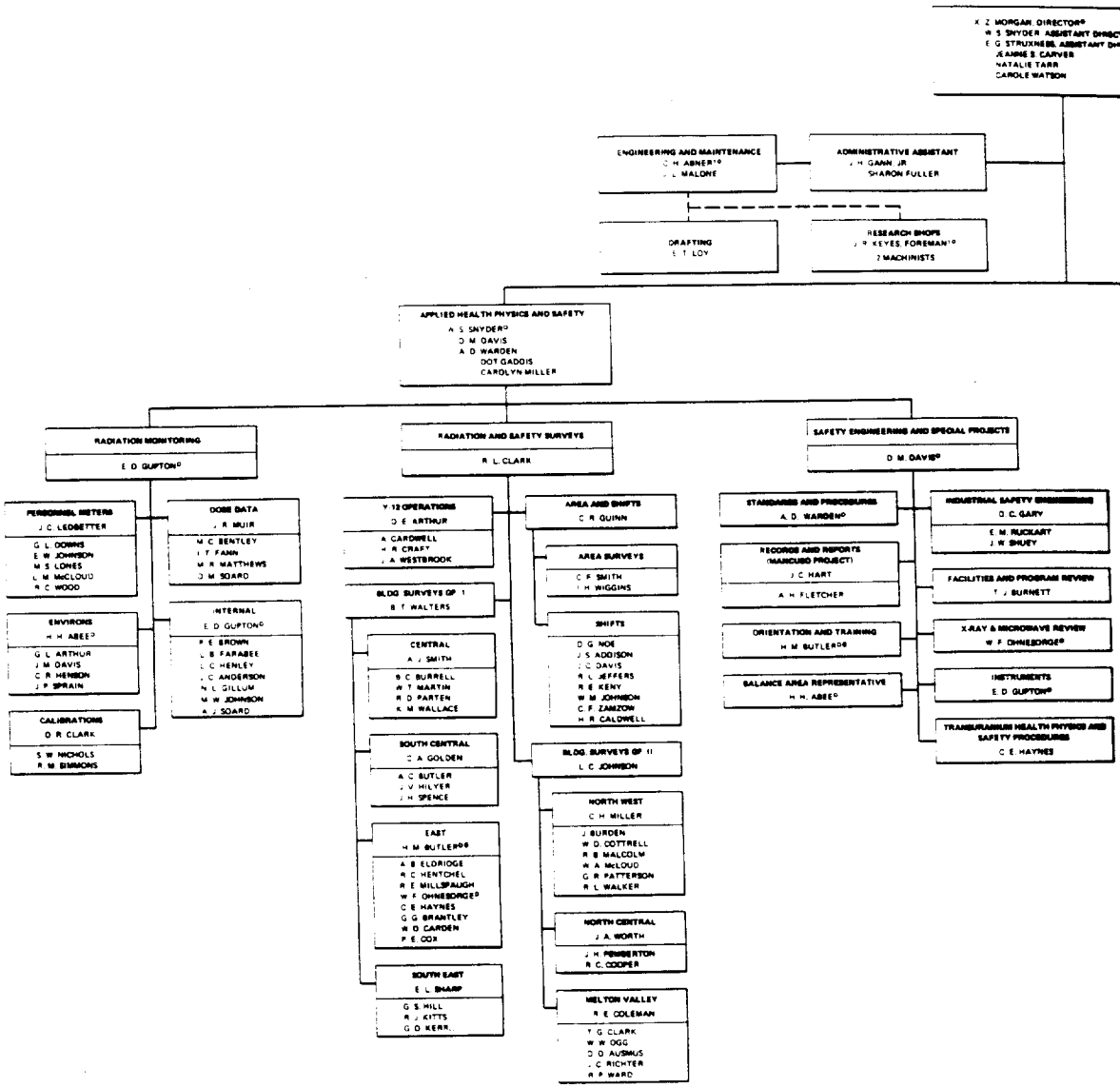

EQUAL CAPACITY
RADIATION CONTROL OFFICER DIVISION
SAFETY OFFICER
LEAVE OF ABSENCE
PART TIME EMPLOYEE
ALIEN GUEST
SELF EMPLOYED
STUDENT
CENTRAL DATA PROCESSING FACILITY (ORGDP)
AEC PREDOCTORAL FELLOWSHIP
ORAU PREDOCTORAL FELLOWSHIP
B & C DIVISION
NEUTRON PHYSICS DIV
B & E DIVISION
ON LOAN TO CIVIL DEFENSE
PART TIME E Q B & G INC
NEW YORK UNIVERSITY
OHIO WESLEYAN UNIVERSITY
CHEMICAL TECHNOLOGY DIV
PART TIME UNIVERSITY OF KENTUCKY
UNIVERSITY OF NORTH CAROLINA
UNIVERSITY OF TENNESSEE
GENERAL ENGINEERING DIVISION
REACTOR CHEMISTRY DIVISION
ECOLOGICAL SCIENCES DIVISION
KANSAS STATE GEOLOGICAL SURVEY

1147988